Quantifying Predator-Prey Interactions: Methods, Challenges, and Applications

Pamela E. Moriarty

A dissertation

submitted in partial fulfillment of the

requirements for the degree of

Doctor of Philosophy

University of Washington

2018

Reading Committee:

Timothy Essington, Chair

Gordon Holtgrieve

Eric Ward

Program Authorized to Offer Degree:

School of Aquatic and Fishery Sciences

University of Washington

Abstract

Quantifying Predator-Prey Interactions: Methods, Challenges, and Applications

Pamela E. Moriarty

Chair of the Supervisory Committee:
Timothy Essington, Professor
School of Aquatic and Fishery Sciences

Knowledge of predator-prey interactions is vital in many subfields of ecology, including food web ecology, behavioral ecology, and population ecology. Information on predator-prey interactions is obtained from a variety of sources, including stomach contents, biochemical tracers such as stable isotopes, fecal matter, and direct observation. These data sources are used to infer the predator's diet and each presents analytical and interpretation challenges. In this dissertation, I pursue research to improve the analysis, interpretation, and application of varied data sources to study predator-prey interactions. My first chapter develops a mixture model to increase the accuracy and precision of diet estimates from stomach content data by addressing several challenges inherent to most stomach content datasets. I extend this model in my second chapter to address sample interdependence, which is a common issue due to sample collection methods. My third chapter addresses the challenges of applying stable isotope analysis to jellyfish due to their unique physiology and proposes a path forward to be able to use this data source effectively. My fourth chapter predicts the effect of hypoxia, a common environmental

stressor, on energy flow from zooplankton to zooplanktivorous fish by merging multiple data sources in a Bayesian integrated assessment. Together, my dissertation research identifies and addresses some common challenges of analyzing predator-prey interactions.

Table of Contents

INTRODUCTION 2

1. A NOVEL METHOD TO ESTIMATE PREY CONTRIBUTIONS TO PREDATOR DIETS 5

1.1 Introduction 5

1.2 Methods 8

1.2.2 Model Testing 13

1.2.3 Applications 16

1.3 Results 17

1.4 Discussion 20

APPENDIX A1 34

2. A MULTI-LEVEL MODEL TO ESTIMATE DIET COMPOSITIONS WITH NON-INDEPENDENT SAMPLES 35

2.1. Introduction 35

2.2. Methods 38

2.3. Results 45

2.4. Discussion 46

3. CHALLENGES AND OPPORTUNITIES FOR APPLYING STABLE ISOTOPE ANALYSIS TO JELLYFISH FOOD WEB ECOLOGY 53

3.1. Introduction 53

3.2. The Mechanisms of Stable Isotope Applications in Food Webs 56

3.3. Implications for Stable Isotope Applications to Jellyfish 61

3.4. Consequences of Assumptions in Stable Isotope Methodology 70

3.5. Discussion 72

APPENDIX A3 78

4. THE EFFECT OF HYPOXIA ON TROPHIC CONNECTIVITY BETWEEN FISH AND ZOOPLANKTON VARIES ACROSS ECOLOGICAL SCALES 80

4.1. Introduction 81
4.2. Methods 84
4.3. Results 97
4.4. Discussion 102
SYNTHESIS 128
REFERENCES 131

List of Tables

Table 1.1 The parameters in the mixture model, along with their corresponding distributions and meanings. 25

Table 1.2 . True values used in sensitivity scenarios for parameters that were held constant..... 25

Table 2.1 The parameters in the mixture model, along with their corresponding distributions and meanings. 49

Table 2.2 True values used in sensitivity scenarios for parameters that were held constant..... 49

Table 2.3 Mean absolute error for each estimation method in each simulation scenario..... 49

Table 3.1 The different scenarios applied to stable isotope analysis data in order to correct for methodological choices. A dash indicates that no correction for that methodology choice was applied, though there is believed to be an effect. Numbers in parentheses indicate the value of the correction applied to the isotope value. The first number indicates the correction for carbon and the second number indicates the correction to the nitrogen value. 77

Table 4.1 Scores for the 10 fold cross-validation analysis. Each column is a variable measured for Pacific herring consuming euphausiids. Lower scores indicate a better fit by the model..... 106

Table 4.2 Scores for the 10 fold cross-validation analysis. Each column is a variable measured for Pacific hake consuming euphausiids. Lower scores indicate a better fit by the model. 106

List of Figures

Figure 1.1 Conceptual flowchart of the mixture model, which splits stomachs into the three cases of $p_i = 0$, $0 < p_i < 1$ and $p_i = 1$. The parameters relevant to each case are shown along with the distributions used to estimate them in the mixture model. 26

Figure 1.2 The continuous relationship between $E(M_s)$ and P_i, which can take a range of shapes, is simplified into a discrete relationship of presence / absence in the mixture model. During model testing, data with concave up, concave down and linear covariance between p_i and $m_s|\phi$ was generated with varying degrees of concavity to test the mixture model's robustness to this simplification. The degree of concavity was altered by varying the value of x in the power function, $E[Msj] = E[Msj|\neg\phi] + (\text{maxconsumption} - E[Msj|\neg\phi]) * Pjx$..... 27

Figure 1.3 Effect of overdispersion in probability of prey occurrence (R_Φ; a, d), probability of only that prey occurring given it does occur ($R_{\Phi p=1}$; b,e), and diet fraction when the prey is present (P .; c,f) on the accuracy (top) and standard error (bottom) of diet fraction estimates. Vertical line shows the true diet fraction. Results are based on 100 simulated data sets each consisting of 200 samples. Box plots indicate median, interquartile range (boxes) and 150% interquartile range (lines). 28

Figure 1.4 Effect of extreme events in stomach masses (e.g., a few very full stomachs) on the accuracy of diet fraction estimates across multiple values of stomach mass when the prey type is present, ((a-c) $M_s|\Phi = 20$, (d-f) $M_s|\Phi = 50$) and across multiple values of the probability of an extreme event occurring, ((a,d) P(extreme event) =0.01, (b,e) P(extreme event) =0.05, (c,f) P(extreme event) =0.1). Scenarios for P(extreme event) = 0.02, 0.2 were also explored and results were consistent with the plots shown here. Horizontal lines

show the true value of c_i. Each box represents 100 simulated datasets of 200 stomachs. Box plots indicate median, interquartile range (boxes) and 150% interquartile range (lines). 29

Figure 1.5 . Effect of extreme events in consumption consumption (e.g., a few very full stomachs) on the precision of diet fraction estimates across multiple values of stomach mass when the prey type occurs ((a-c) $M_s|\Phi = 20$, (d-f) $M_s|\Phi = 50$) and across multiple values of the probability of an extreme event occurring ((a,d) P(extreme event) = 0.01, (b,e) P(extreme event) = 0.05, (c,f) P(extreme event) = 0.1). Scenarios for P(extreme event) = 0.02, 0.2 were also explored and results were consistent with the plots shown here. Horizontal lines show the true value of c_i. Each box represents 100 simulated datasets of 200 stomachs. Box plots indicate median, interquartile range (boxes) and 150% interquartile range (lines)..... 30

Figure 1.6 Effect of covariance between diet fraction Pi and total stomach contents' mass on the accuracy and precision of the mixture model, a convention mean (red line) and conventional weighted mean (blue line). Varying degrees of concavity in the data were created by using a power function, $E[Msj] = E[Msj|\neg\theta] + (\text{maxconsumption} - E[Msj|\neg\theta]) * Pjx$ and varying x. Each box represents 100 simulated datasets of 200 stomachs. Box plots indicate median, interquartile range (boxes) and 150% interquartile range (lines). 31

Figure 1.7 Estimates and standard error when the mixture model, a conventional mean, and conventional weighted mean are applied to a common prey type in diet datasets for four predators with varying life histories, a) Pacific herring, Clupea pallasii, b) English sole,

Parophrys vetulus, c) lingcod, Ophiodon elongates, and d) spiny dogfish, Squalus acanthias. Error bars are standard error. 32

Figure 1.8 . Estimates and standard error when the mixture model, a conventional mean, and conventional weighted mean are applied to a prey type demonstrating correlation between stomach mass and diet fraction. All three methods are applied to diet datasets for four predators with varying life histories, a) herring consuming glass shrimp, b) English sole consuming amphipods, c) spiny dogfish consuming Pacific herring, and d) lingcod consuming great sculpin. Error bars are standard error. Insets are actual data with regression lines, plotted as total stomach contents' mass versus diet fraction. 33

Figure 2.1 Conceptual flowchart of the fixed effects mixture model, which splits stomachs into the three cases of $p_i = 0$, $0 < p_i < 1$ and $p_i = 1$. The parameters relevant to each case are shown along with the distributions used to estimate them in the mixture model. Figure from Moriarty et al. (2017). 50

Figure 2.2 Prey contribution estimates and standard deviation under three simulation testing scenarios, 1) simulating $r\theta k$ from a beta distribution, 2) simulating $r\theta k$ from a student's t distribution, and 3) simulating $r\theta k$ from a bimodal normal distribution. Simulated data for each scenario was estimating under 3 models, 1) the random effects Bayesian mixture model, 2) the non-hierarchical Bayesian mixture model with pooling all data, and 3) the non-hierarchical Bayesian mixture model with subsampling one stomach per sampling group. 51

Figure 2.3 The estimated contribution of Atlantic herring to spiny dogfish under three models, 1) Bayesian mixture model with random effects, 2) treating each stomach as an independent

sample, and 3) subsampling one stomach per sampling event. Error bars are standard deviation. 52

Figure 3.1 The steps in stable isotope analysis (boxes) and the assumptions required for each (bullet points), each of which can influence results and conclusions. 74

Figure 3.2 Isotope signatures for homogenized bodies of of lion's mane jellyfish, Cyanea capillata, in comparison to the isotope signature of their bell. Each point is an individual jellyfish, lines indicate 1:1 lines. 75

Figure 3.3 The estimated biplot position of jellyfish using different methodological assumptions, in comparison to other taxa in the food web. Numbers next to jellyfish points correspond to the numbered scenarios in table 1. Error bars = standard deviation. Euphausiids are bulk samples (different points represent collection by different sampling groups), for fish and jellyfish: n = 20. 76

Figure 4.1 Map of the study area, Hood Canal, in Washington, USA. Black circles indicate the sampling sites. 107

Figure 4.2 Dissolved oxygen levels at each sampling site over the season in both a) 2012 and b) 2013 (red). A dissolved oxygen score of 1 indicates the entire water column had DO < 4mg l^{-1}, while a score of 0 indicates none of the water column had DO < 4 mg l^{-1}. 108

Figure 4.3 Stomach fullness for Pacific herring at sites a) Dabob, b) Duckabush, c) Hoodsport and d) Union (note that the y axes differ between plots). Stomach fullness is a function of mass of stomach contents and the length of the individual fish. Points are mean stomach fullness for Pacific herring caught at that site, month, and year. Lines are the mean model prediction and shaded areas represent the 95% prediction intervals. 109

Figure 4.4 Acoustic densities for Pacific herring (a-d) and Pacific hake (e-h) at Union (a,e), Hoodsport (b, f), Duckabush (c, f), and Dabob (d, h) (units = m^2 nmi^{-2}). Points are mean acoustic densities for each species at that site, month, and year. Acoustic densities were averaged over the water column along each transect and then across transects. Lines are the mean model prediction and shaded areas represent the 95% prediction intervals…. 110

Figure 4.5. Euphausiids available for consumption by Pacific herring (a-d) and Pacific hake (e-h) at Union (a,e), Hoodsport (b,f), Duckabush (c,g), and Dabob (d,h) (units = m^2 nmi^{-2}). Prey availability is a function of zooplankton community composition, size selectivity by the predator in that month, and zooplankton acoustic densities. Points are mean prey availability for that species at that site, month, and year. Lines are the mean model prediction and shaded areas represent the 95% prediction intervals. 111

Figure 4.6 The difference in predicted mean per-capita consumption under actual hypoxic conditions and no hypoxia by Pacific herring over the season at Union (a, b), Hoodsport (c, d), Duckabush (e, f), Dabob (g, h). Per-capita consumption depends on stomach fullness and diet composition of the predator. Top panel in each panel pair depicts the difference in the probabilities of at least a 20% increase in per-capita consumption and a 20% decrease in per-capita consumption. The lower panel in each panel pair depicts the proportional change of per-capita consumption. The line is the mean predicted proportional change and the shaded area shows the 95% prediction intervals.…..... 112

Figure 4.7 The difference in predicted mean per-capita consumption under actual hypoxic conditions and no hypoxia by Pacific hake over the season at Union (a, b), Hoodsport (c, d), Duckabush (e, f), Dabob (g, h). Per-capita consumption depends on stomach fullness and diet composition of the predator. Top panel in each panel pair depicts the difference

in the probabilities of at least a 20% increase in per-capita consumption and a 20% decrease in per-capita consumption. The lower panel in each panel pair depicts the proportional change of per-capita consumption. The line is the mean predicted proportional change and the shaded area shows the 95% prediction intervals. 113

Figure 4.8 The difference in predicted mean population consumption under actual hypoxic conditions and no hypoxia of euphausiids by Pacific herring over the season at sites Union (a, b), Hoodsport (c, d), Duckabush (e, f), Dabob (g, h). Population-level consumption depends on per-capita consumption and acoustic density of the predator. Top panel in each panel pair depicts the difference in the probabilities of at least a 20% increase in per-capita consumption and a 20% decrease in per-capita consumption. The lower panel in each panel pair depicts the proportional change of per-capita consumption. The line is the mean predicted proportional change and the shaded area shows the 95% prediction intervals..... 114

Figure 4.9 The difference in predicted mean population consumption under actual hypoxic conditions and no hypoxia of euphausiids by Pacific hake over the season at sites Union (a, b), Hoodsport (c, d), Duckabush (e, f), Dabob (g, h). Population-level consumption depends on per-capita consumption and acoustic density of the predator. Top panel in each panel pair depicts the difference in the probabilities of at least a 20% increase in per-capita consumption and a 20% decrease in per-capita consumption. The lower panel in each panel pair depicts the proportional change of per-capita consumption. The line is the mean predicted proportional change and the shaded area shows the 95% prediction intervals. 115

Figure 4.10 The difference in predicted mean relative consumption under actual hypoxic conditions and no hypoxia of euphausiids by Pacific herring over the season at sites A (a, b), site B (c, d), site C (e, f), site D (g, h). Relative consumption depends on euphausiid availability and the total consumption by the herring population. Top panel in each panel pair depicts the difference in the probabilities of at least a 20% increase in relative predation and a 20% decrease in relative predation. The lower panel in each panel pair depicts the proportional change of relative predation. The line is the mean predicted proportional change and the shaded area shows the 95% prediction intervals..... 116

Figure 4.11 The difference in predicted mean relative consumption under actual hypoxic conditions and no hypoxia of euphausiids by Pacific hake Union (a, b), Hoodsport (c, d), Duckabush (e, f), Dabob (g, h). Relative consumption depends on euphausiid availability and the total consumption by the hake population. Top panel in each panel pair depicts the difference in the probabilities of at least a 20% increase in relative predation and a 20% decrease in relative predation. The lower panel in each panel pair depicts the proportional change of relative predation. The line is the mean predicted proportional change and the shaded area shows the 95% prediction intervals..... 117

ACKNOWLEDGEMENTS

The Department of Defense National Defense Science and Engineering Graduate (NDSEG) Fellowship, National Science Foundation grant OCE-1154648AM001 and the School of Aquatic and Fishery Sciences provided funding for this research. I would also like to thank my advisor, Timothy Essington, for support throughout all aspects of my dissertation and time as a graduate student. My committee members, Gordon Holtgrieve, Julie Keister, and Eric Ward, have each provided additional feedback and invaluable insight. Halley Froehlich, Kiva Oken, Christine Stawitz, Emma Hodgson, Laura Koehn, Megsie Siple, Elizabeth Ng, Morgan Arrington, and Andy Whitehouse have exceeded all possible expectations of officemates and have taught me so much about statistics, ecology, and life. Over my time as a graduate student, countless other individuals have provided comments on manuscript drafts; I thank them all for spending their valuable time providing me with feedback and suggestions.

The fourth chapter would not have happened without the help of many individuals. I would like to thank John Horne, Sandy Parker-Setter, and Mei Sato for their patience and help with providing and interpreting the acoustics data. Zooplankton data was available thanks to the hours of processing by Amanda Winans, BethELee Hermann, Lingbo Li, and Zack Oyafuso. Jen Nomura, David Duggins, and Scottie were invaluable in the field, as were the many volunteers. Rebekah Stiling, Lilia Bannister, and Sarra Tekola spent innumerable hours staring at partially digested zooplankton with the utmost patience to analyze fish stomach contents.

INTRODUCTION

Understanding predator-prey interactions is central to ecological theory and applications. Food web ecology is concerned with patterns of predation linkages (Polis and Hurd 1996, Marshall 2007), how strong and weak interactions structure food webs (Huxel and McCann 1998, McCann et al. 1998, Prugh 2005), and how energy moves through trophic levels. Behavioral ecology is commonly interested in the factors influencing niche width, including predator choice of prey type (Charnov 1976, Randall and Myers 2001, Navia et al. 2007, Catano et al. 2014). Additionally, population ecology inherently depends on interactions between predators and prey to understand how those affect each population (Gurney and Nisbet 1998). The pervasive role of predator-prey interactions throughout many fields of ecology has led to the development of a wide array of approaches for studying them.

Predator-prey interactions can be viewed through different lenses in order to focus on different aspects of the system. Energetic food webs represent the amount of energy moving between functional groups and are a common way to represent food webs. Their ability to predict system-level processes makes them a useful tool in some situations (Moore and De Ruiter 2012). They also provide some information on the importance of specific functional groups in an ecosystem (Paine 1980).

Accordingly, a range of both analytical and statistical tools now exist to gain information on these energetic linkages. Analytical tools, such as stable isotope analysis (Peterson 1999, Hobson and Bond 2012), stomach content data (Hyslop 1980, Locke et al. 2012) and fatty acid analysis (Iverson 2009) have come into use at different times. Each analytical method requires the development of unique methodology in order to apply it accurately and precisely across

taxonomic groups and ecosystems. Additionally, each method of obtaining information on predator-prey interactions produces a different type of data that has its own set of challenges when analyzing it. Therefore, not only are various statistical methods used for each analytical tool, but may also vary depending on the purpose of the study. The use of effective statistical tools can greatly increase the information we can gain from the data.

However, many of these analytical and statistical tools are increasingly being used for a wider range of applications than for which they were initially developed. Some analytical tools, such as stable isotope analysis, are accompanied by well-developed statistical methods that allow for quantitative estimates (Phillips et al. 2005, Semmens et al. 2009, Ward et al. 2011), but others, such as stomach contents, are not (Ahlbeck et al. 2012). As the need for quantitative estimates of prey contributions to predator diets, or diet estimates, has risen this has increasingly limited our use of stomach content data. Similarly, over the last couple of decades, ecologists have recognized that taxonomic groups that have previously been ignored, such as jellyfish (Richardson et al. 2009) and microbes (Legendre and Rivkin 2008, Turk et al. 2008) may play ecologically important roles. In the case of jellyfish, this has led to a large increase in the number of studies focused on them. As this has occurred, existing analytical tools, such as stable isotope analysis and stomach contents have been increasingly been applied to them (Sosik and Simenstad 2013, Nagata et al. 2015b), but not always with appropriate consideration as to the potential differences among taxonomic groups.

In particular, the appropriate use of analytical and statistical tools for quantifying predator-prey interactions allows us to better assess changes in predator-prey interactions. Predator-prey interactions change over time and space, as they are driven by environmental conditions (Holyoak et al. 2005), such as temperature and oxygen levels in aquatic systems

(Sandberg 1997, Higham et al. 2015). As environmental change occurs, predator-prey interactions are then susceptible to change. The statistical and analytical tools described here can be applied to study how these predator-prey interactions change as environmental changes occur.

Here, I focus on developing methods to study predator-prey interactions to improve our use of existing methodological tools and apply our existing tools to study how environmental conditions drive predator-prey interactions. My first chapter is focused on developing a novel method to quantitatively estimate prey contributions to predator diets that addresses several challenges that are common across many stomach datasets. Additionally, my novel estimation method creates a likelihood-based framework for diet fraction estimates. In my second chapter, I build on the likelihood framework I've created by using Bayesian estimation methods to address sample inter-dependence in stomach data. This model extension allows the model I developed in chapter one to be more broadly applicable. In my third chapter, I investigate the challenges of applying stable isotope analysis to jellyfish (class: Scyphozoa) posed by their unique body composition and physiology. I lay out the path forward to be able to accurately interpret stable isotope ratios for this taxon. Finally, I use an integrated assessment to determine how environmental change, such as the development of hypoxia, alters energy flow from zooplankton to zooplanktivorous fish in Hood Canal, Washington, USA. By simultaneously measuring individual, population, and system-level processes and their interactions, I produce a nuanced picture of the effects of hypoxia on energy flow.

1. A NOVEL METHOD TO ESTIMATE PREY CONTRIBUTIONS TO PREDATOR DIETS

Stomach content data are frequently used to characterize predator feeding habits, often by describing the proportional contribution by weight or number of each prey type (diet fractions). These data pose several statistical challenges for analysis and estimation that have hindered our ability to create quantitative diet fraction estimates from stomach content data. To address these challenges, we developed a novel, likelihood-based mixture model to quantitatively estimate diet fractions. Simulation testing indicated that estimated diet fractions from the mixture model were more precise than those estimated either from a (stomach-mass) weighted mean or the sample mean, and were more accurate than a sample mean. Additionally, we applied the mixture model, a weighted mean, and sample mean to stomach content data for multiple types of predators. For three of four of these datasets, the mixture model demonstrated higher precision than and similar accuracy to a weighted-mean, and similar precision and better accuracy than a sample mean. The mixture model represents an important step in advancing statistical methods to address the challenges of stomach content data.

1.1 INTRODUCTION

Ecological research fundamentally requires understanding the feeding habits of predators. From a behavioral ecology perspective, we are commonly interested in measuring prey breadth, and the factors influencing niche widths (Charnov 1976, Randall and Myers 2001, Navia et al. 2007, Catano et al. 2014). Data on predator feeding habits are also used to better understand top-down and bottom-up effects in predator-prey systems, including how distinct patterns of prey use

might govern predator-prey interaction strengths (Polis and Hurd 1996, Marshall 2007). These data are also essential for creating food webs and understanding their structures and dynamics (Huxel and McCann 1998, McCann et al. 1998, Prugh 2005). Finally, feeding habits information is critical for parameterizing models to predict the outcome of predator –prey interactions (Stewart et al. 1981, Christensen and Walters 2004, Rose et al. 2008, Fulton et al. 2011). Despite the pervasive role of feeding habit information, there has been surprisingly little development of methods for quantitative estimation of predator diets.

For many species, predator feeding information is often derived from sampling stomach contents (i.e. stomach content data). Stomach content analysis is ubiquitously used in studies of fish diets (MacKinlay and Shearer 1996), as well as for seabirds (Montalti and Ruben Coria 1993), jellyfish (Barz and Hirche 2007, Jaspers et al. 2015), sea turtles (Colman et al. 2014, Williams et al. 2014), and marine mammals (Fernandez et al. 2014, Matley et al. 2015). Analysis of stomach content data collected involves two distinct components: 1) measuring total prey amounts in the stomach (total stomach contents' mass or number) (Elliot and Persson 1978) and 2) calculating the fraction of total prey that consists of individual prey types (diet fractions). While there is a large body of literature examining distinct ways to analyze stomach content data, there has been little development of formal statistical methods.

There are few commonly used mass-based analysis methods for estimating diet fractions. One is to use the average of individual diet fractions, treating each stomach as an independent data point (Nielsen et al. 1983, Liao et al. 2001). Alternatively, all stomachs can be pooled and the proportion of the total summed diet mass consisting of each prey type can be calculated (Nielsen et al. 1983). Additionally, a weighted mean (weighting individual stomach proportions by total stomach contents' mass) is sometimes employed, which is analogous to the pooling

method, but allows for calculation of confidence intervals (Nielsen et al. 1983).

These analyses are relatively straightforward to compute, but unfortunately don't address the challenging characteristics of stomach content data. One challenge of analyzing stomach content data is that feeding rates may be related to the prey type consumed- when certain prey items are present they may be likely to be consumed in high quantities. For example, on the occasions that rarely available schooling prey is available, a generalist predator may consume it at high rates. This creates covariance at the individual level between the amount a predator consumes and the prey type eaten that is not reflective of population-level consumption (Hyslop 1980, Liao et al. 2001). Another challenge is that stomach content data are often skewed such that a small number of samples have much higher stomach content masses than the average of all the samples. At a population level, these rare events could comprise a high proportion of total feeding, so are important data to include in predator diet estimates. However, rare events are difficult to estimate precisely, and their presence in a small sample can greatly influence diet fraction estimates (Ahlbeck et al. 2012).

Methods for stomach content data should ideally be based on an appropriate likelihood function to estimate the prey contribution. Likelihood functions for individual sample proportions are possible, but are generally not existent for weighted mean proportions. However, the use of a likelihood based framework in ecology and fisheries, whether in maximum likelihood (ML) or Bayesian models, offers several advantages (Hilborn and Mangel 1997). Likelihood based estimation of parameters allows for formal model selection, using criteria such as AIC (Burnham and Anderson 1998), so that distinct alternative hypotheses can be evaluated in a statistically rigorous way. As diet estimates are used as inputs for other models (Christensen and Walters 2004, Fulton et al. 2004, Plagányi et al. 2014), formally selecting the best estimate

could allow for more accurate inputs to other models. A likelihood framework also allows for merging prior information on predator diets (such as stable isotope analyses, expert judgment or previous sampling) with stomach content data (Ainsworth et al. 2010). Finally, likelihood based approaches can be extended to address the potential lack of independence among stomachs collected during a single sampling event.

Here, we present a novel statistical method to quantitatively estimate prey contributions to a predator's diet that addresses all three challenges discussed above: 1) extreme events in predator stomach contents' mass (defined here as an individual stomach having a total contents mass greater than twice the interquartile range), 2) covariance between stomach contents' mass and diet fraction within the data and 3) uses a maximum-likelihood framework. Then, we demonstrate the use of the mixture model by applying it to datasets for different predators with varying life histories.

1.2 METHODS

We begin by explaining the construction of our model to quantitatively estimate predator diet fractions. Then we evaluate the sensitivity of our model to simplifying assumptions using simulated data and compare its accuracy and precision to existing methods for analyzing stomach content data. Finally, we apply our model to datasets for different predators to determine how the methods compare in real world situations.

1.2.1 Model Development

Diet fraction, defined as the mean proportional contribution of a single prey type, *i*, to a predator's diet, C_i (Table A1.1), is equal to the ratio of the expected mass of prey type *i* in the stomachs, $E[M_i]$, divided by the expected total mass of the stomachs' contents, $E[M_s]$,

[1] $$E[C_i] = \frac{E[M_i]}{E[M_s]}.$$

The desired properties of an estimator for $E[C_i]$ are that it, and its confidence intervals, are bound between 0 and 1, inclusively, and that it is based on a likelihood function to permit model selection and maximum likelihood estimation. There are two existing distinct frameworks, the mean and weighted mean, to estimate $E[C_i]$. Using the mean proportion of prey type *i* in individual stomachs implies that given stomachs from *N* individual consumers, each with prey content mass M_{ij} and total stomach content mass M_{sj}, where $1 < j < N$, $E[C_i] = mean(p_i) = \frac{\sum_{j=1}^{N} \frac{M_{ij}}{M_{sj}}}{N}$. In contrast, using the weighted mean or pooling all stomachs is equivalent to estimating $E[C_i] = weighted\ mean\ (p_i, M_i) = \frac{\sum_{j=1}^{N} M_{ij}}{\sum_{j=1}^{N} M_{sj}}$. If M_{ij} and M_{sj} are independent, these two sample-based methods will, on average, produce equivalent estimates.

Likelihood Estimation

To create a likelihood based framework that will ensure the estimator is bound between 0 and 1, we model M_i as the product of the total stomach contents' mass (M_s) and the mean fraction of diet that consists of prey type *i* (P_i), where both stomach mass and stomach diet fraction are now random variables, described by probability density functions $f(M_s)$ and $g(P_i)$, respectively. However, to account for the fact that P_i and M_s may not be independent, we allow $g(P_i)$ to also be a function of stomach content mass, $g(P_i,M_s)$, so the mean of $g(P_i)$ depends on M_s. Thus, in our framework, the numerator of equation 1 is the integration over P_i and M_s:

$\int_0^1 \int_{\mathbb{R}_*^+}^{\infty} g(P_i, M_s) P_i M_s f(M_s) dM_s \, dP_i$. The denominator is obtained by integrating over M_s in the typical way, producing:

[2] $$E[C_i] = \frac{\int_0^1 \int_{\mathbb{R}_*^+}^{\infty} g(P_i,M_s) P_i M_s f(M_s) \, dM_s \, dP_i}{\int_{\mathbb{R}_*^+}^{\infty} M_s \, f(M_s) \, dM_s},$$

In the simple case where $g(P_i,M_s)$ is independent of M_s, this simplifies to $C_i = \int_0^1 P_i \, g(P_i) \, dP_i$, which is simply the expectation of P_i. When $g(P_i, M_s)$ depends on M_s, the integral in the numerator of equation 2 has no analytical solution except when $g(P_i, M_s)$ is linear in M_s. However, this case is generally not practical because P_i must be bound between 0 and 1, and typical methods to achieve this constraint, such as piecewise linear models, would not produce an analytical solution.

Additionally, there is a second calculation problem when using equation 2. This equation requires a probability density function that allows for a greater than zero density when P_i equals 0 or 1, but has zero density when P_i is less than 0 or greater than 1. No continuous probability density function has this property. One solution for a likelihood function is to create a mixture model and introduce two new variables. The first, Φ, is an indicator variable to represent the presence of prey type *i* in a stomach and is described by r_Φ, the probability of presence. Correspondingly, stomachs not containing the prey type *i* are denoted by $\neg\Phi$. The second random variable, $\Phi_{p=1}$, indicates the stomach consisted entirely of prey type *i* given it contained prey type *i* with the probability of this event denoted by $r_{\Phi p=1}$.

Although including mixture models at first appears to complicate the analytical formulation, it provides an opportunity to account for potential covariance between P_i and M_s. Namely, we make two assumptions regarding how stomach mass is related to stomach contents. One, we assume that the probability density function for M_s differs between stomachs that

contain prey type *i* and those that do not. Two, we assume there is no additional covariance between P_i and M_s among stomachs that contain the prey (Figure 1.1). Under these assumptions, the model simplifies greatly, such that the numerator of equation 2 becomes:

[3] $$E[M_i] = \left(r_\Phi\left(1 - r_{\Phi p_i=1}\right)E\left(P_i|\Phi, 1 - \Phi_{p=1}\right) + r_\Phi r_{\Phi p_i=1}\right)E(M_s|\Phi)$$

And the denominator of equation 2 can be expressed as:

[4] $$E[M_s] = r_\Phi E(M_s|\Phi) + (1 - r_\Phi)E(M_s|1 - \Phi)$$

Then, the full expectation is

[5] $$E[C_i] = \frac{\left(r_\Phi\left(1-r_{\Phi p_i=1}\right)E\left(P_i|\Phi, 1 - \Phi_{p_i=1}\right)+ r_\Phi r_{\Phi p_i=1}\right)E(M_s|\Phi)}{r_\Phi E(M_s|\Phi)+(1-r_\Phi)E(M_s|1-\Phi)}.$$

Another advantage of this mixture formulation is it consists of distinct parameters that can be estimated separately from the data using maximum likelihood estimation (MLE). Here, the probability of prey type *i* occurring is estimated using a Bernoulli probability density function, $\Phi \sim Ber(r_\Phi)$ (Table 1.1), where Φ indicates the presence of prey type *i*. Similarly, the probability of only prey type *i* occurring given that prey type *i* has occurred is also estimated from a Bernoulli density function, $\Phi_{pi=1} \sim Ber(r_{\Phi pi=1})$, where $\Phi_{pi=1}$ indicates only the presence of prey type *i* given prey type *i* has occurred. A common choice for estimating proportional data is a beta distribution, so we model $g(P_i)$ as a beta distribution, $P_i \sim Beta(\alpha_1, \alpha_2)$. The mean diet fraction can be written as the mean of the beta distribution with parameters α_1 and α_2, $\alpha_1/(\alpha_1 + \alpha_2)$. The probability densities of the total stomach contents masses for those containing prey type *i*, $f(M_s|\Phi)$, and those not containing prey type i, $f(M_s|\neg\Phi)$, could be modeled using any non-negative continuous distribution. Because of its flexibility, we used a gamma distribution, so $M_s|\Phi \sim Gamma(k_\Phi, 1/\theta_\Phi)$, with $E[M_{s\Phi}] = k_\Phi\theta_\Phi$ and $M_s|\neg\Phi \sim Gamma(k_a, 1/\theta_a)$, so $E[M_{sa}] = k_a\theta_a$. The gamma distribution's thick tails, as compared to other common choices (normal, lognormal),

allow us to model the stomach data while including the stomachs with extreme content masses in the distribution's long tails.

Using these probability density functions, the total likelihood function for the model we present here is expressed as three components: diet fractions equal to 0, diet fractions between 0 and 1, and diet fractions for single-prey stomachs:

$$[6] \qquad L = \prod_j \begin{cases} \frac{1}{\Gamma(k_a)\theta^{k_a}} p_{ij}^{k_a-1} e^{-\frac{p_{ij}}{\theta_a}} * (1 - r_\Phi), & p_{ij} = 0 \\ \frac{1}{\Gamma(k_\Phi)\theta^{k_\Phi}} p_{ij}^{k_\Phi-1} e^{-\frac{p_{ij}}{\theta_\Phi}} * r_\Phi * r_{\Phi p=1} * \frac{p_{ij}^{\alpha_1-1}(1-p_{ij})^{\alpha_2-1}}{Beta(a_1,\alpha_2)}, & 0 < p_{ij} < 1 \\ \frac{1}{\Gamma(k_\Phi)\theta^{k_\Phi}} p_{ij}^{k_\Phi-1} e^{-\frac{p_{ij}}{\theta_\Phi}} * r_\Phi * r_{\Phi p=1}, & p_{ij} = 1 \end{cases} .$$

(Note that we follow standard statistical notation by using upper case variables to indicate random variables and lower case letters to indicate outcomes, *i.e.* data.)

Parameterization

For the purpose of parameter estimation and calculating error, we reparameterized the model so that the main parameter of interest, $E[C_i] = \widehat{c_\iota}$, was a leading parameter. That is, rather than estimate the eight components of the model independently, and use those to generate $\widehat{c_\iota}$ as a derived parameter, we rearranged the model form so that $\widehat{c_\iota}$ was being estimated simultaneously with the remaining parameters. This allowed us to estimate the variance – covariance matrix of $\widehat{c_\iota}$ and other parameters of interest. Asymptotic error for the parameters was calculated using the inverted hessian matrix. Specifically, we rearranged the equation such that $M_s|\neg\Phi$ was calculated as a derived parameter,

$$[7] \qquad E[M_s|\neg\Phi] = \frac{E[M_s|\Phi]\ r_\Phi(E[P_i] + r_\Phi r_{\Phi p=1} - E[C_i] - E[P_i] r_\Phi r_{\Phi p=1})}{E[C_i](1-r_\Phi)} .$$

Additionally, the gamma and beta likelihood functions each require estimation of two parameters that together give the mean and variance of the distribution. To aid model interpretation, we directly estimated the mean and variance for these distributions (i.e., $E[P_i]$, $Var[P_i]$), rather than the distribution parameters (i.e., α_1, α_2), as the mean and variance have clear biological meanings in this context.

1.2.2 Model Testing

We tested the mixture model via simulation analysis. Specifically, we generated data with particular properties and a known diet fraction from an operating model (with a known "truth"), fit our estimation model to these data, and then compared the true and estimated values. We performed several simulation tests; each asked specific questions about the performance of the model under particular conditions. Results were compared across three modeling approaches: (1) the mixture model, (2) the conventional sample mean, (3) the conventional sample weighted mean.

Base Operating Model

We generated data so that each stomach had a specified probability, r_{Φ}, of having $p_{ij}>0$. For stomachs with $p_{ij}>0$, we then assigned $p_{ij}=1$ with probability $r_{\Phi p=1}$. Stomach masses were drawn for $p_{ij}=0$ from a gamma distribution, $m_{sj}|\neg\Phi \sim Gamma(k_a,\theta_a)$. For stomachs for which p_{ij} was assigned to be > 0, then the bivariate data (p_{ij}, m_{sj}) for each stomach was calculated from

$$[8] \qquad (p_{ij}, m_{sj}) = \begin{cases} p_{ij} \sim \beta(\alpha_1, \alpha_2), m_{sj} \sim Gamma(k_\phi, \theta_\phi), if\ p_{ij} \neq 1 \\ p_{ij} \sim 1, m_{sj} \sim Gamma(k_\phi, \theta_\phi), if\ p_{ij} = 1 \end{cases}$$

For each model testing scenario, we compared the mean and variance of the prey contribution, $\hat{c}_i$, estimated by the mixture model to those estimated using the conventional mean and conventional

weighted mean, as well as to the true value from the operating model. This allowed us to compare the accuracy and precision of the commonly used methods to the new method. We generated 100 data sets, each containing 200 stomachs, for each parameter value tested. Preliminary testing indicated that generating and estimating more than 100 datasets did not alter results or conclusions. Also, preliminary testing on the effect of sample size indicated that sample size affected model precision, but not accuracy. All parameter estimation was performed in R3.1.0 (R Core Team 2014).

To confirm that the numerical routines were converging on the parameter values that maximize the likelihood (MLEs), we also calculated the MLE for each parameter individually in addition to estimating them jointly. The estimate for $\widehat{c_i}$ was then calculated from these individual estimates using equation 5. If the estimate of $\widehat{c_i}$ from estimating all parameters jointly was within 20% of the MLE of $\widehat{c_i}$ obtained by estimating them individually, then we considered the estimation to have converged on the MLE. This confirmation procedure was used throughout all model testing analyses.

Mean Absolute Error

Our first test was designed to determine whether the model parameters could be reliably estimated when all of the model assumptions were true. For this, we generated data directly from the base operating model and estimated the parameters with the model we developed. We calculated the mean absolute error (MAE) for each parameter in the model as,

[9] $$MAE = \frac{1}{N}\sum_{i=1}^{N}|estimated - true|.$$

Overdispersion

Our second test was to evaluate whether the model estimates were robust to overdispersion in stomach contents mass, the distribution of diet fractions, or the presence / absence of prey in stomachs. To simulate overdispersion, we generated data from the basic operating model described above, but treated the distribution parameters of Φ, $\Phi_{p=1}$ and p_i as random. For Φ and $\Phi_{p=1}$, R_Φ and $R_{\Phi p=1}$ were drawn from a beta distribution, so they would be bounded between 0 and 1, while the parameters for P_i, A_1 and A_2, were drawn from a gamma distribution, so they would be greater than 0. Other parameter values were held constant between simulations (Table 1.2).

Extreme Events in Total Stomach Contents' Mass

We evaluated the model's accuracy in estimating $\widehat{c_i}$ under scenarios in which the data contained extreme events in stomach contents' masses (e.g. a few very full stomachs). First, we used the basic operating model, but each stomach had some chance of being an extreme event. For extreme events, we simulated its stomach mass, m_{ej} by $m_{ej} \sim Gamma(k_e, \theta_e)$, where m_{ej} indicates the mass of the jth stomach is an extreme event. We simulated data with these extreme events under multiple combinations of parameter values. We used the same variance for all stomachs (Table 1.2) with two values of $m_e|\phi$, $E[m_e|\phi] = 20$ and 50, and five probabilities that a stomach was an extreme event, $P(\text{extreme event}) = 0.01, 0.02, 0.05, 0.1, 0.2$.

Additionally, we simulated data that had more extreme outliers when $p=0$ (e.g. a very few particularly full stomachs when the predator had not eaten the prey type). This scenario was based on our analysis of predator stomach content data (below). Specifically, here we simulated the case where stomachs that did not contain the prey type had a 0.2% chance of having a sample mass 50 times greater than the other stomachs, such that $E[m_e|\neg\phi] \sim 50*Gamma(k_a, 1/\theta_a)$. Again,

we modified the basic operating model previously described. Data were simulated for $c_i = 0.3$ and 0.6.

Covariance Between Diet Fraction and Mass of Stomach Contents

We used simulated data to test the simplifying assumption that the mixture model makes about the relationship between total stomach contents' mass of a predator and the proportion of the stomach contents that consists of a particular prey. Namely, the mixture model assumes that there are distinct stomach content masses when the prey item is present vs. absent, but that otherwise there is no relationship between diet fraction and stomach mass. Biologically, this implies that the total amount a predator consumes in a feeding episode depends solely on whether the predator has eaten the prey type in this feeding episode, and not how dominant the prey type is in the stomach. We sought to test the robustness of this assumption by generating data from an operating model in which there is a more complex relationship between p_i and m_s. Specifically, we continued to use the basic operating model described above, except we assumed that when a stomach contained the prey type the mean stomach mass was a function of p:

[10] $$E[M_{sj}] = E[M_{sj}|\neg\Phi] + (max\ consumption - E[M_{sj}|\neg\Phi]) * P_j^x$$

We created linear covariance by setting $x = 1$, concave down covariance by $0 < x < 1$ and concave up covariance by $x > 1$ (Figure 1.2). For concave up and concave down covariance we tested a range of values for x.

1.2.3 APPLICATIONS

We applied the mixture model, the conventional weighted mean, and conventional mean to stomach content data for four fish species with varying predation strategies and life histories.

We obtained diet data for two small-bodied predators, Pacific herring, *Clupea pallasii*, and English sole, *Parophrys vetulus*, that have clear dominant prey types (euphausiids and polychaetes, respectively). We also used data for two large, generalist predators: Pacific spiny dogfish, *Squalus suckeyi*, and lingcod, *Ophiodon elongates*. All samples were collected in the Salish Sea, Washington, U.S.A. The stomach content data for Pacific herring, *Clupea pallasii*, were collected in Hood Canal, from June to October 2013 by midwater trawling (Sato et al, *in prep*). Both the English sole and dogfish were sampled throughout Puget Sound by bottom trawling over multiple seasons from 2004-2005 (Reum and Essington 2008). Finally, we also used diet information from lingcod collected individually in the San Juan Archipelago between spring 2004 and fall 2005 (Beaudreau and Essington 2009). As herring, English sole, and dogfish were caught in high numbers in single tows, only one stomach sample per trawl was used when estimating $E[c_i]$ to lower the likelihood of pseudoreplication. For each of the four datasets, we estimated the diet fractions of the most common prey and a prey type that exhibited covariance between p_i and $m_s|\phi$.

1.3 RESULTS

1.3.1 Model Testing

We generated data from the basic operating model while varying the parameter values over their ranges to confirm our mixture model's ability to accurately estimate $\widehat{c_i}$ over the range of parameter values. The mixture model accurately estimated the true parameter values across the range of parameter values. The maximum mean absolute error (MAE) for all parameters was 0.018 (Table A1.2), indicating parameter estimates were robust over the ranges tested. The range of MAE for $\widehat{c_i}$ was 0.004 to 0.015 and increased with the true value of c_i.

Overdispersion

The mixture model, the conventional mean, and conventional weighted mean differed in their sensitivity to overdispersion in the parameters controlling the frequency of the prey type's occurrence, the frequency of $P_i=1$, and the distribution of individual diet fractions (P_i). The new mixture model and the conventional weighted mean accurately estimated $\widehat{c_i}$ when there was overdispersion in any of these random variables, while the conventional mean underestimated $\widehat{c_i}$, especially when the frequency of $P_i=1$ was overdispersed (Figure 1.3a-c). The precision (here, measured as the standard error of the estimate) of estimates was relatively similar across estimation methods and overdispersion scenarios, but tended to be slightly greater for the conventional sample mean (Figure 1.3d-f).

Extreme Events in Stomach Contents' Mass

The estimation methods differed in their sensitivity to extreme events in total stomach contents' mass. For all scenarios explored here (each varying the magnitude and frequency of samples with extreme stomach mass), the conventional mean underestimated diet fraction, while the mixture model and conventional weighted mean tended to accurately estimate diet fraction (Figure 1.4). The error in diet fractions estimated using a conventional mean was substantial, ranging from 0.08 – 0.12 (range of median values). The precision of estimates showed different patterns. Specifically, the conventional weighted mean generally had the lowest precision, especially when extreme events were uncommon, but of high magnitude (Figure 1.5). The precision of estimates from the mixture model were similar to, but slightly less than those of the conventional mean.

Covariance Between Diet Fraction and Mass of Stomach Contents

When the simulated data contained covariance between p_i and m_s, the accuracy of estimates from the mixture model varied depending on the shape of covariance (Figure 1.6a). The mixture model was least accurate in the presence of linear covariance. When concave up or down covariance was present, the degree of concavity had little effect on the accuracy of the diet fraction estimate, such that the median underestimate of diet fraction was consistently about 0.05 (10% different from true value). In comparison, a conventional weighted mean was consistently accurate in estimating $\widehat{c_i}$, and a conventional mean was consistently more inaccurate than the mixture model. While these simulations tested positive covariance, we would expect the same patterns of bias, but in the opposite direction, for negative covariance.

The precision of the mixture model also varied depending on covariance shape and concavity (Figure 1.6b). With concave down covariance, the precision of the mixture model increased as the concavity of the relationship between p and m_s increased. The error from the mixture model was approximately equal to the error from a conventional weighted mean and conventional mean at $x = 1/4$ and was more precise at lower values for x. However, for $x \geq 1$, the precision of the mixture model did not depend on the concavity and was consistently less precise than a conventional weighted mean or conventional mean.

1.3.1 Applications

For each dataset, we first estimated the diet fractions of the most common prey, as determined by the conventional mean. Estimates derived from the mixture model and the conventional weighted mean were broadly similar, but not identical (Figure 1.7). In three of the

four applications, the estimates were as expected from the simulation analysis- the mixture model and conventional weighted mean estimates were similar, which were both very different from the conventional mean estimates, suggesting there was covariance between stomach total mass and diet fraction in the data. In the fourth application, Pacific herring, both the mixture model and conventional weighted mean estimates were much less than the conventional mean, though all estimates had large error (Figure 1.7a). In all applications, the precision of estimates derived from the mixture model and conventional weighted means was similar, and was generally less than that of the conventional mean (Figure 1.7).

In most instances when there was covariance between total stomach content mass and diet fraction, the mixture model produced estimates that were similar to those of the conventional weighted mean (Figure 1.8). This was counter to our expectations that followed from our simulation study. In particular, we expected that estimates from the mixture model would be intermediate to the highly biased conventional mean, yet this expectation was true in only one of the four cases (Figure 1.8b). The lack of similarities between the simulation study and applications to actual data likely reflects the facts that there was greater variance in the real data, and the patterns of covariance between m_s and p_i were not as strong as those simulated.

1.4 DISCUSSION

The mixture model represents a beneficial new method to quantitatively estimate prey contributions to predator diets using stomach content data. It advances the statistical modeling of these data by providing a robust, likelihood-based method that can be applied to complex data. The model was applied here to fish stomach content data, though this method is broadly applicable to other data types as well. The accuracy and precision of the mixture model was

generally comparable to that of the conventional weighted mean approach. In most scenarios, the two methods performed similarly, and are both more accurate than using the simple average of individual diet fractions, as would be expected based on Ahlbeck et al. (2012). The mixture model performed particularly well compared to more conventional methods when there were a small number of very full stomachs in the sample set. Additionally, the mixture model does not require the user to make a decision on whether to weight stomachs by their stomach fullness or treat them as equally informative, which has traditionally been a challenge when working with stomach content data (Nielsen et al. 1983). While the model will produce biased estimates when there is a strong pattern of covariance between sample stomach mass and diet fraction, applications to real data did not indicate that this scenario was common.

The introduction of a likelihood framework into diet estimation methods greatly increases the range of uses for diet data. Analysis methods that include likelihood frameworks have been developed for count data (Fletcher et al. 2005, de Valpine and Harmon-Threatt 2013, Lynch et al. 2014), but this mixture model is explicitly created for proportional data. Formal model selection is standard in other areas such as regression (Hilborn and Mangel 1997, Burnham and Anderson 1998) and is typically done using AIC or likelihood ratio tests. Both of these can now be carried out for diet data with the mixture model framework. Additionally, the existence of a likelihood function provides the ability to use Bayesian methods (Gelman and Hill 2007), which permits various model extensions (e.g., including prior information based on stable isotope analysis or previous stomach content analysis). For instance, one possibility is extending the mixture model to develop a hierarchical model to account for lack of independence among samples. Individual stomachs captured in a single sampling event are frequently not independent samples (Nielsen et al. 1983). A hierarchical-based extension of our likelihood framework would

allow one to directly estimate the level of independence rather than making extreme assumptions (i.e., all samples in a collection event are wholly independent or dependent) (Gelman and Hill 2007).

When data includes stomachs with large stomach masses, analysts would typically choose between a conventional weighted mean or conventional mean by balancing benefits and costs of the two methods. As an example, consider the case of a single stomach that contains one large prey item whose mass represents a substantial fraction of the total sampled mass. Previously, in such a case, analysts have had to choose whether to pool samples (or equivalently use a conventional weighted mean), or to use a conventional sample mean (Nielsen et al. 1983). The former would clearly overstate the importance of that prey item, while the latter is known to impose a substantial bias (Ahlbeck et al. 2012). With the mixture model, the analyst does not need to make this choice, because the estimation procedure is highly robust to these events that often complicate stomach content analysis.

Simulation testing indicated potential bias of the mixture model when the relationship between stomach fullness and stomach contents was more nuanced than the model assumed. We also analyzed stomach contents for the four predator types in cases where the conditions for bias were most likely to occur. In three of these four cases, there was little evidence of bias in the mixture model. We did not observe the mixture model estimating a diet fraction intermediate to conventional mean and conventional weighted mean estimates. This implies that in many cases, the conditions that gave rise to bias in simulations may be uncommon in real datasets. A careful examination of diet data for covariance between p_i and m_s, and comparison of estimates from the mixture model to other methods, can reveal the potential for bias in the mixture model. An initial

examination of the diet data should, however, be part of any analysis (Hilborn and Mangel 1997, Burnham and Anderson 1998, Gelman and Hill 2007).

The model framework can also be adapted to minimize the potential bias caused by the model simplification of estimating two discrete stomach masses. The choice to have two distinct stomach content parameters for stomachs that do and do not contain prey type *i*, $m_s|\Phi$, when $p_i > 0$, and another stomach mass when the prey is absent, $m_s|\neg\Phi$, when $p_i = 0$, allows us to partially address the covariance between p_i and m_s. However, there is no constraint on the number of distinct prey mass distributions that can be assumed, and including more prey masses could remove much of this bias. For example, one could estimate a distinct conventional mean stomach mass for stomachs when $p_i = 1$, or divide the mass data into multiple cases based on the observed relationship between p_i and m_s. A continuous functional relationship between $E[m_s]$ and p_i could also be assumed to avoid making this assumption at all.

Most methods for estimating diet fractions only estimate the contribution of a single prey type to the predator's diet, rather than estimating the predator's entire diet composition simultaneously (Liao et al. 2001, Ahlbeck et al. 2012). If this is done for each prey type, the resulting estimates will not sum to precisely 1. A multivariate beta distribution, known as the Dirichlet distribution, could be used to estimate the diet fractions for all consumed prey types at once. In fact, this was the method employed by Ainsworth et al. (2010) to combine estimates from multiple data sources. However, the Dirichlet cannot be used to estimate diet contributions if any of the samples contain p_i=0 or p_i =1, *i.e*. each prey type needs to be present in each sample. Standard application of the Dirichlet also weights all samples identically regardless of stomach fullness.

The new model is an important step forward in quantitatively estimating predator diets and is also broadly applicable to other data types involving proportional data. There are, of course, limitations to diet data that are not addressed by our method. These include differential digestion (Baker et al. 2014), regurgitation during the sampling process, and small sample sizes that may not capture rare, but ecologically important, events. However, the mixture model opens the door to addressing other challenges of proportional stomach content data by providing a likelihood framework for diet fractions estimates, while generally providing accurate and precise estimates of diet fractions estimates.

Table 1.1 The parameters in the mixture model, along with their corresponding distributions and meanings.

Parameter	Distribution	Parameter Definition
c_i	-	Mean contribution of prey type i to a predator's diet
P_i	$\beta(\alpha_1,\alpha_2)$	Mean fraction of the predator's diet made up of prey type i
$M_s\|\Phi$	$\Gamma(k_{present}, 1/\theta_{present})$	Mean mass of stomachs containing prey type i
$M_s\|\neg\Phi$	$\Gamma(k_{absent},1/\theta_{absent})$	Mean mass of stomachs not containing prey type i
Φ	$Ber(r_\Phi)$	Frequency of occurrence of prey type i in samples
$\Phi_{pi=1}$	$Ber(r_{\Phi pi=1})$	Frequency a sample only contains prey type i given it contains prey type i
σ_Φ	-	Standard deviation of Φ
$\sigma_{\neg\Phi}$	-	Standard deviation of $\Phi_{pi=1}$
$\sigma_ß$	-	Standard deviation of P_i

Table 1.2 . True values used in sensitivity scenarios for parameters that were held constant.

Scenario	r_θ	$r_{\theta p=1}$	$m_s\|\theta$	$\sigma_{ms\|\theta}$	$\sigma_{ms\|\neg\theta}$	p_i	σ_p	c_i
Overdispersion	-	-	4	1	1	-	.1	.5
Extreme Events	0.5	0.5	4	1	1	0.5	0.1	-
Covariance Between p_i and m_s	0.5	0.5	-	0.1	0.1	0.5	0.4	0.5

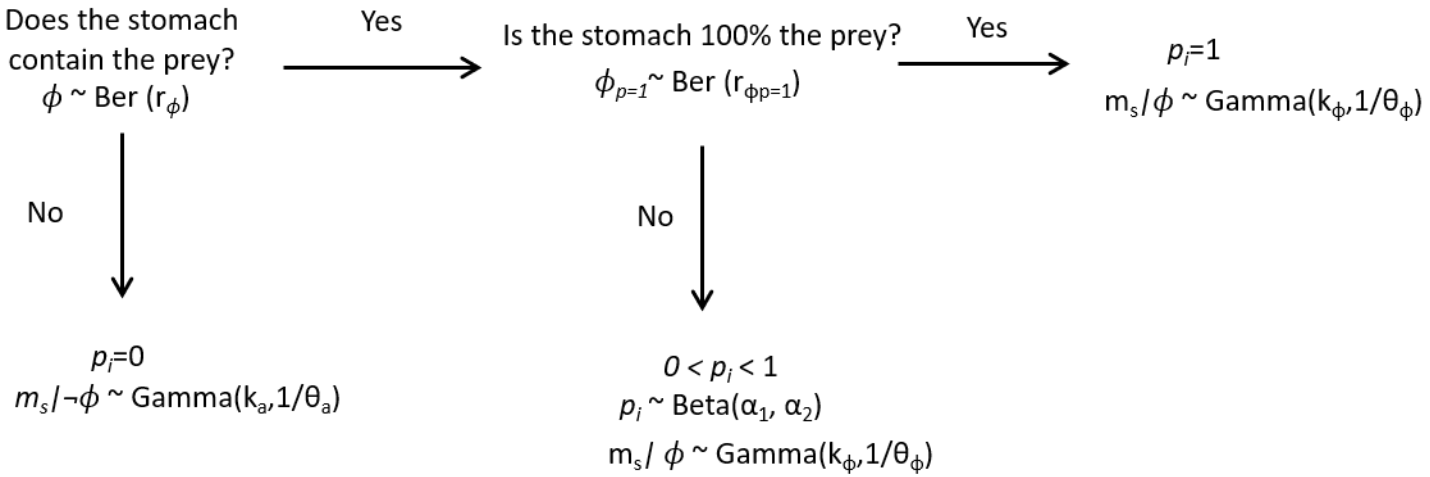

Figure 1.1 Conceptual flowchart of the mixture model, which splits stomachs into the three cases of $p_i = 0$, $0 < p_i < 1$ and $p_i = 1$. The parameters relevant to each case are shown along with the distributions used to estimate them in the mixture model.

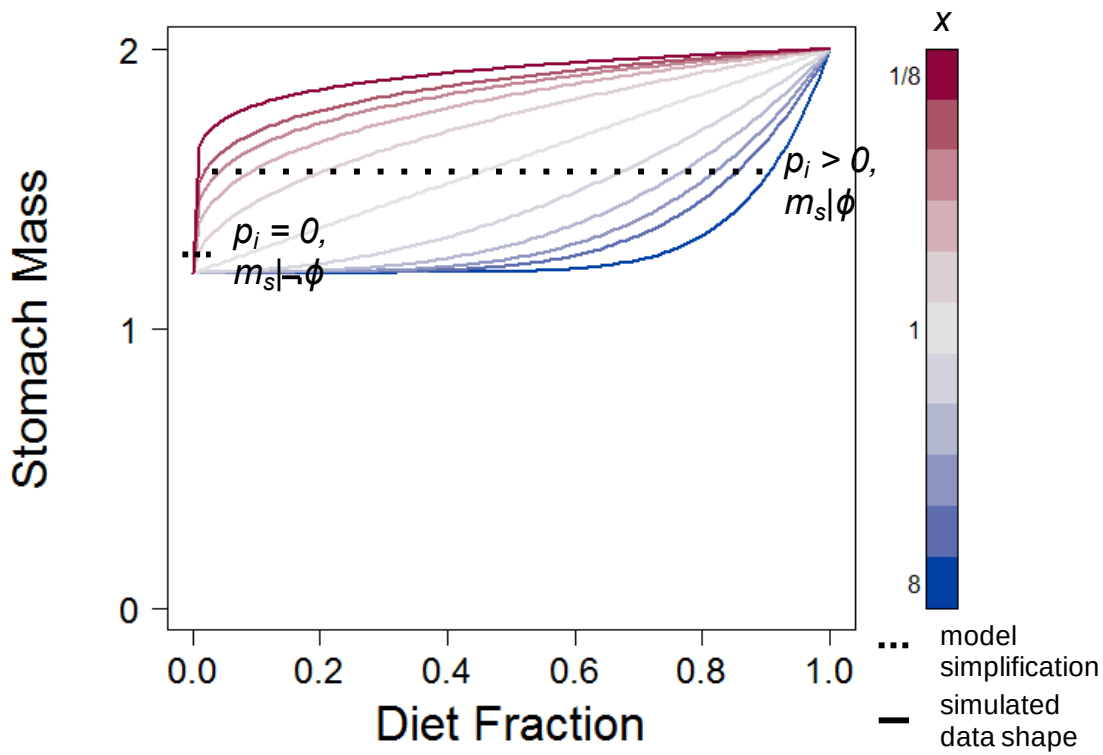

Figure 1.2 The continuous relationship between $E(M_s)$ and P_i, which can take a range of shapes, is simplified into a discrete relationship of presence / absence in the mixture model. During model testing, data with concave up, concave down and linear covariance between p_i and $m_s|\phi$ was generated with varying degrees of concavity to test the mixture model's robustness to this simplification. The degree of concavity was altered by varying the value of x in the power function, $E[M_{sj}] = E[M_{sj}|\neg\phi] + (max\ consumption - E[M_{sj}|\neg\phi]) * P_j^x$.

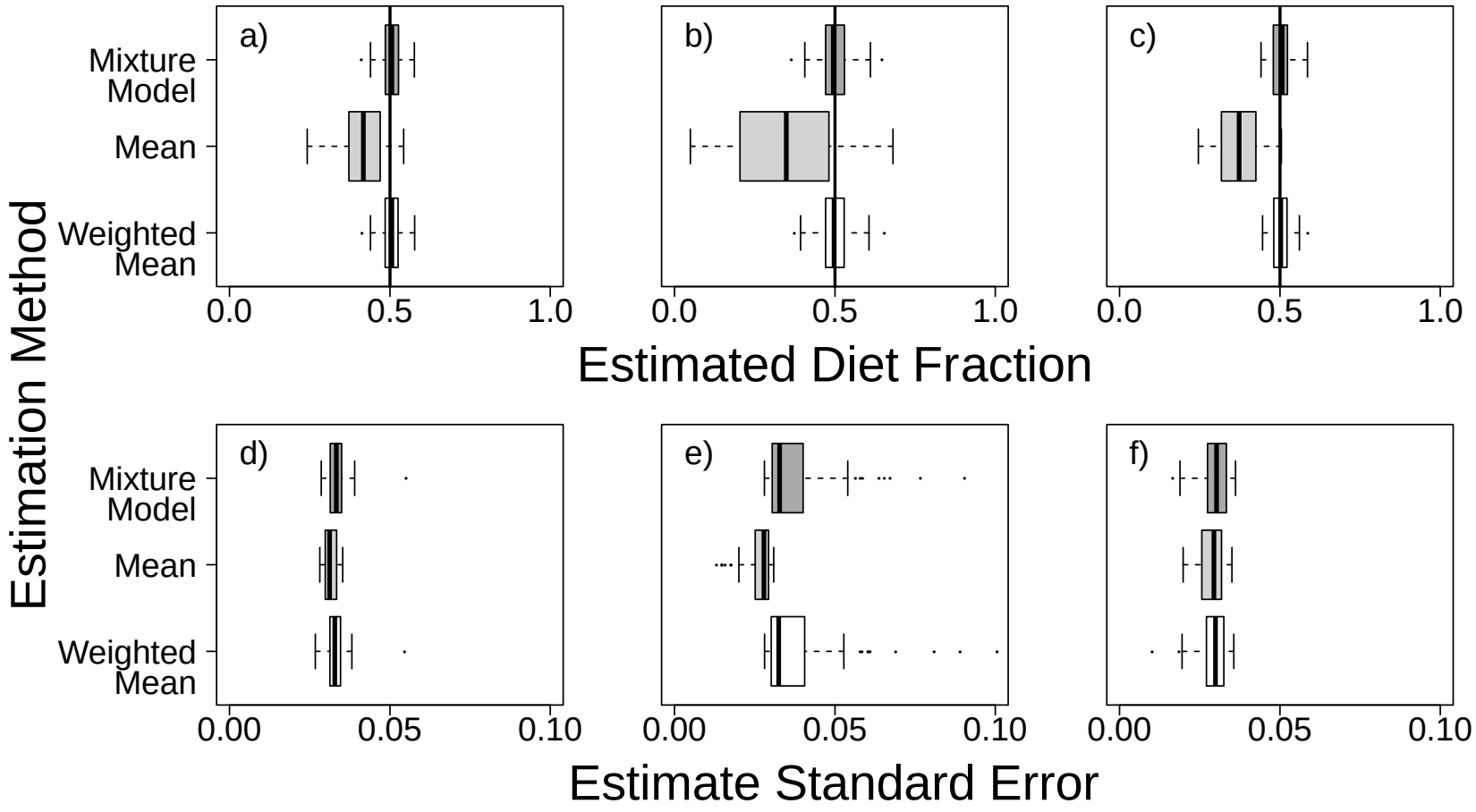

Figure 1.3 Effect of overdispersion in probability of prey occurrence (R_{Φ}; a, d), probability of only that prey occurring given it does occur ($R_{\Phi p=1}$; b,e), and diet fraction when the prey is present ($P_{.}$; c,f) on the accuracy (top) and standard error (bottom) of diet fraction estimates. Vertical line shows the true diet fraction. Results are based on 100 simulated data sets each consisting of 200 samples. Box plots indicate median, interquartile range (boxes) and 150% interquartile range (lines).

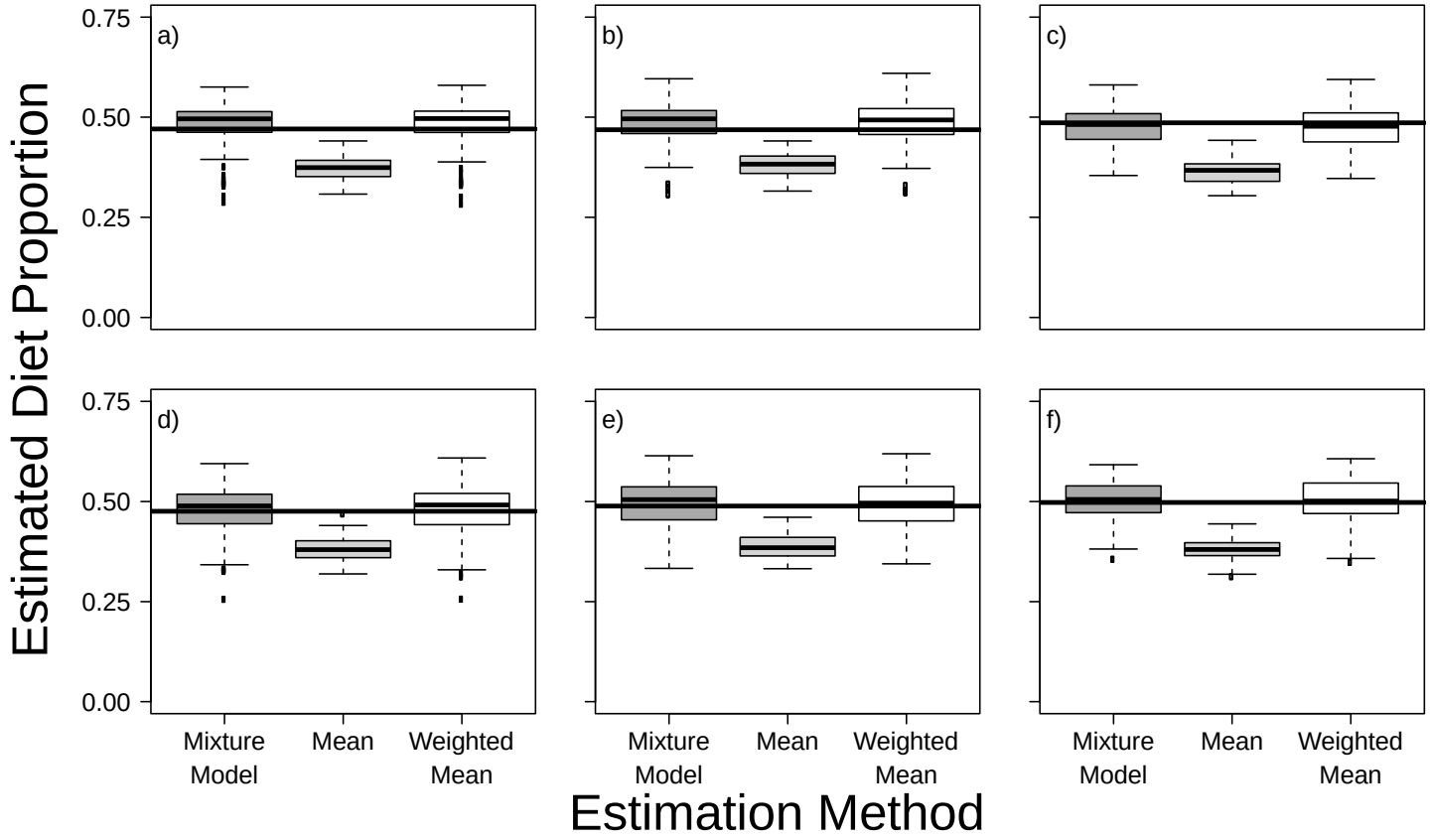

Figure 1.4 Effect of extreme events in stomach masses (e.g., a few very full stomachs) on the accuracy of diet fraction estimates across multiple values of stomach mass when the prey type is present, ((a-c) $M_s|\Phi = 20$, (d-f) $M_s|\Phi = 50$) and across multiple values of the probability of an extreme event occurring, ((a,d) P(extreme event) =0.01, (b,e) P(extreme event) =0.05, (c,f) P(extreme event) =0.1). Scenarios for P(extreme event) = 0.02, 0.2 were also explored and results were consistent with the plots shown here. Horizontal lines show the true value of c_i. Each box represents 100 simulated datasets of 200 stomachs. Box plots indicate median, interquartile range (boxes) and 150% interquartile range (lines).

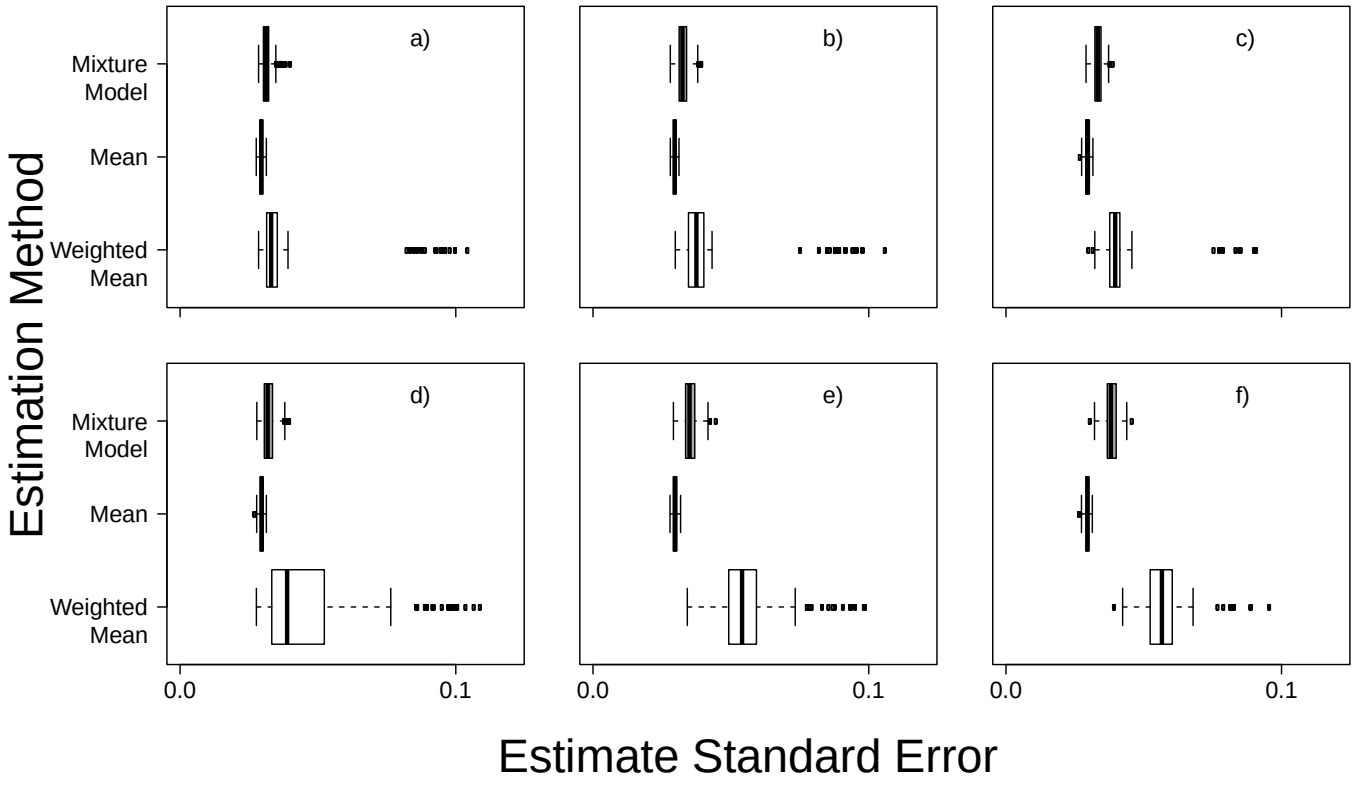

Figure 1.5 . Effect of extreme events in consumption consumption (e.g., a few very full stomachs) on the precision of diet fraction estimates across multiple values of stomach mass when the prey type occurs ((a-c) $M_s|\Phi = 20$, (d-f) $M_s|\Phi = 50$) and across multiple values of the probability of an extreme event occurring ((a,d) P(extreme event) = 0.01, (b,e) P(extreme event) = 0.05, (c,f) P(extreme event) = 0.1). Scenarios for P(extreme event) = 0.02, 0.2 were also explored and results were consistent with the plots shown here. Horizontal lines show the true value of c_i. Each box represents 100 simulated datasets of 200 stomachs. Box plots indicate median, interquartile range (boxes) and 150% interquartile range (lines).

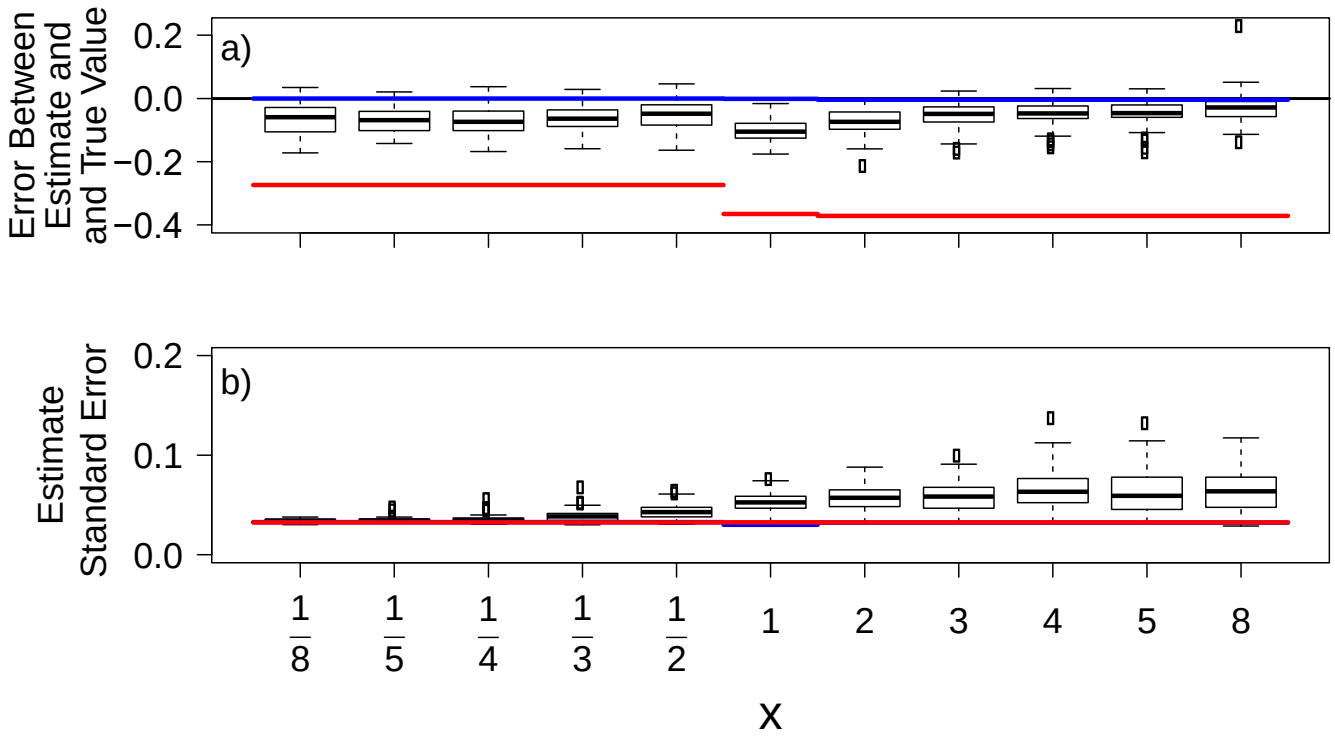

Figure 1.6 Effect of covariance between diet fraction Pi and total stomach contents' mass on the accuracy and precision of the mixture model, a convention mean (red line) and conventional weighted mean (blue line). Varying degrees of concavity in the data were created by using a power function, $E[M_{sj}] = E[M_{sj}|\neg\theta] + (max\ consumption - E[M_{sj}|\neg\theta]) * P_j^x$ and varying x. Each box represents 100 simulated datasets of 200 stomachs. Box plots indicate median, interquartile range (boxes) and 150% interquartile range (lines).

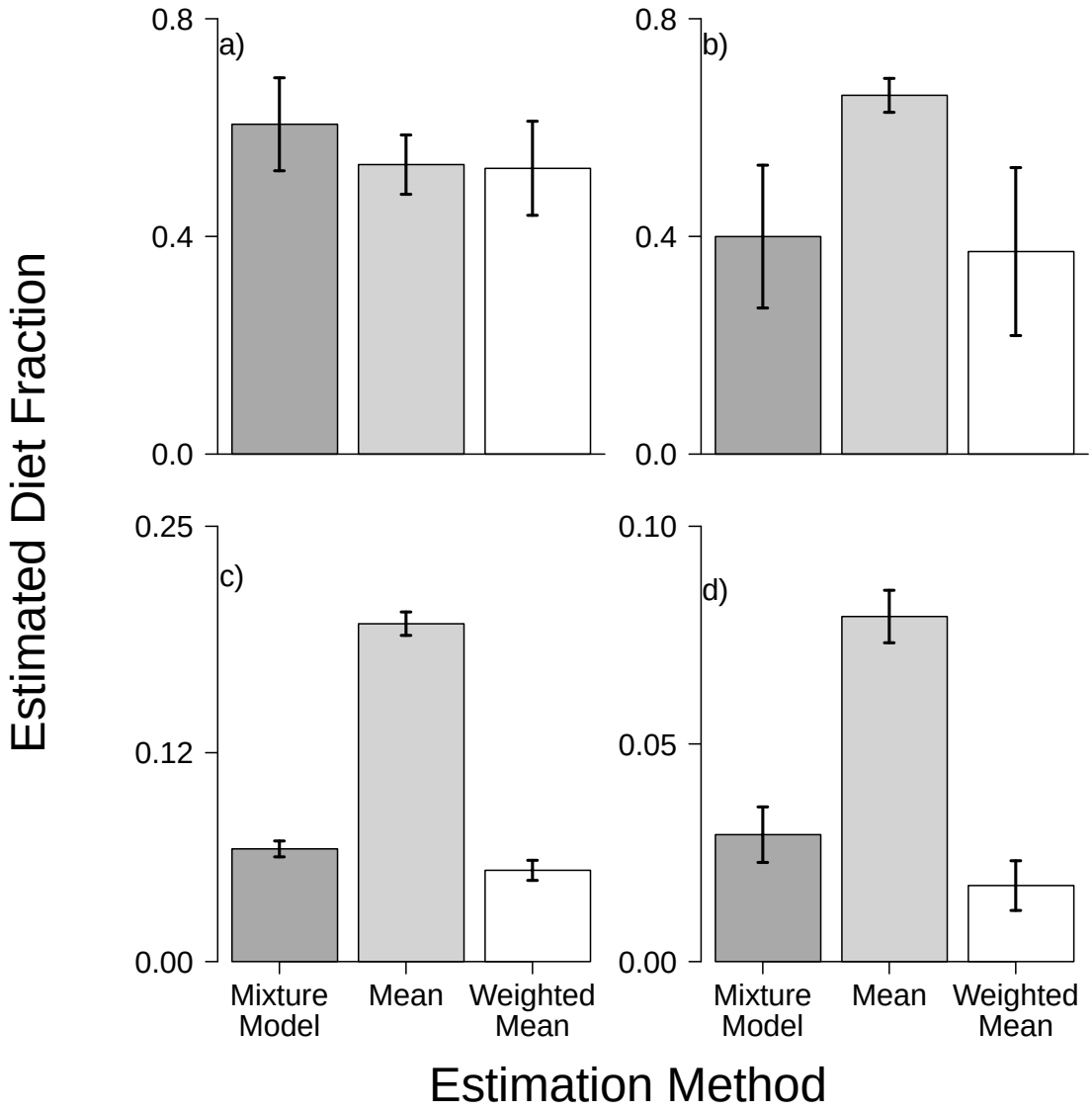

Figure 1.7 Estimates and standard error when the mixture model, a conventional mean, and conventional weighted mean are applied to a common prey type in diet datasets for four predators with varying life histories, a) Pacific herring, Clupea pallasii, b) English sole, Parophrys vetulus, c) lingcod, Ophiodon elongates, and d) spiny dogfish, Squalus acanthias. Error bars are standard error.

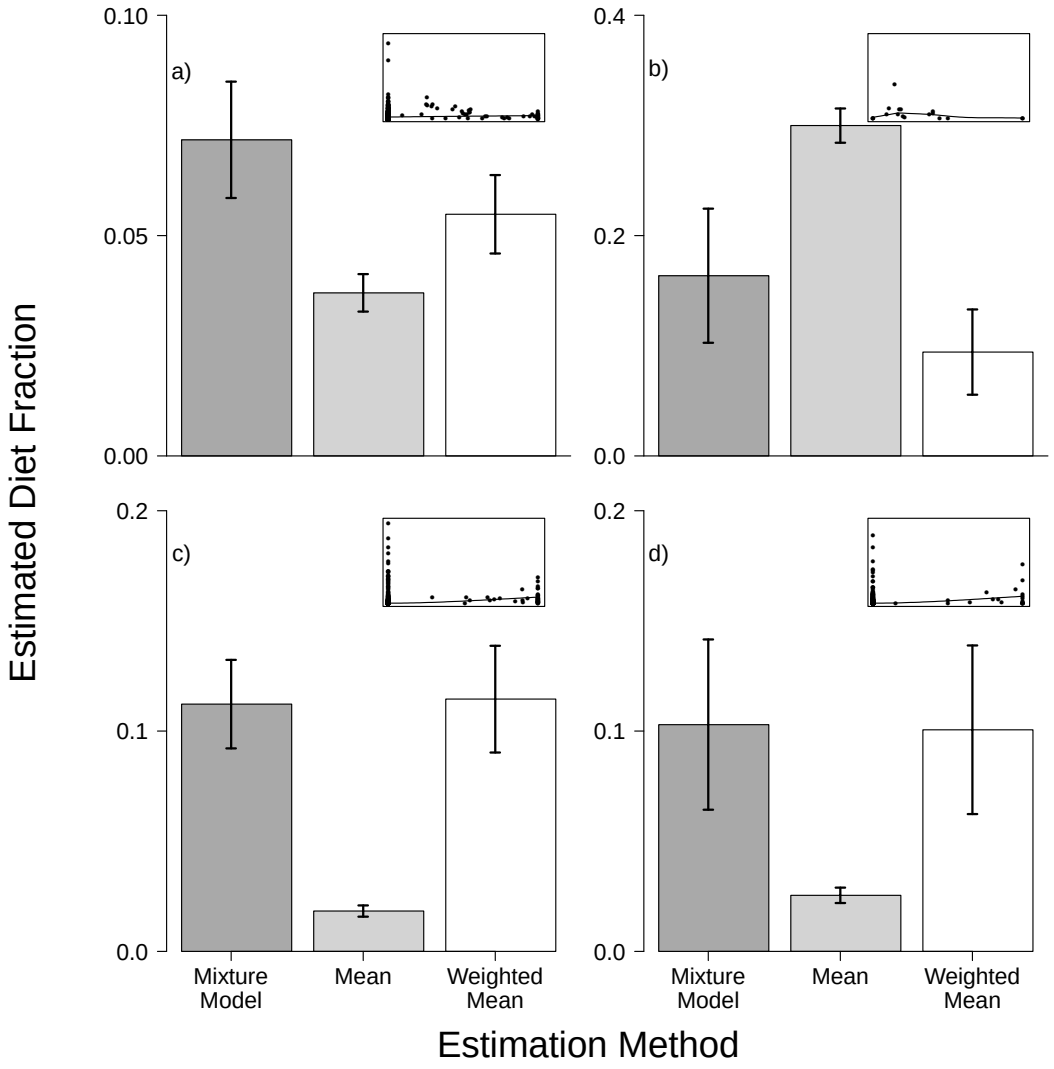

Figure 1.8 . Estimates and standard error when the mixture model, a conventional mean, and conventional weighted mean are applied to a prey type demonstrating correlation between stomach mass and diet fraction. All three methods are applied to diet datasets for four predators with varying life histories, a) herring consuming glass shrimp, b) English sole consuming amphipods, c) spiny dogfish consuming Pacific herring, and d) lingcod consuming great sculpin. Error bars are standard error. Insets are actual data with regression lines, plotted as total stomach contents' mass versus diet fraction.

APPENDIX A1

Table A1.1. Mean absolute error (MAE) when each parameter in the mixture model was varied over a range of values. The minimum and maximum MAE do not necessarily correspond to the minimum and maximum parameter values.

Parameter	Range	MAE Range
r_ϕ	0.1-0.9	0.021-0.089
$r_{op=1}$	0.1-0.9	0.024-0.034
$m_s\|\phi$	1.0-10	0.027-0.036
c_i	0.1-0.6	0.012-0.035
σ_ϕ	0.1-2	0.027-0.032
$\sigma_{\neg\phi}$	0.1-2	0.026-0.031
p	0.1-0.9	0.027-0.036
σ_p	0.01-0.4	0.026-0.030

2. A MULTI-LEVEL MODEL TO ESTIMATE DIET COMPOSITIONS WITH NON-INDEPENDENT SAMPLES

ABSTRACT

Practical constraints on field data collection often result in samples that are not statistically independent of each other due to opportunistic and/or bulk sampling. Stomach content data, which is ubiquitous throughout marine ecology, is particularly prone to this issue. Frequently, this non-independence is unaccounted for during analyses, causing resulting estimates to be unrealistically precise. A recently developed mixture model to analyze stomach content data provides a likelihood framework for diet estimates. We make use of this likelihood framework to extend the model by using random effects to estimate effective sample size and explore the resulting model's behavior by combining simulation analysis and applications to real data. The resulting random effects mixture model has comparable accuracy to previously existing analysis methods. Here, we only explored adding a single random effect to one parameter. Before extensive application, the behavior of the model with multiple levels of random effects and random effects on different parameters should be considered.

2.1. INTRODUCTION

Understanding ecological systems requires understanding interactions among taxa. These interactions are fundamental to food web ecology (Marshall 2007), behavioral ecology (e.g. Randall and Myers 2001, Catano et al. 2014), and predator-prey interactions (McCann et al.

1998). Studying these interactions among taxa requires methods to estimate what predators are feeding on and the variation in their feeding over time and space. Direct observation of predation events is frequently not possible; for that reason we often use stomach content analysis to draw inferences about predation after the event has occured. This is a common method to obtain predator diet information across taxa (e.g. Cortes 1997, Ashworth et al. 2014, Baker et al. 2014).

Stomach content data presents many analytical difficulties. One common challenge is the presence of extreme events where a few individuals consume far more than other individuals in the population (Ahlbeck et al. 2012). Other times, there may be covariance between what a predator eats and how much it eats (Hyslop 1980, Liao et al. 2001). That is, when a prey item is present it is likely to be consumed in high quantities. This frequently occurs for mobile predators in patchy environments. For instance, sea raven are less likely than other fish in the Northeast Atlantic to consume herring, but when they do, they consume a large quantity (Deroba 2018). Additionally, predator diets are composed of multiple items, whose proportions together must sum to one, which can present statistical challenges for estimation. Several of these issues were addressed by Moriarty et al. (2017), which allowed for both covariance and extreme events in consumption. However, this method only estimates a single prey type at a time, rather than the entire vector of prey diet proportions. Other recent models (Ainsworth et al. 2010, Coblentz et al. 2017) estimate the entire vector of prey diet proportions, but did not did not address these other features of stomach content data.

Another challenge is the frequent lack of statistical independence among stomach samples. Collection events often capture multiple individuals at once and then a stomach sample is collected from each individual (Cortes 1997). As these stomachs are collected from the same collection event, they cannot be considered independent samples. For instance, in aquatic studies,

many fish are commonly collected in the same place around the same time, such as by trawling, electrofishing, seining, etc. These individuals are not true random samples of the population, but by being in the same place at the same time, are more likely to have similar diets (Cortes 1997). As statistical methods generally assume samples are independent (e.g. Gelman and Hill 2007), this lack of independence in the data creates an extra challenge when working with stomach content data.

This interdependence among samples collected in the same collection event is not a problem unique to analyzing stomach content data, but arises throughout ecological data. A common solution is to estimate the effective sample size for each observation; several methods to do this have been proposed for fisheries catch data. For example, age composition data that are used in fisheries stock assessments (which are often large in number and non-independent) are weighted according to estimated effective sample size. This may be done by using sample importance resampling (McAllister and Ianelli 1997, Arni et al. 2013) or bootstrapping (Sondre and Pennington 2003, Stewart and Hamel 2014) to estimate effective sample size. Effective sample size has also been estimated using methods based on either non-linear least squares regression or profile maximum likelihood estimation (Candy 2008). However, none of these have been used with data from stomach contents.

Instead, there are a few ways that existing methods to analyze stomach content data handle this issue of lack of independence. A stratified subsampling scheme can be used, where one stomach from each collection event is randomly chosen. This ensures each sample included is independent, but requires dismissing data that were collected and the information contained in them. Alternatively, all samples from each collection event may be pooled, treating the entire collection event as a single datum (e.g. Tirasin and Jorgensen 1999). However, this ignores

variation amongst stomach samples (Gelman and Hill 2007) and therefore also risks losing information.

A straightforward approach for stomach content data would be to use a hierarchical model, which can directly account for sample inter-dependence, while including all samples in the model. Hierarchical models partition variation by collection event, so the data determines how many independent samples there are (Gelman 2004, Gelman and Hill 2007). This multi-level, or hierarchical, modeling approach requires a likelihood function, which was recently developed for stomach content data by Moriarty et al. (2017). Here, we extend that model to incorporate sample interdependence. We aim to estimate the contribution of prey to a predator's diet, while using a multilevel model to allow for more realistic estimates of precision.

2.2. METHODS

We extend the model described in Moriarty et al. (2017) to address sample interdependence. Moriarty et al. (2017) presented a mixture model based on the concept that diet fraction, defined as the mean proportional contribution of a single prey type, *i*, to a predator's diet, C_i, is equal to the ratio of the expected mass of prey type *i* in the stomachs divided by the expected total mass of the stomachs' contents,

$$E[C_i] = \frac{E[M_i]}{E[M_S]}.$$

This mixture model classifies stomachs into three categories: 1) those that did not contain prey type *i*, 2) those that only contain prey type *i*, and 3) those that contain both prey type *i* and other prey types (Figure 1). The resulting model is a mixture model that acts comparably to a weighted mean, while creating a likelihood framework for the contribution of the prey type to the

predator's diet. Within this, we let the proportion of a stomach that is prey type *i*, P_i, be dependent on M_s. This results in the full model equation,

$$E[C_i] = \frac{\int_0^1 \int_{\mathbb{R}_*^+}^{\infty} g(P_i, M_s) P_i M_s f(M_s)\, dM_s\, dP_i}{\int_{\mathbb{R}_*^+}^{\infty} M_s\, f(M_s)\, dM_s},$$

We estimate two different total stomach contents masses, M_{sa} is the stomach mass of predators who did not eat prey type *i* and M_{sp} is the stomach mass of predators who did eat prey type *i* (Table 2.1), to allow covariance between what a predator eats and how much it eats. This allows for the possibility that a predator has a higher consumption rate when feeding on a particular prey type. This, along with some additional math detailed in Moriarty et al. (2017), leads to the expression for population level diet fraction:

$$E[C_i] = \frac{\left(r_\Phi\left(1-r_{\Phi p_i=1}\right)E\left(P_i\middle|\Phi, 1-\Phi_{p_i=1}\right)+ r_\Phi r_{\Phi p_i=1}\right)E(M_s|\Phi)}{r_\Phi E(M_s|\Phi)+(1-r_\Phi)E(M_s|1-\Phi)}.$$

The parameters on the right-hand side are estimated based on a series of likelihood functions expressed as three components: when diet samples lack the prey type ($p_{ij} = 0$), when diet samples contain they prey type plus other prey types ($0 < p_{ij} < 1$), and when diet samples contain only the prey ($p_{ij} = 1$):

$$L = \prod_j \begin{cases} \frac{1}{\Gamma(k_a)\theta^{k_a}} p_{ij}^{k_a-1} e^{-\frac{p_{ij}}{\theta_a}} * (1-r_\Phi), & p_{ij} = 0 \\ \frac{1}{\Gamma(k_\Phi)\theta^{k_\Phi}} p_{ij}^{k_\Phi-1} e^{-\frac{p_{ij}}{\theta_\Phi}} * r_\Phi * r_{\Phi p=1} * \frac{p_{ij}^{\alpha_1-1}(1-p_{ij})^{\alpha_2-1}}{Beta(a_1,\alpha_2)}, & 0 < p_{ij} < 1 \\ \frac{1}{\Gamma(k_\Phi)\theta^{k_\Phi}} p_{ij}^{k_\Phi-1} e^{-\frac{p_{ij}}{\theta_\Phi}} * r_\Phi * r_{\Phi p=1}, & p_{ij} = 1 \end{cases}.$$

The probability of prey type *i* occurring and the probability of only prey type *i* occurring given that prey type *i* has occurred are each estimated using a Bernoulli probability density function, Φ

$\sim Ber(r_{\Phi})$, where Φ indicates the presence of prey type *i* and $\Phi_{pi=1} \sim Ber(r_{\Phi pi=1})$, where $\Phi_{pi=1}$ indicates only the presence of prey type *i* given prey type *i* has occurred. We model the probability density of diet fractions, $g(P_i)$, as a beta distribution, $P_i \sim Beta(\alpha_1, \alpha_2)$. The probability densities of the total stomach contents masses for those containing prey type *i*, $f(M_s|\Phi)$, and those not containing prey type i, $f(M_s|\neg\Phi)$ are modelled using a gamma distribution, so $M_s|\Phi \sim Gamma(k_{\Phi}, 1/\theta_{\Phi})$, with $E[M_{s\Phi}] = k_{\Phi}\theta_{\Phi}$ and $M_s|\neg\Phi \sim Gamma(k_a, 1/\theta_a)$, so $E[M_{sa}] = k_a\theta_a$. For more detailed reasons on choosing these distributions, see Moriarty et al. (2017).

To address the issue of sample interdependence, we add random effects to this mixture model. Random effects presume that the parameter(s) they're applied to varies among sample groups (e.g. vary between collection events or sites), while constraining those group estimates to share a common distribution. We include a single level of random effects here, but potentially any number, nested or not, could be included to model parameter variability by collection event, location, season, etc. The main benefit is that adding random effects avoids assuming sample independence, while also avoiding subsampling, so that we can retain all our data for use. Unfortunately, this additional layer of model complexity results in a model with the need for more complex integration methods. As a result, we move to a Bayesian framework due to integration methods being better developed than for maximum likelihood estimation.

We added random effects by presuming that the probability that a stomach contains prey type *i*, r_{Φ} , varies among collection events. Ecologically, this represents a case when predators in certain collection events are more likely to have consumed prey type *i* than predators in other collection events. The occurrence of prey type *i* in a sample in the k^{th} collection event is a Bernoulli random variable, Φ, drawn with probability r_{Φ_k},

$$\Phi \sim Ber(r_{\Phi_k}).$$

The *k* probabilities are drawn from a common distribution. Here, we use a beta distribution,

$$r_{\Phi_k} \sim \beta(\alpha_{\Phi 1}, \alpha_{\Phi 2}).$$

The beta distribution is a natural choice for random variables that are bounded from 0 to 1. Both $\alpha_{\Phi 1}$ and $\alpha_{\Phi 1}$ are estimated parameters, with weakly informative priors, $\alpha_{\Phi} \sim half - normal(0, 10)$. The probability that a stomach only contained prey type *i* given it contained prey type *i* used a uniform prior with nearly all proportions equally likely *a priori*, $r_{\Phi p1} \sim Beta(1, 1)$. Parameters for estimation of stomach mass, M_{sp}, σ_p, used improper uniform priors calculated by Stan. The multipliers, M_{mult} and σ_{mult} had standard normal priors.

To move to a Bayesian framework, we reparameterized certain model elements to improve performance of numerical intergration routines. The gamma function contains two parameters that must be estimated, that together give the mean and variance of the distribution. We directly estimated the mean and variance for this distribution (i.e., $E[M_s|\ \Phi]$, $Var[M_s|\ \Phi]$), rather than the distribution parameters (i.e., k_{Φ}, $1/\theta_{\Phi}$). Parameterizing this distribution in terms of the mean and variance is more interpretable than shape and scale parameters, but also provides the ability to use an informed prior for the mean and variance of stomach masses if relevant information is known from other studies. Additionally, we used a reparameterization to estimate M_{sa} and σ_a, such that $M_{sa} = M_{mult} * M_{sp}$ and $\sigma_a = \sigma_{mult} * \sigma_p$. Reparameterization can often effectively aid in model convergence (Stan Development Team 2017b).

2.2.1. Model Testing

We tested this Bayesian mixture model via simulation analysis. We generated data with known parameters and specific properties from an operating model, fit our Bayesian mixture

model to these data, and compared the true and estimated values. For each simulation test, we compared the estimated values across three approaches: 1) the random effects model, 2) assuming all samples were completely independent and applying the non-hierarchical model, 3) subsampling one stomach per trawl and applying the non-hierarchical model. We performed several simulation tests to test the model under specific conditions.

Base Operating Model

The base operating model is similar to that described in Moriarty et al. (2017), but modified slightly to generate hierarchical data. The probability of prey occurrence is variable between sampling groups, such that for *k* sampling groups the probability of prey being present is $r_{\Phi_k} \sim \beta(\alpha_1, \alpha_2)$. For stomachs with $p_{ij}>0$, we then assigned $p_{ij}=1$ with probability $r_{\Phi p=1,}$ which did not vary by collection event. When the prey was absent, stomach masses were drawn from a gamma distribution, $m_{sj}|\neg\Phi \sim Gamma(k_a,\theta_a)$. For stomachs for which the prey type was present then stomach mass was calculated from $m_{sj} \sim Gamma(k_\phi, \theta_\phi)$. The diet fraction was drawn from a beta distribution, $p_{ij} \sim \beta(\alpha_1, \alpha_2)\ if\ p_{ij} \neq 1$, or if it was the only prey type present, then was assigned $p_{ij} = 1$.

For each testing scenario, we compared the mean and variance of $\widehat{c_i}$, the prey contribution, estimated by the random effects model to those estimated using the non-hierarchical Bayesian models. We used two non-hierarchical methods: assuming complete independence and subsampling the data. We generated 100 data sets, each containing 20 collection events, wherein each collection event contained 10 to 200 stomachs, parameter values are listed in Table 2.2. The number of stomachs per event was chosen randomly for each event using the 'sample' function in base R. All parameter estimation was run in Stan (Stan

Development Team 2017b) with the NUTS algorithm (Homan and Gelman 2014, Carpenter et al. 2017, Stan Development Team 2017b) using rstan v2.15.1 (Stan Development Team 2017a) in R v 3.4.0 (R Core Team 2017). For each iteration of the model, we ran 3 chains with 3,000 iterations after a warm-up period of 1,500 iterations. Chains were not thinned. Model outputs were checked to ensure there were no divergent transitions and that the scale reduction, $\hat{R}$, was $0.95 < \hat{R} < 1.05$ (Gelman and Rubin 1992). Chains and posterior distribution plots of a random subset of iterations were visually inspected for convergence.

Mean Absolute Error

Our first test was to determine whether the prey contribution to the predator could be reliably estimated when all of the model assumptions were true. For this, we generated data directly from the base operating model, so that random effects were drawn from a beta distribution, $r_{\Phi_k} \sim Beta(\mu_\Phi,\ \sigma_\Phi)$, and estimated c_i with the model we developed. This simulated a simple scenario where the hierarchical Bayesian mixture model should perform well. We then estimated all model parameters using the Bayesian mixture model. We calculated the mean absolute error (MAE) for $\hat{c}_i$ as,

$$MAE = \frac{1}{N}\sum_{i=1}^{N}|estimated - true|.$$

Overdispersion in frequency of occurrence.

The next step was to determine the model's robustness under higher amounts of overdispersion in r_{Φ_k}. For this, we wanted to simulate data where $r_{\Phi_k} \sim t(1)$. This simulates a scenario where r_{Φ_k}'s have a wide distribution. To ensure $r_{\Phi_k} > 0$, we applied a logit

transformation and drew $logit(r_{\Phi_k}) \sim t(1,\ logit(\overline{r_\Phi}))$ where $\overline{r_\Phi}$ is the mean of the random effects distribution.

Bimodal distribution in frequency of occurrence

Our model presumes a single probability density function can describe the fraction of samples stomachs that contain the prey item, but it is possible that there could be two or more different generating functions. Therefore, our final test determined the model's robustness when r_{Φ_k}'s were distributed bimodally. That is, mean probability of prey occurrence was either very high or very low,

$$r_{\Phi_k} = \begin{cases} r_{\Phi_{k1}} \sim Beta(\mu_{\Phi 1}, \sigma_{\Phi 1}) \\ r_{\Phi_{k2}} \sim Beta(\mu_{\Phi 2}, \sigma_{\Phi 2}) \end{cases}.$$

The number of collection events falling under each mean probability was chosen randomly, such that $n_{r_{\Phi k1}} \sim Bin(n_{groups},\ 0.5)$, where n_{groups} is the number of collection events. Then, $n_{r_{\Phi k2}} = ngroups - n_{r_{\Phi k1}}$.

2.2.2. Applications

We applied the Bayesian mixture model to a hierarchical dataset of spiny dogfish stomach contents data. The data was procured from the Northeast Fisheries Science Center Food Web Dynamics Program (Link and Almeida 2000). The dogfish were captured in bottom trawl surveys in the Northwest Atlantic, ranging from North Carolina, USA to Nova Scotia, Canada between 1977 and 2010. Individual dogfish captured in the same trawl were considered to be part of the same collection event. The dataset did not include a trawl identification, so trawls were determined to be the same trawl if their beginning latitude and longitude matched and they were

performed the same day. The dataset included stomach content information on over 20,000 dogfish stomachs.

We analyzed the diet contribution of Atlantic herring, *Clupea harengus*, to the spiny dogfish. For simplicity in this example application, we subset the trawls that contained all three cases (e.g. the trawl had dogfish stomach samples that only contained Atlantic herring, dogfish stomach samples that did not contain Atlantic herring, and dogfish stomach samples that contained Atlantic herring along with other prey). This resulted in 424 individual spiny dogfish stomachs that spanned 24 separate trawls.

2.3. RESULTS

2.3.1. Model Testing

Our Bayesian mixture model performed equally well under all three simulated scenarios (Figure 2.2). For all three estimation models, the average accuracy across many simulations was correct. However, the mean absolute error, a measure of likely accuracy of any individual application, varies across the estimation methods (Table 2.3). The random effects model consistently had the lowest MAE, while the subsampling method's MAE was up to six times higher.

As expected, the prey contribution estimates were less precise (higher standard error of $\hat{c}_i$) when we used the random effects model compared to the extreme case of assuming all samples were independent, but more precise than subsampling a single sample from each collection event. This indicates that the method is correctly assigning an intermediate level of precision that is being informed by the sample sizes and the extent of interdependence from samples in the same collection event.

2.3.2. Applications

All three estimation methods, 1) the Bayesian mixture model with random effects, 2) assuming complete independence of stomachs caught in the same collection event, and 3) subsampling one stomach per collection event, led to comparable estimates of the contribution of Atlantic herring to spiny dogfish (Figure 2.3). As expected, standard deviation of subsampling was larger than for the first two methods due to the smaller sample size. The error estimates were the same for the independence and random effects model due to the small sample size of dogfish within each trawl, suggesting in these cases there may not be much benefit to using the random effects model. Estimates of the probability that an individual consumed Atlantic herring, r_{Φ_k}, were estimated to be, $r_{\Phi_k} \sim Beta(10.3, 10.9)$, which has a mean of 0.485 and standard deviation of .01.

2.4. DISCUSSION

The addition of random effects to our earlier model is an effective approach to address the common challenge of sample independence in diet data. By avoiding data subsampling (and using one stomach per collection event) or ignoring the issue and treating all stomachs as independent, we produce accurate estimates of prey contributions to the predator's diet without overestimating precision. In the example application here, the variance of probability of prey occurrence among collection events was small, so the addition of the random effect had a minimal effect on the precision of $\hat{c}_i$. By adding random effects as an extension to the Moriarty et al. mixture model we also preserve the benefits that the base model provides. Namely, the resulting mixed effects mixture model still addresses the challenge of covariance between what a

predator eats and how much it eats and the occurrence of outliers in consumption amount (Moriarty et al. 2017), while taking advantage of the likelihood framework to address sample interdependence. Both of these features were present in the dogfish-herring data.

Here we explored the effect of adding random effects to the probability of a predator consuming the prey type (r_{Φ_k}). However, random effects could be added to any parameter(s) in the model. The choice of which parameters to apply random effects to is context dependent depending on the model goal and knowledge about the data's structure (Gelman and Hill 2007). For instance, in our application to spiny dogfish we were able to determine which dogfish were captured simultaneously and that multiple trawls were not performed sequentially at the same site. As a result of this knowledge, considering an individual trawl as a collection event was a logical choice. Other times, multiple trawls may be performed at the same site, in which case it may be a better choice to consider each site as a grouping variable. It is also necessary to consider the ecological interpretation of the choice(s) of where to add random effects in the model. By adding a random effect to the probability of prey occurrence, our model assumes that the probability of prey consumption varied among trawls that were performed at different times and/or places. Instead treating each site as a collection event creates the assumption that all trawls at the same site have the same probability of prey type consumption, regardless of when the trawls were performed. As each time a random effect is added to a parameter, the total number of parameters increases by the number of collection events, it is necessary to consider and carefully choose which parameter(s) and data levels do require a random effect and not blindly add them to many parameters throughout the model.

Another recent attempt to use random effects for quantitative diet analysis also found it to be an effective method for allowing for variation in diets among sites when analyzing diet

specialization (Coblentz et al. 2017). Coblentz et al. employed a similar hierarchical Bayesian approach to ours for analyzing diet specialization. Their use of random effects also allowed for quantifying variation among collection events.

The use of this mixture model with random effects is a promising method to quantitatively analyze stomach content data. As we only present an initial analysis of how random effects affect model behavior, additional exploration of the use of random effects in this mixture model is warranted before extensive application. Yet, combining this mixture model with random effects appears to be a promising method to quantitatively analyze stomach content data.

Table 2.1 The parameters in the mixture model, along with their corresponding distributions and meanings.

Parameter	Distribution	Parameter Definition
c_i	-	Mean contribution of prey type i to a predator's diet
P_i	$\beta(\alpha_1,\alpha_2)$	Mean fraction of the predator's diet made up of prey type i
$M_s\|\Phi$	$\Gamma(k_{present}, 1/\theta_{present})$	Mean mass of stomachs containing prey type i
$M_s\|\neg\Phi$	$\Gamma(k_{absent},1/\theta_{absent})$	Mean mass of stomachs not containing prey type i
Φ_k	$Ber(r_{\Phi k})$	Frequency of occurrence of prey type i in samples from group k
$\Phi_{pi=1}$	$Ber(r_{\Phi pi=1})$	Frequency a sample only contains prey type i given it contains prey type i
σ_Φ	-	Standard deviation of Φ
$\sigma_{\neg\Phi}$	-	Standard deviation of $\Phi_{pi=1}$
$\sigma_ß$	-	Standard deviation of P_i

Table 2.2 True values used in sensitivity scenarios for parameters that were held constant.

Scenario	r_θ	$\sigma_{r\theta}$	$r_{\theta p=1}$	$m_s\|\theta$	$\sigma_{ms\|\theta}$	$\sigma_{ms\|\neg\theta}$	p_i	σ_p	c_i
Beta	0.6	0.2	0.5	1	0.2	0.2	0.6	0.1	0.4
t	0.6	0.2	0.5	1	0.2	0.2	0.6	0.1	0.4
Bimodal	0.8, 0.3	0.05, 0.05	0.5	1	0.2	0.1	0.6	0.1	0.4

Table 2.3 Mean absolute error for each estimation method in each simulation scenario.

Simulation Scenario	Estimation Model	MAE
Beta	Random Effects	0.012
	Independent	0.021
	Subsampling	0.070
t	Random Effects	0.033
	Independent	0.036
	Subsampling	0.072
Bimodal	Random Effects	0.012
	Independent	0.022
	Subsampling	0.070

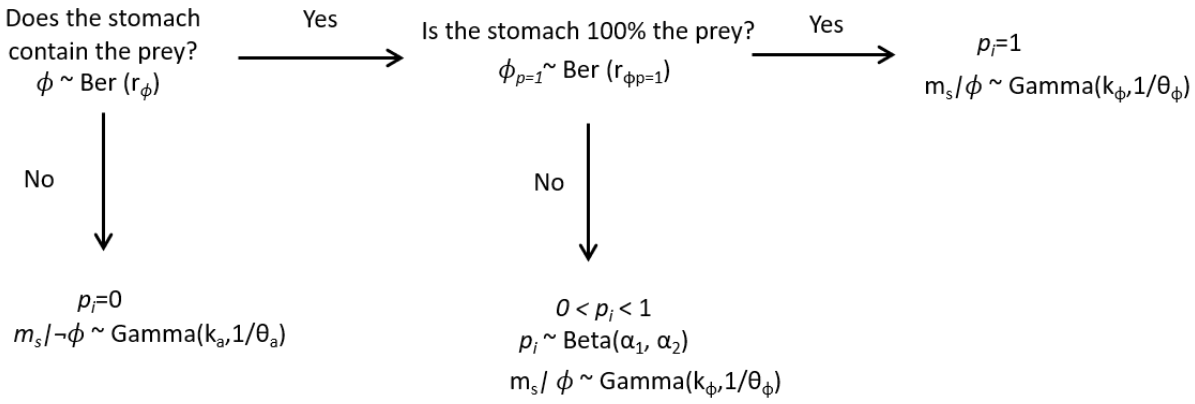

Figure 2.1 Conceptual flowchart of the fixed effects mixture model, which splits stomachs into the three cases of $p_i = 0$, $0 < p_i < 1$ and $p_i = 1$. The parameters relevant to each case are shown along with the distributions used to estimate them in the mixture model. Figure from Moriarty et al. (2017).

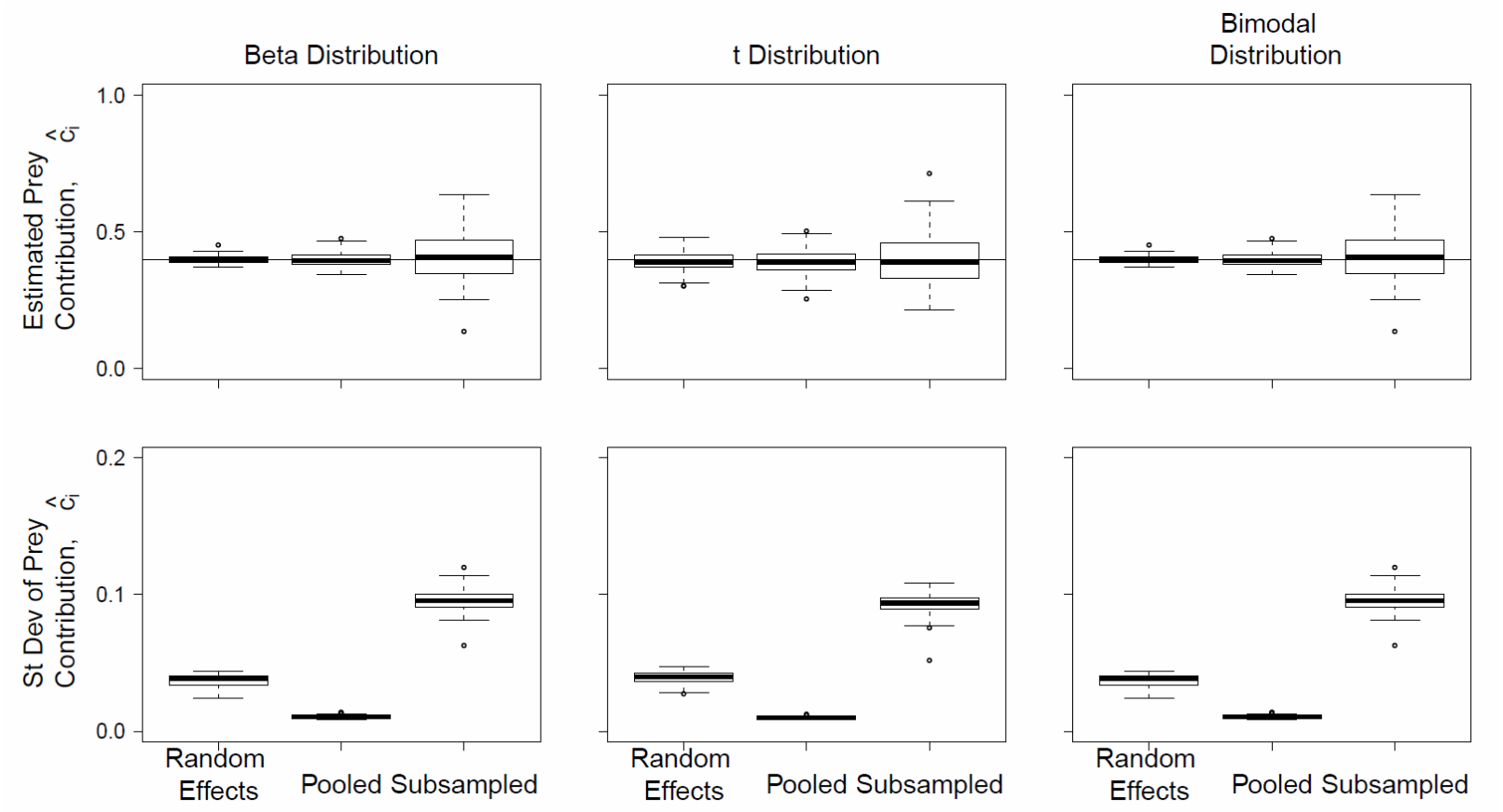

Figure 2.2 Prey contribution estimates and standard deviation under three simulation testing scenarios, 1) simulating r_{θ_k} from a beta distribution, 2) simulating r_{θ_k} from a student's t distribution, and 3) simulating r_{θ_k} from a bimodal normal distribution. Simulated data for each scenario was estimating under 3 models, 1) the random effects Bayesian mixture model, 2) the non-hierarchical Bayesian mixture model with pooling all data, and 3) the non-hierarchical Bayesian mixture model with subsampling one stomach per sampling group.

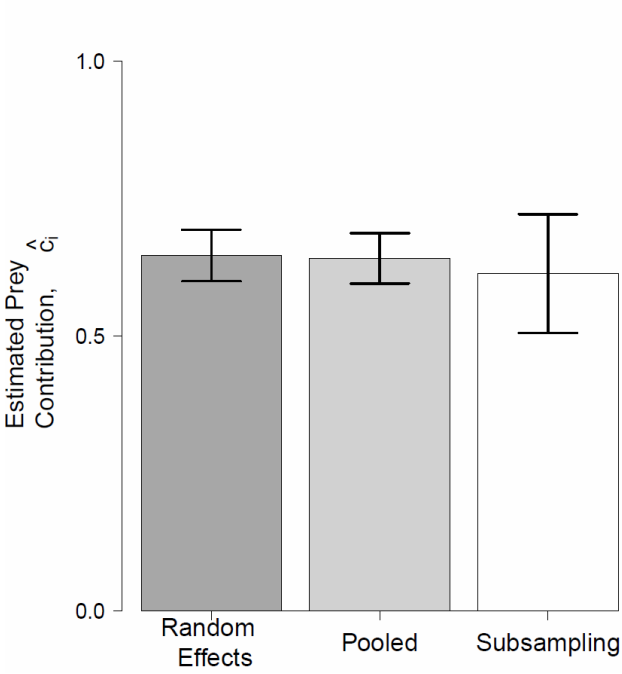

Figure 2.3 The estimated contribution of Atlantic herring to spiny dogfish under three models, 1) Bayesian mixture model with random effects, 2) treating each stomach as an independent sample, and 3) subsampling one stomach per sampling event. Error bars are standard deviation.

3. CHALLENGES AND OPPORTUNITIES FOR APPLYING STABLE ISOTOPE ANALYSIS TO JELLYFISH FOOD WEB ECOLOGY

ABSTRACT

As interest in the ecological role of jellyfish (class: Scyphozoa) has grown, an increasing number of studies have sought to determine their structural and functional roles in food webs. Stable isotope analysis is often used to obtain information about dietary sources. However, most of these studies have used assumptions and methodology developed for teleost fish, ignoring the unique body composition and physiology of jellyfish. Limited studies addressing the use of jellyfish stable isotope ratios have generally found unexpected effects of methodology on isotope ratios and unusual fractionation rates, though reasons for these unexpected effects remain unresolved. Here, we link the underlying mechanisms that cause fractionation to the unique physiology of jellyfish and to these unusual stable isotope results. We also consider what the unusual stable isotope methodology results imply about less-known aspects of jellyfish physiology. The path towards accurate application and interpretation of stable isotopes to jellyfish requires a lengthy array of studies to understand the mechanisms driving fractionation in this taxa. We propose that the quickest path forward requires the use of compound specific isotope analysis of amino acids in controlled laboratory studies, along with standardized sample handling methodology. Obtaining a clear understanding of fractionation in jellyfish, however, will require a more nuanced view of their unique body composition and physiology, whose effects need to be determined through a longer series of controlled experiments.

3.1. INTRODUCTION

Interest in the ecological role of jellyfish (class: Scyphozoa) has grown over the last decade. Jellyfish are now recognized to be important in food webs by moving energy into microbial pathways (Condon et al. 2011), by competing with commercially and culturally important fish for prey (Ruzicka et al. 2016), and serving as an important prey source for higher trophic levels (Thiebot et al. , McClellan et al. 2010, Heaslip et al. 2012). Additionally, they may be useful negative indicators of the health of an ecosystem (Samhouri et al. 2009).

Stable isotope analysis is a commonly used technique to characterize trophic interactions, and the implications of these interactions for competition, population dynamics, and habitat use. Such analyses have proven to be particularly useful in aquatic systems, where direct observation of feeding is typically infeasible. For many organisms, stomach content analysis is a simple way to determine predator diets, but jellyfish's tendency to regurgitate their stomach contents when handled makes this technique challenging (Jennifer Purcell pers. comm.). As a result, stable isotope analysis has been used to infer feeding of jellyfish (D'Ambra et al. 2013), measure their isotopic niche in comparison to fish (RM et al. 2015) and estimate their predation on commercially important fish (Brodeur et al. 2002). While promising, applications of stable isotopes to better understand jellyfish predation on and competition with other organisms depends on accurate information on how jellyfish accumulate and alter stable isotope composition, how stable isotope ratios vary among tissues, and how collection methods might alter stable isotopic ratios.

Accurate comparisons among taxa necessitate standardized stable isotope methodology. In aquatic systems, stable isotope analysis has most frequently been applied to fish and crustaceous zooplankton. This widespread use of stable isotopes for fish and crustaceous zooplankton has led to multiple attempts to standardize methodology for these taxonomic groups

(Post 2002, Vanderklift and Ponsard 2003, Boecklen et al. 2011, Hopkins and Ferguson 2012). As a result, consistent methods have emerged to standardize stable isotope analysis, the effects of variation in lipid content (Post et al. 2007, Logan et al. 2008), nutrient content (Adams and Sterner 2000) and tissue type (Mohan et al. 2016), are generally known for these taxonomic groups, though more information is continuously being determined. Even so, methods and assumptions used in studies sometimes ignore this knowledge and do not consider the potential effect of their methods and taxa on sample isotopic values (e.g., Baeta et al. 2017, Cornelissen et al. 2018).

Currently, standard stable isotope analysis assumptions derived from fish and zooplankton studies are typically applied to jellyfish without consideration on whether they are appropriate (e.g., Kellnreitner et al. 2013, Ingram et al. 2016, Naman et al. 2016, Vansteenbrugge et al. 2016). For instance, trophic discrimination and effects of sample preservation choices in jellyfish has been assumed to be the same as they are in fish. However, these assumptions have begun to be revealed as invalid for jellyfish.

Physiology is known to be important in determining isotopic ratios. For example, there is strong evidence that the nitrogen fractionation is related to factors such as the consumer's body composition (e.g., Caut et al. 2009), excretion form (e.g., Vanderklift and Ponsard 2003) and diet quality (e.g., Sick et al. 1997). Jellyfish are gelatinous organisms with low complexity, no specialized systems, and a water content of 95-98% (Doyle et al. 2007). Given their unique physiology, it is not safe to assume that jellyfish process elemental isotopes through the same processes as fish, crustaceous zooplankton, or other taxa. Fortunately, as applications of stable isotopes to jellyfish has grown, there has been increased effort to determine the best stable isotope methods specifically for jellyfish. These jellyfish-specific findings have begun to confirm

that the use of stable isotopes with jellyfish may be quite different than for vertebrates. However, the underlying physiological basis for these differences has largely been ignored.

Here, we aim to determine how stable isotopes can best be applied to study jellyfish interactions given our existing knowledge. We consider the biochemical basis for fractionation and how it applies to the unique physiology of jellyfish. For this, we create a framework for the use of stable isotopes with jellyfish that synthesizes existing jellyfish specific knowledge and how that differs from methodological standards for other taxonomic groups. Throughout, we highlight considerations for further research into the consequences of jellyfish physiology for stable isotope analysis.

3.2. The Mechanisms of Stable Isotope Applications in Food Webs

Here we posit that the unique composition and physiology of jellyfish means that specific knowledge and understanding of jellyfish are needed for robust application of stable isotope analysis on these species. For that reason, we briefly review the mechanisms that shape an organism's isotopic ratio and the aspects of jellyfish physiology that are most pertinent to these mechanisms. To meaningfully interpret stable isotope data from jellyfish it is necessary to consider how their body composition affects isotope fractionation.

The basic tenet of stable isotope analysis is that the ratios of naturally-occurring stable isotopes reflect the diet sources of an organism. In food web analyses, carbon and nitrogen are most commonly used (Boecklen et al. 2011). Carbon is useful to discern the original source of fixed carbon (e.g. allocthonous vs. autochthonous production, benthic vs. littoral, etc.), whereas nitrogen is often used as a measure of trophic level. Together, the two can reveal the relative dietary contribution of different sources, based on the distinct isotopic composition of sources.

At the simplest level, stable isotope analysis rests on the notion that "you are what you eat" (Deniro and Epstein 1978). That is, the ratio of heavy to light carbon (^{13}C:^{12}C) or nitrogen (^{15}N:^{14}N) in a consumer is indicative of the ratio in its diet. However, these ratios can be modified by processes collectively referred to as fractionation. Most fractionations are mass-dependent and occur due to the difference in weights between isotopes of the same element (Fry 2006). Enzymes that degrade or create complex molecules (e.g., amino acids, fatty acids) catalyze reactions between substrate molecules. Enzyme kinetics typically occur more rapidly on lighter substrates, so that these reactions preferentially uptake the lighter isotope. Consequently, the products of enzyme-substrate reactions will be lighter, on average, than their substrates (Gannes et al. 1998).

For nitrogen, transamination and deamination (the catabolism of amino acids) are the main enzymatic reactions responsible for fractionation. When consumers obtain nitrogen from their diet, the assimilation and excretion of this nitrogen requires transamination and deamination, which then results in fractionation. Nitrogen is also stored in several pools in the body and sometimes is available from a symbiotic relationship with the consumer's gut microbial communities (McMahon and McCarthy 2016). Movement of nitrogen among these pools is also connected through transamination and deamination, providing more opportunities for fractionation to occur.

The extent of carbon and nitrogen fractionation depends on multiple factors. One prominent factor is the assimilation efficiency of the predator (Doyle et al. 2007). Assimilation efficiency is the ability of an organism to retain consumed elements and incorporate them into body tissues. Organisms that retain most of their consumed carbon and/or nitrogen will have less fractionation of that element than those that excrete large amounts of the element (Fry 2006).

This is because there is reduced net discrimination of lighter over heavier isotopes as nearly all of the element consumed is assimilated to synthesize proteins (i.e., the system follows Rayleigh distillation) {Kendall, 1998 #1769}.

Similarly, the size of the available source pool of the element in the prey also affects fractionation rates. A large pool of the available substrate means the element is less limiting, which leads more opportunity to preferentially uptake the lighter isotope (Pearson et al. 2003). Conversely, when an element is scarce relative to demands there is less potential for discrimination among isotopes during nutrient uptake. This relationship between element source pools and fractionation has been found in a range of taxa, including songbirds (Pearson et al. 2003), rats (Caut et al. 2008) and guppies (Dennis et al. 2010).

These factors are particularly germane to jellyfish because of their unique C:N ratios relative to their prey. Jellyfish are nitrogen rich and carbon poor (Pitt et al. 2013). Their main prey is zooplankton, (Purcell and Sturdevant 2001), which are typically nitrogen poor and carbon rich in comparison (Pitt et al. 2009b). As a result, jellyfish must retain most nitrogen they consume. This is supported by the low amounts of nitrogenous waste they excrete (Pitt et al. 2013). Their high nitrogen retention, along with small nitrogen source pool, predicts low nitrogen fractionation. In order to meet their high nitrogen needs, jellyfish likely consume far more carbon than needed, which is supported by their high excretion rates of dissolved organic matter and mucus (Pitt et al. 2013). This low carbon retention and high carbon availability predict high carbon and low nitrogen fractionation in jellyfish.

In addition, nitrogen fractionation specifically is affected by additional factors. An organism consuming a diet that closely matches dietary needs ("high diet quality") may have lower isotope fractionation, i.e. the 'consumption hypothesis' (e.g. Robbins et al. 2005). High

quality diets are those that have similar elemental and macromolecule profiles as the consumer. In these cases, the close match between amino acid demands and their diet reduces the demand for amino acid synthesis (Sick et al. 1997). Synthesized amino acids are are enriched in heavy nitrogen because amino acid precursors (e.g. glutamate) become enriched owing to deamination pathways that preferentially remove lighter nitrogen into ammonia and urea waste products. As a result, the low synthesis needed due to consuming a high quality diet has fewer transamination and deamination steps (Gannes et al. 1997), leaving less opportunity for fractionation to occur.

For jellyfish, there is likely poor match between dietary amino acid profiles and amino acid needs. Jellyfish's main prey, zooplankton, have a markedly different amino acid profile than jellyfish, as well as having a much lower nitrogen content (Pitt et al. 2009b). Low quality prey, as zooplankton are for jellyfish, would predict high nitrogen discrimination rates. However, fractionation is related to overall diet quality, rather than diet quality of individual diet components (Robbins et al. 2010). Other dietary sources of jellyfish, such as dissolved organic matter (Pitt et al. 2009b, Skikne et al. 2009), are frequently ignored, but may result in an overall high quality diet that may result in low nitrogen fractionation.

The form of excretion product also dictates the amount of nitrogen trophic fractionation (Germain et al. 2013). In marine food webs, excretion form tends to differ between lower and higher trophic levels, potentially causing ^{15}N fractionation rates to vary with trophic level. Ammonia excreting taxa tend to have lower fractionation than urea excreting taxa (Vanderklift and Ponsard 2003). This may be due to the different lengths of their formation processes. Ammonia is produced directly from the available pool of the amino acid, glutamic acid, by deamination. In contrast, urea production requires two deamination steps, which involve multiple nitrogen reservoirs. This broader distribution of nitrogen across pathways and reservoirs may

lead to more enrichment (Germain et al. 2013). Like most other marine taxa, jellyfish excrete ammonia (Arai 1997).

Carbon fractionation is complex; in general, isotope ratios of carbon are less altered by trophic transfers, averaging an increase of 0-1‰ (Peterson and Fry 1987). This small shift is due to a couple of factors. Respiration preferentially expels ^{12}C (DeNiro and Epstein 1977, Michener and Lajtha 2007, Thurber 2014), leaving the body slightly enriched in ^{13}C. Meanwhile, carbon can be enriched due to synthesis of non-essential and catabolism of essential fatty acids (Dalsgaard et al. 2003, Iverson et al. 2004). Non-essential fatty acids are synthesized from stores of available carbon in the body. As metabolism preferentially uptakes the lighter isotope, which is then lost during respiration, these stores become mildly enriched in ^{13}C (Iverson et al. 2004). Similarly to nitrogen, diet composition can also affect carbon trophic fractionation, such that higher amounts of available carbon in the source pool are correlated to higher fractionation rates (Michener and Lajtha 2007).

Respiration rates of jellyfish are much lower than other pelagic taxa (Pitt et al. 2013), though if scaled to carbon content rather than wet-weight, their respiration rates are similar to other metazoans (Acuña et al. 2011). The body of a jellyfish is primarily composed of mesoglea, which is an extracellular structure composed of water, collagen, and salt (Pitt et al. 2013). This mesoglea contains few or no cells, leading to the low respiration rates relative to their wet weight. Depending on whether wet weight or carbon content are used for scaling, jellyfish respiration rates would predict low to average carbon fractionation (Pitt et al. 2013).

When considering physiology in relation to isotope ratios, we should recognize that bulk stable isotope ratios represent the aggregate effect of fractionation of individual amino acids and fatty acids and their relative proportions. In most taxa, certain amino acids show high

fractionation, such as glutamic acid in nitrogen and glysine in carbon, while others have minimal fractionation from the diet, such as phenylalanine (Hare et al. 1991, Chikaraishi et al. 2009, Boecklen et al. 2011). The weighted averaged of the fractionation rates for each individual amino acid, weighted by the proportion they compose of the total amino acid pool, should closely approximate the bulk isotope fractionation rate. As a result, understanding of bulk isotope fractionation rates and the biochemistry driving the variation in these rates, can often be improved by considering patterns of individual amino acid fractionation and their proportions in the tissue being sampled (Boecklen et al. 2011, Chikaraishi et al. 2014).

The amino acid composition of jellyfish is unique compared to many taxa. For *Pelagica noctiluca*, their amino acid composition was almost identical to that of the entire zooplankton community, except for an unusually large amount of glysine (Malej et al. 1993). In particular, the comparable levels of glutamic acid and phenylalanine in the jellyfish are particularly unusual and suggest that both or neither must fractionate with each trophic transfer (Malej et al. 1993). The high amounts of glysine may be due to uptake of dissolved organic matter, which is known to be assimilated by jellyfish (Pitt et al. 2009b, Skikne et al. 2009) and is likely needed due to their high collagen content. Body tissues of jellyfish are dominated by mesoglea, which is largely composed of collagen. Collagen is 33% glycine and the glycine in collagen is known to have high carbon fractionation, ~8‰ (Hare et al. 1991). This high need for glysine predicts high carbon fractionation, in contrast to the low carbon fractionation predicted by their low respiration rates.

3.3. Implications for Stable Isotope Applications to Jellyfish

The process of applying stable isotope analysis to any type of organism involves multiple steps: 1) sample collection, 2) sample preservation, 3) processing the sample, 4) analyzing the sample, and 5) interpreting the data (Figure 1). Here, we focus on how the methods and assumptions used in these steps might alter stable isotopic ratios of jellyfish, thereby distorting inferences about their trophic position.

3.3.1. Sample Collection

A single tissue is often collected from each organism for stable isotope analysis. The choice of tissue to sample depends on the ecological question of interest. As stable isotopes are used to reconstruct the diet of a consumer based on a single tissue, it is necessary to understand the tissue turnover and routing, the process by which isotopes are differentially routed to specific tissues and body compartments, associated with that tissue (Gannes et al. 1998). In fish, muscle tissue is often used, which has a mean turnover of weeks to months in most taxa, but is highly dependent on growth rate (Boecklen et al. 2011). Muscle also represents the greatest fraction of whole body mass giving it a clear ecological interpretation when information about consumer diet is of interest. Similarly, marine mammals are also often sampled using muscle tissue, though blood and skin are also commonly used as these can also be obtained non-lethally (Newsome et al. 2010). In contrast, due to their small size, zooplankton are sampled as bulk samples, where many entire individuals are combined whole to form a single sample.

For jellyfish, there is no established consensus regarding whether different tissues or whole individuals should be sampled. For practical reasons, it is often necessary to sample the whole individual when they are small and have low carbon content (e.g. Vansteenbrugge et al. 2016). However, for larger species, the bell tissue is frequently collected (e.g. Brodeur et al.

2002, Fleming et al. 2011, Fleming et al. 2015) under the rationale that the majority of an individual's mass is stored in the bell (D'Ambra et al. 2014, MacKenzie et al. 2017). However, it is unclear how nutrients are routed into different tissues and whether this leads to distinct isotopic signatures among tissues. D'Ambra et al (2014) found that there were no differences between the isotopic signatures of C and N in the bell compared to the whole body of *Aurelia sp.*, suggesting in this species or that the bell is representative of the whole individual. However, Towanda and Thuesen (2006) found that bell tissue from *Phacellophora camtschatica* was enriched in carbon compared to other tissues. Finally, our analysis of the large-bodied *Cyanea capillata* showed that bell tissues provided no reliable information on measured whole-individual isotopic signatures (Figure 2, Supplement A). These conflicting results indicate species-specific differences in routing into tissues or that other factors are confounding the measurements. As assimilation efficiency varies widely with prey availability (Pitt et al. 2009a), this may also affect whether, and how much, routing occurs due to the link between assimilation efficiency and fractionation.

Choosing a tissue to sample is further complicated by our little knowledge of tissue turnover rates in jellyfish, making ecological interpretations of stable isotope data difficult. Turnover rates have only been measured in *Aurelia sp.* where they were measured as 18-20 days for both the bell and whole individual (D'Ambra et al. 2014). The consistent turnover rate aligns with the consistent isotope signature between tissues measured in this study, further supporting the possibility that the bell represents the whole individual.

Interpretation of jellyfish stable isotopic ratios in ecological studies is currently limited due to the conflicting results on whether isotopic ratios in jellyfish vary among tissues and uncertain turnover rates. To more thoroughly determine turnover rates, more controlled

laboratory studies where diets can be manipulated are needed. Turnover rates need to be estimated for several species, separately on tissues that may be of interest, due to the possibility of tissue and species-specific effects (Vander Zanden et al. 2015). Isotopic routing into tissues is similarly best determined in laboratory experiments that are motivated by specific hypotheses that tie physiological mechanisms to isotopic composition. Application of stable isotope analysis to individual tissues in jellyfish and prey will reveal whether routing is occurring, resulting in different isotopic ratios among tissues. If so, we will have a clearer understanding of the different composition of the tissues and why they differ in isotopic signature. This knowledge of turnover rates and routing will allow us to choose an appropriate tissue to sample for the ecological question of interest.

3.3.2. Sample Storage

After collection, samples are frequently stored by freezing. On some occasions, samples may be dried fresh, but this is usually not an option when working in the field. Freezing is typically considered the preferred form of storage (compared to immersion in ethanol or formalin), because gain or loss of mass from the sample is inhibited.

Freezing does not affect isotopic ratios in samples most taxa, including fish, some invertebrates, octopus, or kelp (Bosley and Wainright 1999, Ponsard and Averbuch 1999, Kaehler and Pakhomov 2001, Sweeting et al. 2007). However, a study focused on zooplankton did find mild enrichment carbon and nitrogen isotopes in zooplankton (Feuchtmayr and Grey 2003). Feuchtmayr and Grey (2003) propose that mechanical breakdown of the cells may have led to leaching of carbon and nitrogen when samples were thawed and prepared.

Multiple studies have demonstrated that freezing effects jellyfish isotopic ratios. Specifically, freezing samples elevated ^{15}N:^{14}N ratios by ~2‰ in *Aurelia aurita* in two studies in different systems, the Beaulieu River in southern England and Strangford Lough in Ireland, while ^{13}C:^{12}C was unaffected (Fleming et al. 2011, MacKenzie et al. 2017). This enriched nitrogen isotope is contradictory to assumptions made for other taxa and marks an important difference in sampling from other taxa. This unexpected, but consistent finding that freezing alters isotopic ratios indicates that interpretation of jellyfish SIA values needs to account for effects of freezing, particularly if they are being compared to other taxa.

Despite being found in multiple studies, as well as Feuchtmayr and Grey (2003), there is not a clear mechanism for this nitrogen enrichment due to freezing. One possibility is that this finding results from separation of proteins in the process of freezing and thawing, as suggested by Feuchtmayr and Grey (2003) and Dannheim et al. (2007). Jellyfish may be especially prone to this given their high water content. If extreme care is not taken to grind the entire sample after it has been dried and separated, part of the sample may be left behind, resulting in altered nitrogen isotopic values, as may have occurred in Feuchtmayr and Grey (2003). This could be tested experimentally by comparing tissues that have been frozen to those that were homogenized and then frozen. Isotope ratios of large bulk samples of infaunal macrozoobenthic species are also altered due to freezing and it has been suggested that this is caused due to the large mass of collected samples, which may allow for the microbial communities to metabolize some components due to the long time it takes for the sample to fully freeze (Dannheim et al. 2007). Because of their high water content, jellyfish samples are also large relative to other organisms. To determine if the long time to freezing is a mechanism causing enrichment, standard freezing of samples can be compared to flash freezing samples, as in Feuchtmayr and Grey (2003).

3.3.3. Sample Preservation

Preserving a sample after its collection and storage involves multiple steps, including drying the samples. Oven drying and freeze drying are both commonly used and are assumed to not affect isotopic signatures across a range of taxa including fish, octopus, kelp, invertebrates, (Kaehler and Pakhomov 2001), and elasmobranchs (Kim and Koch 2012). Both methods remove water from the sample, but are not thought to remove nitrogen or carbon and therefore are assumed to preserve a sample's isotope ratios.

Recent evidence suggests this assumption may be invalid for jellyfish. A study across four jellyfish species found that oven drying, as compared to freeze drying, elevated ^{15}N:^{14}N for two of the species, while the other two species were unaffected (Kogovsek et al. 2014). The nitrogen isotopic ratios were elevated by up to 2.5‰ while ^{13}C:^{12}C ratios were unchanged. This enrichment of nitrogen is an especially concerning result, as oven drying appears to have an inconsistent result between species.

There are several possible mechanistic explanations for how oven drying changes isotopic signatures. Because large effect sizes often come from studies with small sample sizes, it is possible that these documented effects are simply statistical noise. Replication is essential to ensure it is not statistical error. If the results are confirmed, follow up studies are needed to understand the mechanisms and which species are most affected. For instance, because of the high water content of jellyfish, oven drying takes days to weeks to complete. Extended drying time may lead to microbial growth in samples. The growth of microbial communities may itself change the isotope ratios (McMahon and McCarthy 2016) by leading to gaseous loss of nitrogen. These potential mechanisms are supported by the lack of a difference when samples in Kogovsek

et al. (2014) were dialysed (water removed) before drying. These potential effects of drying method can be avoided by freeze drying or dialyzing samples before oven drying. Until the mechanism for oven drying affecting nitrogen isotope ratios is resolved, these need to be standard methods for processing jellyfish tissue samples.

3.3.4. Sample Analysis

Preserved samples are analyzed for isotope ratios using an elemental analyzer coupled to an isotope ratio mass spectrometer. A ground sample is combusted and isotope ratios in the resulting gas are measured. The sample mass required varies as a function of the mass spectrometer's sensitivity and percent of carbon and nitrogen in the tissue. A minimum amount of carbon and nitrogen are needed for the elemental analyzer mass spectrometer to provide accurate measurements. If the amount of carbon and nitrogen in the sample is too low, then the isotope ratio is typically underestimated, while a very high amount will overwhelm the instrument (Fry 2006). The high salt content in ground jellyfish samples require a higher sample mass to be combusted than for taxa such as fish and zooplankton. Through preliminary work, studies applying stable isotopes to jellyfish have found an optimal sample mass of between 2.4-12 mg, dependent upon species, which is much higher than the 0.5-1.0 mg typically required for most animals (Supplement A, D'Ambra et al. 2014, Kogovsek et al. 2014, Fleming et al. 2015). If preliminary work is not performed to determine an appropriate mass of sample for use in the specific equipment being used, isotopic ratio estimates are likely to be inaccurate.

3.3.5. Trophic Fractionation

When stable isotopes are used to determine a consumer's diet or food web structure, fractionation per trophic level has to be assumed to estimate relationships among taxa. In marine food webs, authors often assume 0‰ fractionation for carbon and 3.4‰ per trophic level for nitrogen (Minagawa and Wada 1984). These fractionation rates are derived from averages across many taxa (Boecklen et al. 2011), but are now thought to vary with trophic level (Hussey et al. 2014). Despite increasing awareness of the biases introduced by assuming a constant fractionation across taxa and trophic levels, standard fraction values frequently continue to be applied (e.g. Baeta et al. 2017, Iglesias et al. 2017).

Trophic fractionation estimates specifically for jellyfish are beginning to be determined, but may be very different from the commonly used standard fractionation rates based on other taxa. D'Ambra et. al. (2014) estimate trophic fractionation rates of 4.0‰ for carbon and 0.1‰ for nitrogen (D'Ambra et al. 2014); to our knowledge, this is the only jellyfish-specific analysis of stable isotope fractionation rates. While these estimates are very different from those measured in fish and zooplankton, they align with fractionation in other soft-bodied invertebrates. For instance, nitrogen fractionation in annelids ranges from -0.8‰ to -3.0‰ depending on the food source, while carbon fractionation ranged from -3.6‰ to 3.6‰ (Thurber 2014). In sea cucumbers, carbon fractionation rates averaged 4.2‰, while nitrogen fractionation rates (average 2.4‰) were similar to fish and zooplankton (Watanabe et al. 2013). Thus, while jellyfish may be unusual when compared to fish and crustaceous zooplankton, they may be typical for soft-bodied invertebrates.

Furthermore, the amino acid composition of jellyfish potentially supports little trophic fractionation in bulk nitrogen and high fractionation in bulk carbon. In other taxa, the fractionation of bulk nitrogen is largely due to fractionation in the amino acid phenylalanine, so

the lack of phenylalanine fractionation in jellyfish supports the idea of little bulk nitrogen fractionation. Similarly, jellyfish have a higher glysine content than most other taxa. As glysine exhibits high carbon fractionation, this could drive unusually high bulk carbon fractionation.

A lack of trophic fractionation in nitrogen in jellyfish suggests that their assimilation and/or excretion processes differ from many other taxa. The lack of enrichment may indicate that there is not an opportunity to discriminate between nitrogen isotopes. This may occur for a couple of reasons. First, they have high nitrogen demands due to their high protein content, potentially such that they are nitrogen limited (Pitt et al. 2013), which could lead to low discrimination in nitrogen. Additionally, they likely consume excess carbon in order to reach their nitrogen needs (Pitt et al. 2013), which may produce high carbon trophic fractionation. Alternatively, as jellyfish have one cavity for consumption and excrement and no specialized systems, their assimilation and excretion pathways may be short. Short pathways may not have many occurrences of transamination or deamination, which would result in low trophic nitrogen fractionation. Finally, their body tissues are dominated by mesoglea, which is largely composed of collagen and therefore largely glycine. Since the glycine in collagen is known to have high carbon fractionation, ~8‰ {Hare, 1991 #1737}, this could lead to the high carbon fractionation observed.

Several steps are needed to understand tropic fractionation in jellyfish. First, studies measuring trophic isotope fractionation need to be repeated. Ideally, they would be repeated with multiple jellyfish species as consumers and with multiple jellyfish diets. If similar unusual trophic fractionation estimates are again measured, then studies to determine the mechanistic basis are required. Ultimately, to fully understand trophic fractionation of nitrogen, studies employing compound specific isotopic analysis of amino acids would be most beneficial.

Controlled laboratory experiments on jellyfish and their prey would allow for collecting detailed information on the trophic fractionation of individual amino acids. By comparing the amino acid profile of jellyfish with their actual prey, rather than the whole zooplankton community as done by Malej et al. (1993), we can gain a nuanced understanding of which amino acids fractionate and which are conserved. This gives us insight into what may be driving the trophic fractionation of the bulk isotopes.

3.4. Consequences of Assumptions in Stable Isotope Methodology

Stable isotopes of jellyfish are frequently analyzed to understand their trophic relationships in comparison to fish species (e.g. Frost et al. 2012, Syvaranta et al. 2012, Ingram et al. 2016, Naman et al. 2016). Unsubstantiated methodological assumptions are likely to alter where jellyfish fall in relation to other taxa on an isotope biplot, posing problems when drawing conclusions. The potential extent of these problems is not fully appreciated.

To illustrate the consequences of methodological methods and assumptions, we calculated the isotope biplot positions that could result from identical stable isotope samples that were analyzed using different methodological assumptions. We used stable isotope samples collected for zooplankton (euphausiids), fish (Pacific herring and Pacific hake), and jellyfish (lion's mane jellyfish) in Hood Canal, Washington, USA at the same sites on the same days (details in supplement A3). Samples for all taxa were frozen upon collection. Fish and zooplankton were freeze dried after returning to the laboratory, while jellyfish were oven dried. All jellyfish samples were bell tissue, with careful attention to not include any gonads in the samples, while fish samples were muscle tissue, and euphausiids were bulk samples.

Our goal was to compare the trophic position of each fish species to the potential trophic position of lion's mane jellyfish. As we were lacking stable isotope ratios for multiple prey sources, we do not quantitatively compare trophic positions of the jellyfish and fish, but use the stable isotope information to demonstrate the potential effects of these different methodological assumptions.

From the raw stable isotope values, we corrected the jellyfish values using several different sets of assumptions about the effects of the methodology used. These were chosen based on what is commonly done in primary literature and what is now known specifically about jellyfish (Table 3.1). The first was to make standard assumptions (i.e. preservation method and drying method had no effect on isotope ratios). We also assigned standard fractionation rates, 3.4‰ and 0‰ for nitrogen and carbon, respectively. Next, we assessed the range of trophic position and energy base that could be estimated solely by uncertainty in fractionation rates. Finally, we assessed the range of estimated trophic level and carbon source pathway that could arise through different assumptions regarding effects of preservation and drying methods. As the effect of oven drying is species dependent, the subset of these scenarios that correct for drying include multiple subscenarios to account for the unknown on whether oven drying would affect lion's mane jellyfish samples.

The different assumptions made about the methodology effects on the jellyfish isotopes affected where jellyfish fall in comparison to potential competitors on an isotope biplot, (Table 1, Figure 3). Quantitative trophic position estimates of jellyfish would vary widely under these different results. The variation among estimates far exceeds the statistical uncertainty associated with the point estimates (Figure 3.3), leading to different conclusions when comparing the trophic position of jellyfish to other taxa, as is frequently done (e.g. McClellan et al. 2010, van der Bank

et al. 2011, Frost et al. 2012, Ingram et al. 2016, Naman et al. 2016). Until mechanisms for fractionation in jellyfish are understood and stable isotopes can be accurately interpreted, stable isotopes cannot accurately be used to compare their trophic position to other taxa.

3.5. DISCUSSION

Jellyfish have distinct physiology that should lead to distinct methodology for accurate applications of stable isotopes in food web ecology, which is increasingly supported by empirical evidence. Currently, we lack the mechanistic understanding of how isotope fractionation occurs in jellyfish, causing seemingly standard decisions to affect measured stable isotope ratios. As the need to understand the trophic role of jellyfish is likely to continue, our first priority is to consider how best to move forward with the application of stable isotopes to this taxon. We believe that the ideal path forward combines standardizing the methodology used and employing additional studies.

Continued use of SIA requires adopting standard collection, preservation, and processing practices, as recently called for by Mackenzie et al. (2017). At a minimum, this would allow for better comparisons amongst studies. For instance, standardizing sample drying methodology is a simple and effective way to address the potential effects of drying samples until underlying biochemical processes for the effects are known. Ultimately, however, it is vital to understand these underlying mechanisms.

We suggest that the most productive path forward is to begin applying compound specific isotopes on amino acids to jellyfish. By analyzing both jellyfish and their prey in controlled laboratory experiments, the use of compound specific isotope analysis on amino acids will serve as replication of the results obtained by D'Ambra et al. (2014), while also providing a nuanced

picture of nitrogen and carbon trophic fractionation. Additional studies will ultimately be required to ascertain the effects and mechanisms of sample storage, preservation, etc. However, in conjunction with standardizing methodology of sample collection, preservation and drying, making use of compound specific isotopic analysis of amino acids has the potential to relatively quickly lead to more robust and meaningful results and conclusions about the trophic position of jellyfish.

Until methods are further developed and jellyfish biochemistry is resolved, applications of stable isotopes to jellyfish should acknowledge uncertainty when drawing comparisons to other taxa. Poor understanding of the biochemical processes strongly dampens our ability to draw accurate conclusions about their trophic position in comparison to other taxa. For instance, application of these fractionation rates estimated by D'Ambra et al. (2014), results in trophic level estimates that place jellyfish above larger predators, such as spiny dogfish (e.g. Nagata et al. 2015, unpublished data- Supplement A, Naman et al. 2016, MacKenzie et al. 2017) or below zooplankton (Figure 3). These trophic position estimates are implausible, suggesting there are poor assumptions somewhere in the stable isotope methodology used. Until these are resolved, the current methodological limitations of applying stable isotopes to jellyfish prohibit us from accurately drawing specific conclusions about the trophic role of jellyfish.

Stable isotope analysis is a common and useful tool for inferring food web linkages, but it requires careful and informed applications to yield interpretable and meaningful results. Existing methods for applications to jellyfish need to be clarified and further developed, so that better information on the ecological role of jellyfish can be ascertained. Pursuing the physiological mechanisms in jellyfish that underlie isotope fractionation, along with careful results interpretations, will ultimately lead to more informative studies of their ecological role.

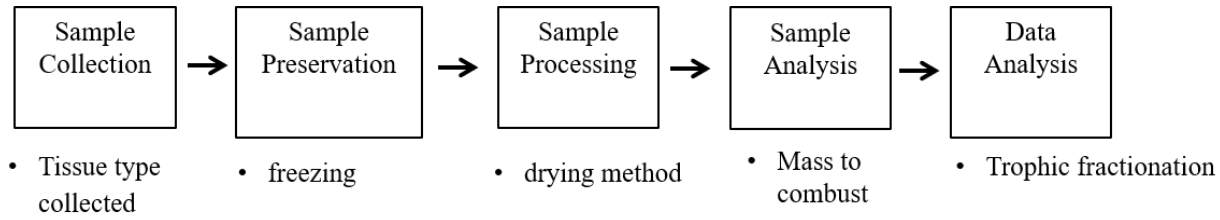

Figure 3.1 The steps in stable isotope analysis (boxes) and the assumptions required for each (bullet points), each of which can influence results and conclusions.

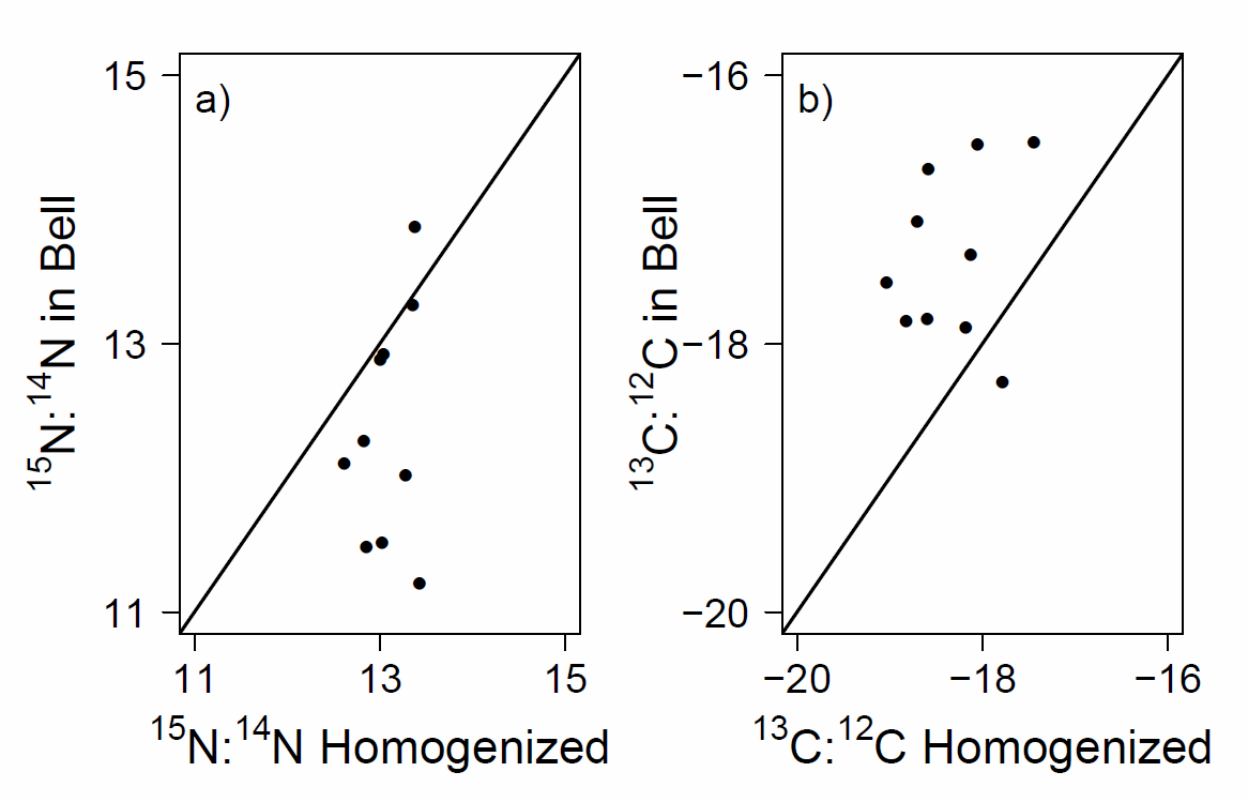

Figure 3.2 Isotope signatures for homogenized bodies of of lion's mane jellyfish, Cyanea capillata, in comparison to the isotope signature of their bell. Each point is an individual jellyfish, lines indicate 1:1 lines.

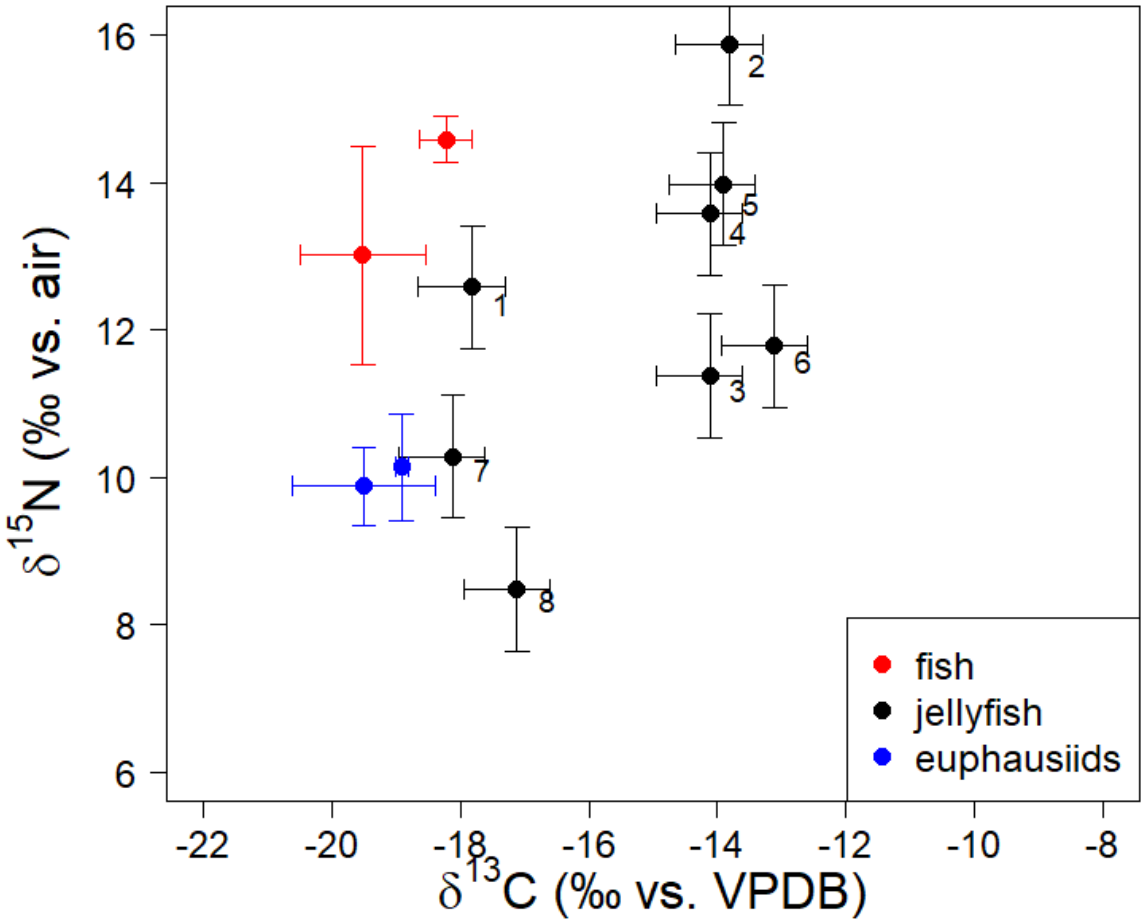

Figure 3.3 The estimated biplot position of jellyfish using different methodological assumptions, in comparison to other taxa in the food web. Numbers next to jellyfish points correspond to the numbered scenarios in table 1. Error bars = standard deviation. Euphausiids are bulk samples (different points represent collection by different sampling groups), for fish and jellyfish: n = 20.

Table 3.1 The different scenarios applied to stable isotope analysis data in order to correct for methodological choices. A dash indicates that no correction for that methodology choice was applied, though there is believed to be an effect. Numbers in parentheses indicate the value of the correction applied to the isotope value. The first number indicates the correction for carbon and the second number indicates the correction to the nitrogen value.

Scenario 1 = treating jellyfish as fish; Scenario 2 = only correcting fractionation; Scenarios 3-4 = ignoring fractionation rates due to implausibility; Scenarios 5 – 8: applying all jellyfish specific knowledge, with oven drying correction dependent on species. Correction values were collected from primary literature: 1) Fleming et al. (2011), 2) MacKenzie et al. (2017), 3) Kogovsek et al. (2014), 4) D'Ambra et al. (2014).

Scenario	Preservation Correction (C, N)[1,2]	Drying Correction (C, N)[3]	Fractionation Rate Applied (C, N)[4]	Jellyfish Corrected d13C	Jellyfish Corrected d15N
1	-	-	-	-17.8	12.6
2	-	-	(-4, 0.1)	-10.4	15.9
3	(0,2)	(0.3, 0.3)	-	-18.1	10.3
4	(0,2)	(-0.7, 2.1)	-	-17.1	8.5
5	(0,2)	(0.3, 2.5)	(-4, 0.1)	-14.1	11.4
6	(0,2)	(0.3, 0.3)	(-4, 0.1)	-14.1	13.6
7	(0,2)	(0.1, -0.1)	(-4, 0.1)	-13.9	14
8	(0,2)	(-0.7, 2.1)	(-4, 0.1)	-13.1	11.8

APPENDIX A3

Methods

We collected samples of common fish and jellyfish for stable isotope analysis in Hood Canal, Washington USA. Individuals were collected via midwater trawling in July 2012 and 2013 in the same region of Hood Canal (near Union, Washington) (see chapter 4 for sampling details). Zooplankton were collected in the midwater trawl net, as well as from zooplankton net tows (see chapter 4 for sampling details).

Tissue samples from jellyfish and fish were collected and preserved. In 2012, we simultaneously collected the dominant jellyfish species, lion's mane jellyfish (*Cyanea capillata)* and the dominant zooplanktivorous fish, Pacific herring (*Clupea harengus)* and Pacific hake (*Merluccius productus*). A piece of bell tissue of ~50-100g was taken from each jellyfish, while being careful to not include tissue from gonads, oral arms, or any other jellyfish part. Muscle tissues were collected for both fish species. In 2013, jellyfish were collected to compare the isotopic signature of their bell to the whole individual. Within 30 minutes of collection, individuals were cut in half. From one half a sample of bell tissue, with no other tissue types visibly present, was collected. The second half was placed in a food processor and blended until visibly homogenized and a sample of the homogenized jellyfish was collected. In both years, all samples were immediately frozen in a chest freezer. Upon returning to land, samples were transferred to a -40C freezer for storage until processing.

To preserve isotope samples, samples were either oven-dried or freeze dried. All fish tissue from both years was freeze dried. Jellyfish collected in 2012 were oven dried at 60C, while jellyfish collected in 2013 were freeze dried. After drying, all samples were ground to a fine, uniform powder using a Wig-l-Bug dental amalgator.

Ground samples were analyzed using a Costech elemental analyzer copled to a Thermo MAT253 isotope ratio mass spectrometer by the University of Washington IsoLab. Each fish sample was analyzed using 0.4 – 0.6mg of dried, ground material. Jellyfish samples were analyzed using 2.5-4mg of dried, ground material due to their lower carbon content (optimal weights were determined by preliminary analyses in conjunction with the University of Washington IsoLab).

4. THE EFFECT OF HYPOXIA ON TROPHIC CONNECTIVITY BETWEEN FISH AND ZOOPLANKTON VARIES ACROSS ECOLOGICAL SCALES

ABSTRACT

Predicting ecological change is challenging. Yet, as environmental stressors continue to alter ecosystems, doing so is increasingly necessary. Hypoxia is an environmental stressor that occurs in coastal systems worldwide and is continuing to increase in extent and intensity. Hypoxia is believed to influence zooplankton-zooplanktivorous fish trophic linkages by affecting organism behavior, community composition, and organism physiology. To predict the effects of hypoxia on energy flow from zooplankton to fish, usually changes in spatial overlap between zooplankton and zooplanktivorous fish are measured and assumed to directly propagate to changes in energy flow through the trophic link. However, hypoxia is also known to affect zooplankton community composition and abundance, fish abundances and fish feeding, and organism reproduction. Here, we simultaneously measure per-capita feeding rates, population level consumption, and prey availability to determine if energy flow from zooplankton to zooplanktivorous fish, represented within by fish predation on zooplankton, in Hood Canal, WA, USA is altered due to hypoxia. To integrate these measurements we use a Bayesian modeling framework, which allows us to predict predation under actual hypoxic conditions and under an alternative scenario where there is no occurrence of hypoxia. By comparing these predictions, we determine that hypoxia increases relative predation of zooplankton by zooplanktivorous fish in Hood Canal, despite no change in their spatial overlap. This increase in relative consumption is

due to a decrease in prey availability under hypoxia, while fish consumption at the population-level stays constant or slightly increases. Our approach reveals effects of hypoxia that would not be obtained by solely considering spatial distributions. Instead, by simultaneously measuring multiple ecological processes that interact, we develop a nuanced picture of how energy flow from zooplankton to zooplanktivorous fish in Hood Canal is altered by hypoxia.

4.1. INTRODUCTION

The need for ecological forecasts of ecosystem changes is growing as the pace of global change continues to increase. Unfortunately, precise predictions are quite challenging because ecological dynamics are governed by a multitude of system processes (Doak et al. 2008) that occur over and interact across individual, population, and system level scales (Heithaus et al. 2008, Tylianakis et al. 2008, Chave 2013, Heffernan et al. 2014, Stillman et al. 2015). Being able to resolve predictions of ecological dynamics requires approaches that can integrate across these scales (Rastetter et al. 2003, Wernberg et al. 2013, Heffernan et al. 2014, Stillman et al. 2015).

Food webs emerge as a result of these cross-scale interactions. Each trophic link in a food web arises as a consequence of individual, population, and community properties and processes (Sentis et al. 2014). These processes include the spatial movements of individual predators and prey, the resulting spatial distribution of predator and prey populations, the feeding preferences of predators, and how those are governed by prey behavioral avoidance responses. Finally, the strength of trophic linkages depends on the relative population sizes of predators, prey, and the species composition of these groups. It follows then that external drivers that alter individual behavior, physiology, population biology, or community composition will be reflected in food web structure and dynamics (Tylianakis et al. 2008).

Food webs are sensitive to environmental stressors due to this multitude of complex underlying processes. Hypoxia is a common environmental stressor, occurring in hundreds of coastal systems worldwide (Vaquer-Sunyer and Duarte 2008) and is continuing to grow in intensity and frequency (Breitburg et al. 2018). While hypoxia occurs alongside and interacts with other environmental stressors such as ocean acidification and increasing temperatures (Conley et al. 2009, Vaquer-Sunyer and Duarte 2011, Melzner et al. 2013, Breitburg et al. 2018), the gradient in hypoxia that occurs within a region often causes it to have a strong ecological influence on marine systems at a regional level (Breitburg et al. 2018).

Hypoxia affects zooplankton-zooplantivorous fish trophic linkages by affecting organism behavior, community composition, and organism physiology. Hypoxia induces behavioral responses that are reflected in spatial distributions of fish and zooplankton (e.g. Pierson et al. 2009, Zhang et al. 2009, Ekau et al. 2010, Essington and Paulsen 2010). These distributional changes can alter spatial overlap between zooplankton and fish, thereby enhancing or reducing availability of zooplankton prey to fish predators (Ludsin et al. 2009, Vanderploeg et al. 2009, Roman et al. 2012). If decreased access to zooplankton are maintained over a longer period of time, fish abundances may decrease as a result of reduced access to prey. Hypoxia also directly affects composition and abundance of zooplankton and fish communities. Zooplankton taxa have short lifespans and varying tolerances to low dissolved oxygen. Short lifespans result in high turnover relative to fish and potentially quick changes in the relative abundances of taxa. Community composition changes in zooplankton may limit or eliminate the preferred prey of fish (e.g. Roman et al. 1993, Uye 1994). The reduced habitat available to fish due to hypoxia may cause fish abundances to decline if competition among them increases (Casini et al. 2008). Finally, hypoxia might induce physiological responses that negatively affect fish. Stress from

low dissolved oxygen may cause a decrease in fish feeding (Pollock et al. 2007) or impair reproduction, hormone production, and cause epigenetic changes (Sokolova 2013, Thomas et al. 2015).

Previous hypoxia studies have focused on measuring effects of individual food web properties, but have not simultaneously measured multiple processes and how those processes affect food web linkages. In particular, spatial distributions have been a focus of many studies (e.g. Ludsin et al. 2009, Ekau et al. 2010, Essington and Paulsen 2010). While understanding how hypoxia affects spatial distributions of organisms is useful, evaluating the effect of hypoxia on only spatial distributions doesn't allow for predictions of effects on trophic linkages. Understanding how ecological dynamics respond to hypoxia and gaining any ability to accurately predict the effects of hypoxia on a food web will require simultaneously measuring multiple food web properties, which is complicated due to their occurrence over multiple resolutions.

Here, we aim to determine how hypoxia affects individual, population, and system-level properties of a marine system. We use nested hypotheses to determine the effect of hypoxia on the trophic link from zooplankton to fish: 1) Does hypoxia alter per-capita feeding rates of zooplanktivorous fish? If so, is this change due to changes in fish diets and/or change in total consumption amount; 2) Does hypoxia alter population level feeding (a function of per-capita feeding and population biomass)? If so, is this change due to change in population biomass and/or change in per-capita feeding? 3) Does hypoxia alter relative predation of zooplankton by zooplanktivorous fish? If so, is this due to change in population level feeding and/or due to change in prey availability?

4.2. METHODS

4.2.1. Sampling

This study was conducted in Hood Canal (Figure 4.1), an estuarine fjord that constitutes the western branch of Puget Sound, Washington, USA. A sill at the mouth of the fjord limits oceanic inputs, which combined with riverine inputs leads to stratification (Babson et al. 2006, Sutherland et al. 2011). The deep bathymetry and long water residence time of Hood Canal make the system naturally prone to seasonal hypoxia (Newton et al. 2007), which usually begins in mid-summer and continues through early autumn. Seasonal hypoxia typically develops earlier and most strongly at the southern end of the system, while the northern end retains higher oxygen levels (Newton et al. 2007). These contrasting regions make Hood Canal an effective natural laboratory for studying the effects of hypoxia.

Sampling Design

We compared stations at opposite ends of the canal through time to differentiate the effects of hypoxia from phenology and location-specific characteristics. Two sampling sites, Union and Hoodsport, were located at the southern end of Hood Canal where hypoxia typically develops in the summer, and two were located in the northern region, Duckabush and Dabob, where oxygen levels usually remain higher (Figure 4.1). Southern sites and northern sites were selected based on bathymetry (Union is similar to Dabob, Hoodsport is similar to Duckabush). We sampled in every fourth week in 2012 and 2013 from early June to early October for a total of 5 sampling periods each year. Our goal was to monitor the system before, during, and after the onset of seasonal hypoxia. As fish feeding and zooplankton spatial distributions are known to have diel patterns, we sampled during the day and night during each sampling period. Hereafter,

sampling variables will be referred to as ‘site’, ‘year’, ‘month’, and ‘diel’ and a ‘sampling event’ refers to a single year-month-site-diel combination.

Oxygen Sampling

To characterize the dissolved oxygen (DO) profile of the water column, we performed CTD casts using a Sea-Bird Electronics SBE 911plus CTD equipped with a SBE 43 DO sensor. The DO sensor was annually calibrated by Sea-Bird and calibrated during field surveys with titrations conducted following the modified Winkler Method (Carpenter 1965). At each site, in each month, 2-4 profiles were conducted during both day and night. The data were processed into 1 m depth bins; environmental conditions were assumed to be horizontally uniform within each site.

Zooplankton Sampling

Zooplankton community composition was determined using a five net Hydro-Bios MultiNet system (https://www.hydrobios.de/product/multinet) equipped with 335-um mesh nets with a 0.25 m^2 mouth opening, double flowmeters, and a CTD sensor. Depth stratified tows were conducted at a speed of 2-4 knots for 1-7 minutes, depending on the thickness of the layer, and were conducted within the acoustic survey areas. Typically, two tows were conducted for each site -year-month-diel combination. Target sample depths were chosen based on backscatter densities observed on the echosounder conducted immediately prior to sampling. Samples were preserved in 5% formalin in seawater buffered with sodium borate and returned to the laboratory for analysis.

Acoustic Surveys

To determine distributions and densities of pelagic fish and zooplankton, acoustic backscattering data was obtained using a Simrad EK60 splitbeam echosounders operating at 38, 70, 120, and 200 kHza as described in Sato et al. (2016). All transducers were deployed attached to a pole on the side of the boat at 2m below the surface and had beam widths of 7°. The echosounders operated with a ping frequency of 0.5 – 2.0 pings s^{-1} with a pulse duration of 512μs. At each site acoustic surveys were performed over a grid of 6-8 parallel transects 500m apart at a boat speed of 5-6 knots. Within a site, the same grid of transects was used for the acoustic surveys during each sampling event.

Fish Sampling

We used midwater trawls to assess the fish community composition and to collect samples for quantifying fish feeding habits. A Marinovich midwater trawl with a 3.2 mm knotless liner in the codend was towed at a boat speed of 2-3 knots and outfitted with a real-time pressure sensor (PI50, Kongsberg Maritime). The vertical opening of the trawl net ranged from 4.8 – 7.0 m. Typically, we aimed to conduct 2 trawls at each year-site-month-diel combination, though the actual number of trawls varied from 1 to 4, for a total of 149 trawls. Trawl duration varied from 3 to 33 minutes depending on the observed backscatter density, but typically lasted for 8 minutes. Trawl depths were chosen to representatively sample the spatial distributions at the site, while also being targeted to depths where fish predators were most dense. During our study, zooplanktivorous fish was mainly comprised of Pacific herring, *Clupea pallasii*, and Pacific hake, *Merluccius productus* (Sato et al. 2015, Sato et al. 2016), so we focused on these two species. Often, we performed one tow through an acoustically-observed dense targeted

backscattering layer (typically hake) and a second that targeted discrete fish aggregations (typically herring).

Following capture, fish were separated by species, each species' catch was weighed using a digital bench scale, and then the number of individuals in each species was counted. When abundance was exceptionally high, > ~15kg, total abundance was estimated by subsampling a weighted portion of the total catch. For each trawl sample, we randomly sampled 100 individuals of each species to measure total lengths. When fewer than 100 were captured we measured all individuals.

To collect information on fish feeding habits, we sampled up to 50 herring stomachs and 50 hake stomachs from the trawls for each sampling event. We aimed to split these equally among the repeated trawls at each sampling event. However, not every trawl captured at least 25 Pacific herring and 25 Pacific hake. When one trawl captured fewer than 25 individuals, we preserved more stomachs from the other trawls in the same sampling event to reach 50 samples. Individual total lengths (mm) of the fish were measured, and stomachs were removed from the individual and preserved in ethanol.

4.2.2. Sample Processing

Zooplankton Sample Processing

Samples for each sampling event were subsampled to determine the zooplankton community composition for that site-month-year. The subsamples were identified to taxa which were counted and measured using the silhouette method (Davis and Wiebe 1985, Little and Copley 2003). Euphausiids were measured from the posterior base of the eye stalk to the end of the sixth abdominal segment (Mauchline 1980). For all other taxa total length was measured.

These counts were converted to biomass using previously derived length-weight relationships (Williams and Robins 1979, Webber and Roff 1995, Lavaniegos and Ohman 2007).

Acoustic Data Processing

Acoustic data were processed using Echoview (version 5.4; Echoview Software Pty Ltd). Vessel noise estimated during the acoustic surveys was removed by linear subtraction. Data shallower than 5 m depth were removed from analyses to eliminate near-field transducer effects and surface bubbles. Similarly, data within 0.5 m of the echosounder-detected bottom were removed from the analysis. Acoustic backscattering strength (Sv, dB re 1 m-1, Maclennan et al. 2002) was classified as zooplankton (dominated by euphausiids and copepods), herring, or hake based on distribution morphologies and backscattering frequency responses (Sato et al. 2015, Sato et al. 2016). Acoustic separation of herring from hake could not be done in the night data when both species migrated near surface and aggregations dispersed. The nautical area scattering coefficient (NASC; m^2 nmi^{-2}), which integrates backscatter through the water column and standardizes area to a square nautical mile, was calculated for all backscatter measurements along all transects at each site. Hereafter, NASC is referred to as 'backscattering density'.

Fish Sample Processing

To analyze individual fish feeding, each fish stomach was dissected open and all stomach contents were weighed together. Contents were then separated by taxonomic group and each group was weighed and counted. Contents that were too digested to identify were classified as 'unknown'. We aimed to process 20 stomachs per sampling event for each species, selected

randomly from the samples collected. If fewer than 20 were caught in a sampling event, which occurred 5 times for herring and 9 times for hake, then we processed all samples available.

As euphausiids were a dominant prey item, we sought to determine the euphausiid sizes consumed by hake and herring. We measured the length of individual euphausiids in a subset of fish stomachs under a dissecting microscope. Stomachs were chosen randomly. For the first 1,000 intact euphausiids measured across stomachs, we measured both carapace length and total length (measured from the base of the eye to the end of the sixth abdominal segment) so that we could estimate the ratio of the two and apply this ratio to euphausiids that were not intact. Euphausiid lengths were measured for each fish species for each month for a total of 898 euphausiids from hake stomachs and 1369 euphausiids from herring stomachs.

4.2.3. Data Analysis

Dissolved Oxygen

We sought to characterize the water quality, represented by DO level, in terms of expected impacts to marine life. Averaging DO over the water column would not provide an accurate measure of the severity of DO conditions to organisms, as biological responses to oxygen can be non-linear (Pollock et al. 2007, Hrycik et al. 2017) and as an average would not incorporate factors such as phytoplankton blooms. Another way to describe conditions is to calculate the proportion of the water column below a prior defined threshold DO value (e.g. 2.0 mg l^{-1}); however, pilot analyses indicated that subsequent statistical results were highly sensitive to the choice of the threshold DO values. To solve these problems, we created a 'Dissolved Oxygen Score' (DO score) that incorporates the vertical extent of the water column with low oxygen and the intensity of oxygen depletion into a single, continuous variable, such that

$$s(DO_i) = \begin{cases} 0 & DO_i > DO_{thresh} \\ f(DO_i) & \text{otherwise} \end{cases}.$$

where DO_{thresh} is the threshold value chosen for where low DO begins to affect marine life and DO_i is the observed dissolved oxygen at depth *i*.

We explored two alternatives for $f(DO_i)$, though both share the common attribute of growing larger as DO_i decreases. We considered a linear function, which would suggest the marginal effect of DO depletion is constant as DO decreases,

$$f(DO_i) = \beta_0 + \beta_1 DO_i,$$

where β_0 is the index score at $DO = 0$ and β_1 is the degree of response, or how much the DO score changes for a 1mg l^{-1} change in DO. This model can be parameterized by specifying DO_{thresh} and f_{ref} where f_{ref} is the value of $f(DO_i)$ when DO_i = 2 mg l^{-1}. As an alternative function, we also explored a log-linear function, such that

$$f(DO_i) = \exp(\beta_0 + \beta_1 DO_i).$$

We parameterized this model using the same DO_{thresh} and f_{ref} values as above. In all cases, we averaged $s(DO_i)$ across all evenly-spaced increments of the water column to generate a scalar that describes DO conditions at the sampling site.

Because the DO values at which biological responses will occur varies among species and systems, we conducted sensitivity analysis by generating DO scores under alternative assumptions of DO_{thresh} and f_{ref}. We considered values of DO_{thresh} = 3 mg l^{-1} and 5 mg l^{-1} for the linear model. Separately, we also parameterized DO_{thresh} and f_{ref} (DO_{thresh} = 4 mg l^{-1}; f_{ref} = 1 at DO = 4 mg l^{-1}) so that it was equivalent to the proportion of water column that had DO below 4 mg l^{-1}.

Bayesian Analyses

We assessed the effect of DO score on the measurements of interest (stomach fullness, diet composition, Pacific herring biomass, Pacific hake biomass, and prey availability) by fitting a linear mixed effects model in a Bayesian framework. The multi-level Bayesian framework allowed us to propagate uncertainty in estimated hypoxia effects on measured quantities (fullness, diet composition, acoustic density, prey availability) and through to derived quantities (per-capita feeding, population-level consumption, relative consumption). Our approach involved fitting the response variable to a model with year, diel, month, and DO score as fixed effects, and site as a random effect to account for lack of independence of samples collected in the same site (Gelman 2014). This framework allowed us to separate site effects from low DO effects, while also modeling seasonal trends. However, it assumed month, diel, and year effects are consistent across sites (e.g., June vs. October has the same effect at each site).

Our base approach to all analyses is to fit linear models with multi-level effects of sampling site and fixed effects for time of day, year, and month. Thus, for any response variable:

$$\mathbf{y} = \beta\mathbf{X} + u\mathbf{Z} + \epsilon$$

where y is vector of observations, X is the model matrix for fixed effects, Z is the model matrix for site effects, β and u are vectors of fixed effect and random effect coefficients, respectively. ϵ is a vector of residuals, assumed to be normally distributed with mean of 0 and standard deviation σ. The standard deviation consists of two components, the model error (σ_{model}) which is estimated, and the observation errors (σ_{obs}) that are quantified outside of the estimation routine:

$$\sigma = \sqrt{\sigma_{model}^2 + \sigma_{obs}^2}$$

The multi-level parameters (site effects) were assumed to follow from a normal distribution with mean equal to μ_μ and standard deviation σ_μ. Data were transformed as needed to be approximately normal: diet fraction was logit transformed, while stomach fullness index and acoustic data were log transformed.

We used weak priors on parameters to aid in model convergence. As per convention, we used Cauchy priors for $\beta_{i,j}$ with location and scale parameters set to 0 and 2.5, respectively (Gelman 2006). A location parameter of 0 represents our prior belief that there are roughly equal odds of a positive or negative effect of each predictor. A scale parameter of 2.5 means that a coefficient of 2.5 is presumed one-half as likely as a coefficient of 0. We used half Cauchy priors for all σ parameters, with location set to 0, where σ_{model} had its scale parameter set to 2.5 and σ_u set to 1. The more restricted prior for σ_u was necessary because with only 4 sites convergence issues arose when it was less constrained. Priors for site effects were also weak, so that $\mu_\mu \sim$ Cauchy (x, 2.5) where $x = 0$ for logit diet fraction, log fish density, and log prey availability and $x = -3$ for log fullness. The location parameter of -3 was based on the log fullness data mostly ranging from -5 to -2.

All Bayesian analyses were run in Stan (Stan Development Team 2017b) with the NUTS (no u-turn sampling) algorithm (Homan and Gelman 2014, Carpenter et al. 2017, Stan Development Team 2017b), using rstan v. 2.15.1 (Stan Development Team 2017a), run in R v 3.4.0 (R Core Team 2017). Models were run with 3 chains of 10,000 iterations each, plus a warm-up period of 5,000 iterations. Chains were not thinned. Models outputs were checked to ensure no divergent transitions occurred, and for convergence by looking for the scale reduction, $\hat{R}$, to be near 1 (Gelman and Rubin 1992). Posterior predictive checks were visually analyzed to evaluate model fit.

Measured Quantities

Using this Bayesian model framework, we sought to model each of the individual and population-level quantities we measured directly: stomach fullness, diet composition, Pacific herring backscattering density, Pacific hake backscattering density, and prey availability.

Stomach fullness indices for each stomach were calculated from total stomach contents' mass and length using the standard equation,

$$fullness = \left(\frac{stomach\ content\ mass}{fish\ length\ (mm)^3}\right) * 100$$

Diet composition for the predators was estimated from stomach contents. For this, we used the estimation model from Moriarty et al. (2017). Stomach masses were variable and sometimes contained covariance between total stomach contents' mass and the importance of a particular prey taxa, as well as sporadic individuals with much higher consumption amounts than the rest of the individuals in that trawl. The Moriarty et al. (2017) method is similar to a weighted mean, but specifically accounts for these issues in the diet proportion estimates, making it preferred here. We created a Bayesian version of this model, which provided more robust estimates of observation error and variance. Uninformative priors were chosen for all parameters (Supplement A4).

Prey and predator biomasses were approximated using acoustic backscatter. Backscattering densities can be converted to biomass estimates using additional assumptions. However, as we seek to document relative changes in energy flux, and not absolute changes, we avoided making these additional assumptions and used backscattering density as an index of biomass. As separate acoustic densities could not be estimated for Pacific herring and Pacific

hake at night, we approximated the nighttime densities using the daytime densities. This required the assumption that fish remain in the same site between day and night.

The availability of prey depends on the zooplankton community biomass and composition, as well as size selectivity of the predators. Preliminary analysis of stomach contents indicated that euphausiids were a dominant prey for both Pacific herring and Pacific hake, with amphipods as a secondary prey. As a result, we focused our analysis on energy flow from euphausiids and amphipods to Pacific hake and herring. Total euphausiid acoustic density was calculated from the zooplankton acoustic density and proportion of the zooplankton biomass that was euphausiids as determined from the zooplankton net tows.

Zooplanktivorous fish are frequently size selective, so the availability of euphausiids as prey is not necessarily equivalent to the biomass of euphausiids in the system. From the size distribution of euphausiids in stomachs of each herring and hake, we used the 25^{th} percentile to estimate the minimum preferred size for each predator species. Then, we calculated the proportion of the euphausiid community that was above this size in each month and year. For amphipods, data on preferred size was not available, so we assumed that there was no size selectivity.

For each year-month, these measurements were combined to estimate prey availability of euphausiids. Prey availability was measured as the product of zooplankton acoustic density, proportion of zooplankton by biomass that was euphausiids, and the proportion of euphausiids at the size consumed by fish,

$$prey\ available = S_A * p_e * \ p_s,$$

where p_e is the proportion by biomass of the zooplankton population that is euphausiids and p_s is the proportion of the euphausiid population that is the preferred size. Similarly, amphipod availability was calculated from

$$prey\ available = S_A * p_a,$$

where p_a is the proportion of the zooplankton population that was amphipods. Noe that as amphipod availability does not consider size selectivity and as different taxa have different backscattering densities, which is not incorporated in these calculations, euphausiid and amphipod availability indices are not directly comparable. Each, however, does indicate relative changes between sites, months, and years for that taxa.

Derived Quantities

We additionally sought to assess how the observed DO levels affected the derived quantities: per capita feeding of each predator on each prey type (the product of prey composition and stomach fullness index), the population-level consumption of each predator of each prey type, and the ratio of consumption to prey biomass. Per-capita feeding was calculated as the product of stomach fullness and the diet composition of the predator. We fit the probability densities, β and μ, for both diet proportion and fullness simultaneously, and propagated uncertainty in those terms to estimate the probability density function of predicted per capita feeding rate, $\hat{p}$. For each site, year, month, diel period combination, given the observed DO metrics:

$$\hat{p} = \exp(\beta(f)\boldsymbol{X} + u(f)\boldsymbol{X}) * \ logit^{-1}(\beta(c)\boldsymbol{X} + u(c)\boldsymbol{Z}),$$

where $\beta(f)$ and $\mu(f)$ are the estimated coefficients fit to log-fullness, and $\beta(c)$ and $\mu(c)$ are the estimated coefficients fit to to logit(c).

Population-level consumption was calculated from per-capita consumption and acoustic backscattering densities. Uncertainty in the density and per-capita feeding estimates was propagated forward, such that

$$\hat{\rho} = \hat{p} * (\exp(\beta(a)\boldsymbol{X} + \mu(a)\boldsymbol{X}),$$

where $\hat{\rho}$ is the predator's population level consumption, $\beta(a)$ and $\mu(a)$ are the estimated estimated coefficients fit to log-backscattering density.

Finally, relative consumption of the prey type ($\hat{r}$) by the predator was calculated from total population consumption and prey availability,

$$\hat{r} = \frac{\hat{\rho}}{\exp(\beta(z)\boldsymbol{X}+\mu(z)\boldsymbol{X})},$$

where $\beta(z)$ and $\mu(z)$ are the estimated coefficients fit to log-prey availability.

From these estimated coefficients, we predicted each derived quantity for each sampling event. We made these predictions under two scenarios: 1) the observed DO conditions and 2) an alternative scenario when there was no hypoxia. From these predictions, we estimated the probability that the observed DO led to an increase or decrease in the derived quantities. We considered an ecologically significant change as being more than a 20% change in the derived quantity value. Therefore, our metric of detecting an effect of DO was the difference in the probability of an increase and the probability of a decrease,

$$\hat{e} = P(> 20\%\ Increase) - P(> 20\%\ decrease)$$

where $\hat{e}$ is the estimated effect of DO. This results in a metric that can range from 1 to -1, where 1 indicates a high probability that low DO led to an increase in the derived quantity, 0 indicates there is no evidence of a change due to DO, and -1 indicates a high probability of a decrease in the derived quantity due to low DO.

We also employed 10-fold cross validation for the measured quantities as a model selection technique to determine the importance of each variable. Cross-fold validation estimates the effect of a subset of the data on the estimated parameter values (Hooten and Hobbs 2014). It excludes a subset of the data, fits the models, predicts the out-of-sample data, and compares those predictions to the actual out-of-sample data. Here, we split the data into 10 groups and performed this process while excluding each group. To compare models using cross-validation results, we used the sum of the score for each group, such that each group's score is the average of the likelihoods of the removed data given the parameters for each of the MCMC iterations. The sum was then multiplied by -2 to be consistent with traditional model selection techniques (Hooten and Hobbs 2014), such that a smaller value means the model had a better fit. That is,

$$\text{Score} = -2 * \sum_{k=1}^{10} \log\left(\frac{\sum_{t=1}^{T}[y_k|y_{-k},\theta^t]}{T}\right).$$

The scores from this 10-fold cross validation were compared between models that did and did not include DO score as a predictor. This allowed us to determine whether including DO score improved our ability to predict the quantity of interest.

4.3. RESULTS

4.3.1. Dissolved Oxygen

All sites reached at least mild hypoxia, with portions of the water column having DO < 4 mg l^{-1} at some times. Sites Union and Hoodsport in the south exhibited higher DO scores (e.g., more hypoxia) in all months than the northern sites, Duckabush and Dabob (Figure 4.2, Figure B4.1). A seasonal cycle was evident in both years, where DO score increased from early to late

season. In 2012, the difference in DO score between the southern sites and northern sites increased over the course of the season, as three of the four sites continued to experience increased hypoxic conditions through October. In 2013 the hypoxic cycle differed such that DO scores peaked at all sites in September and then decreased in October.

4.3.2. Measured Quantities

Herring diet composition was dominated by euphausiids with amphipods of secondary importance (Figure B4.2). Model selection procedures supported a model including year, diel, and site effects (Table 4.1), suggesting that DO was not an important factor driving feeding preferences. This was supported by the full model estimate of $\widehat{\beta_{DO}}$ = -0.38 with a wide prediction interval that includes zero (95% PI = (-1.8, 0.99)).

Euphausiids were also the main prey of Pacific hake, though amphipods were less important than for herring (Figure B4.2). Similarly to the herring, cross-validation did not provide support for models that included DO score, suggesting that DO did not have an influence on hake diet composition (Table 4.2). This finding was further supported by posterior probabilities of the model coefficient estimate of DO ($\widehat{\beta_{DO}}$ = -0.15, 95% PI = (-1.92, 1.59)) in the full model.

Pacific herring stomach fullness was highly variable. Mean fullness did not show clear trends across the season, though it did reach higher rates at the northern sites than at the southern sites (Figure 4.3). Model fits of mean stomach fullness were less variable and elucidated a seasonal pattern among sites. Mean fullness was greatest in the early and latest sampling months. Analysis of Pacific herring stomach fullness revealed poor evidence for an effect of DO on fullness. Models that did not include DO score were slightly preferred by our model selection

procedure (Table 4.1). Additionally, model DO score coefficient estimates were slightly negative (e.g., fullness increased with oxygen levels), but again spanned zero ($\widehat{\beta_f}$ = -0.30, 95% PI = (-1.57,0.95)).

Similarly, there was no evidence of an effect of DO on stomach fullness of Pacific hake. Models that did not include DO had the strongest support (Table 4.2), consistent with model coefficient estimates supported ($\widehat{\beta_f}$ = -0.08, 95% PI = (-1.47, 1.31)).

Backscattering densities of Pacific herring were highly variable over the season and between years without a clear difference among sites (Figure 4.4). Model fits remained variable, though showed some seasonal trends. Fitted densities were higher in July and September largely due to high observed backscattering densities in sites Union and Dabob. However, in 2013, fitted backscattering densities were far less variable and were largely constant over the season and among sites. Models without a term for DO were selected by cross-validation (Table 4.1), which agrees with this high variability and low evidence of a pattern. Similarly, model coefficient estimates did not indicate an effect of DO on backscattering densities ($\widehat{\beta_a}$ = 0.90, 95% PI = (-0.27, 2.01)).

Pacific hake acoustic densities were also highly variable among months in both years (Figure 4.4). Model fits for Pacific hake in 2012 were opposite to that of herring at the southern sites, where hake acoustic densities decline in July and September. However, in 2013, the acoustic densities peak in July and September. Models that do not include DO score as a predictor were selected using cross-validation (Table 4.2). Again, model coefficient estimates for the full model agreed, as $\widehat{\beta_a}$ = -0.01 (95% PI = -0.73, 1.64).

Euphausiid availability for herring and hake consumption was variable, but increased over the season at most sites (Figure 4.5). Model fits reflected this trend and were higher in the

late season at all sites and years. Models that included DO score did have the strongest support for prey availability of both Pacific herring and hake (Tables 4.1, 4.2). Model coefficient estimates indicated a potential negative effect of DO score (e.g., prey availability decreased with increasing hypoxia), though the prediction intervals still included 0 (hake: $\widehat{\beta_p}$ = -1.60, 95% PI = (-3.55, 0.25), herring: $\widehat{\beta_p}$ = -1.58, 95% PI: = (-3.53,0.26)). This pattern of a negative DO score effect was driven by a large increase in euphausiid availability in the northern sites that was either absent or heavily dampened in the southern sites (Figure 4.5).

4.3.3. Derived Quantities

There was marginal evidence suggesting that Pacific herring per-capita consumption of euphausiids decreased with intensified hypoxia (Amphipods shown in supplement B4). We calculated the ratio of predicted mean per-capita consumption when DO score was 0 (no hypoxia) compared to the predicted levels when DO scores were nonzero (from here on referred to as the 'proportional change'). The median proportional change declined in the southern sites, though the posterior variance was large, leading to large credibility intervals (Figure 4.6). We further assessed the role of DO by calculating the difference in posterior probabilities of a 20% increase in per capita consumption and 20% decrease. This metric suggested that DO was about 50% more likely to have induced a decline than an increase, especially in 2013 (Figure 4.6). In contrast, the northern sites showed no change over the season because DO levels were generally high.

Per-capita consumption of Pacific hake showed no evidence of a DO effect (Figure 4.7). The proportional change for per-capita consumption was constant across sites, though credibility intervals were again large. The probability of an increase in per-capita consumption was

approximately equivalent to the probability of a decrease at all sites, supporting this lack of effect.

There was weak evidence that population level consumption was affected by hypoxia for both Pacific herring and hake (Figure 4.8, 4.9). The median proportional change of the population-level consumption increased at the southern sites in the late season for herring, though did not change for hake. The southern sites also had larger credible intervals than the northern sites. For herring, the southern sites also exhibited a slightly greater probability of an increase than a decrease in population-level consumption, suggesting that for herring, population-level consumption may have mildly increased under hypoxia.

There was modest evidence that relative consumption of euphausiids (the ratio of fish consumption to prey availability) increased with hypoxia for both Pacific herring and hake (Figures 4.10, 4.11). For both species, the median proportional change increased in the southern sites, while remaining constant at the northern sites. However, the prediction intervals were quite large, as the model predictions incorporates uncertainty from multiple measured variables. Despite the large credible intervals, the probability that hypoxia increased relative consumption approaches 1 for the southern sites for both hake and herring.

4.3.4. Sensitivity Analyses

While coefficients and predictions varied with different ways of calculating DO conditions, the overall patterns were similar. The strength of model results was marginally sensitive to the choice of threshold in the DO score. When $DO_{threshold} = 3\ mg\ l^{-1}$ was used, the effects of DO on fullness, backscattering densities, and prey availability were weakened,

although the direction of the effects remained consistent. When $DO_{threshold} = 5\ mg\ l^{-1}$, acoustic density estimates were unaffected, though the effect on prey availability decreased.

Model performance was poor when a linear relationship was assumed compared to a log-linear relationship. When a linear model was used, the model severely underfit fullness and prey available.

4.4. DISCUSSION

Predicting ecological changes over a range of resolutions reveals different and more nuanced conclusions than if only a single analytic resolution such as individual or population processes were considered. Individual and population level processes (e.g. feeding and abundance) for fish remained constant for both herring and hake under hypoxic conditions. Yet, a decrease in euphausiid availability with hypoxia led to a change in relative prey consumption: a systems-level process. Including physiological, behavioral, and population processes that influence predator-prey interactions is necessary to reveal how hypoxia affects energy transfer in aquatic food webs.

These results demonstrate the importance of measuring ecological processes at individual, population, and system scales. As discussed in Sato et al. (2016), the lack of changes in spatial overlap between fish and euphausiids due to hypoxia is counter to observations reported from other regions (Ludsin et al. 2009, Vanderploeg et al. 2009, Zhang et al. 2009, Ekau et al. 2010). Furthermore, the total density of zooplanktivores was not sensitive to DO levels observed during the study. This indicates that fish in Hood Canal may be more resilient to mild hypoxia (DO < 4 mg l^{-1}) than expected, perhaps because there are advantages to remaining in low DO areas that we have not discerned, or the cool temperatures lead to a lower O_2

requirement (Sato et al. 2016). It is also possible that while acoustic densities were unchanged by hypoxia, individual fish did not spend long periods of time in hypoxic waters. If their euphausiid prey remained in hypoxic areas, there may have been foraging advantages for fish to feed in hypoxic waters and then leave (Rahel and Nutzman 1994, Roberts et al. 2012), which would not change population-level consumption. As Hood Canal is naturally prone to seasonal hypoxia that has been occurring for decades, the existing food webs there may be more resilient to this environmental stressor. This may be particularly true for the years we sampled, as observed DO was typical for Hood Canal (Dunne et al. 2002).

Spatial overlap between predators and their prey is commonly thought to be a proxy for energy transfer, such that changes in spatial overlap are often believed to directly propagate to changes in energy flux (Ludsin et al. 2009, Vanderploeg et al. 2009, Zhang et al. 2009, Pothoven et al. 2012). During this study time, spatial overlap between predators and prey was maintained in Hood Canal (Sato et al. 2016); yet, there was some evidence of an increase in the relative consumption of euphausiids by herring and hake. By simultaneously measuring consumption, diet, densities, and prey availability, we found a more nuanced picture of how hypoxia affects trophic energy flow. Given the connected nature of ecological processes, assumptions that one ecological process is solely responsible for the outcome of another is likely to be invalid in most situations.

The weak effects of hypoxia on fish feeding and densities in Hood Canal contrast to those observed in other systems and in laboratory experiments, emphasizing the importance of *in situ* observations. Changes in feeding due to the formation of hypoxia have been observed in many systems for a range of fish species (Pollock et al. 2007), potentially limiting growth (Pörtner and Knust 2007). As hypoxia is a long occurring, natural phenomenon in Hood Canal

(Brandenberger et al. 2011), organisms in this system may be adapted to these environmental conditions. In other regions prone to hypoxia, fish are known to have adapted to allow them to survive, grow, and reproduce under hypoxia or even anoxia (Val et al. 1998, Mandic et al. 2009), particularly if the hypoxia co-occurs with other environmental stressors (Pörtner et al. 2005).

Our modeling framework required several assumptions about the measurements and analysis that may affect the results. First, we used acoustic density to represent biomass, as is commonly done (Demer and Hewitt 1995, Ott 2005, Sato et al. 2015). Backscatter is typically converted to biomass by assuming a relationship (Foote 1983) between reflected energy, density, and biomass, and choosing appropriate scalers to represent energy reflected from an average individual and the conversion from length to biomass for each classified species. By using relative backscattering densities, we did not have to choose scalar values. Additionally, the DO score we created avoided choosing a single threshold at which organisms are affected by low DO, but did require making a semi-arbitrary choice for parameter values. Ideally, the choice of the threshold would be based on knowledge of species' physiological tolerances. Unfortunately, not a lot is known about herring and hake DO tolerances, but many pelagic fish exhibit altered behaviors at < 4 mg l^{-1} O_2 (e.g. Pollock et al. 2007, Parker-Stetter and Horne 2009, Hrycik et al. 2017), which formed the basis for our choice of threshold. Finally, both midwater trawling and zooplankton net tows are known to be size selective. As an example, our trawls caught the same length of Pacific herring from spring through fall, though we recognize that the individuals in the population almost certainly grew over that period. Similarly, larger euphausiids preferentially escape zooplankton nets. We chose not to use a correction factor for this escapement, as the best estimate for an escapement correction is linear with length (Wiebe et al. 2013) and would not affect interpretation of our results.

Our research creates a framework for assessing responses to ecological stressors across individuals, populations, and ecosystems. Through our framework of nested hypotheses, we were able to measure changes in physiological, behavioral, and population processes and determine how those influence energy flow. This framework allows for simultaneously measuring multiple ecological processes at different resolutions then merging them to create a detailed analysis of how the ecosystem is responding to environmental change. With continued environmental change, understanding ecological effects at higher resolutions and integrating them to understand effects at the ecosystem scale will continue to be vital. Hood Canal presented a unique opportunity for this paired-site study design.

This integrated analysis framework is particularly beneficial for combining multiple environmental measurements. The necessity of this type of assessment framework for making ecological predictions was recently noted by Breitburg et al. (2018).The challenge of quantitatively measuring environmental effects on marine fish has also been previously noted (Rose 2000). In particular, Rose (2000) noted the challenge, but importance, of including community interactions, as well as the necessity of regional predictions. Our study conclusions support both of these as being necessary. Interpretation of our results would not have been obtained without considering multiple ecological processes and their interactions, as well as studying a region that may be more adapted to hypoxia than many other systems.

Table 4.1 Scores for the 10 fold cross-validation analysis. Each column is a variable measured for Pacific herring consuming euphausiids. Lower scores indicate a better fit by the model.

Model	**Fullness**	**Diet Composition**	**Acoustic Density**	**Prey Available**
Year + Diel	175.30	220.71	90.98	343.97
Year + Diel + Month	180.43	212.45	95.48	315.53
Year + Diel + DO	177.67	220.83	84.04	342.58
Year + Diel + Month + DO	181.72	214.44	91.92	313.25

Table 4.2 Scores for the 10 fold cross-validation analysis. Each column is a variable measured for Pacific hake consuming euphausiids. Lower scores indicate a better fit by the model.

Model	**Fullness**	**Diet Composition**	**Acoustic Density**	**Prey Available**
Year + Diel	117.38	141.74	110.95	343.67
Year + Diel + Month	109.02	141.33	117.51	313.14
Year + Diel + DO	119.00	143.58	114.70	341.88
Year + Diel + Month + DO	110.50	143.37	119.77	310.30

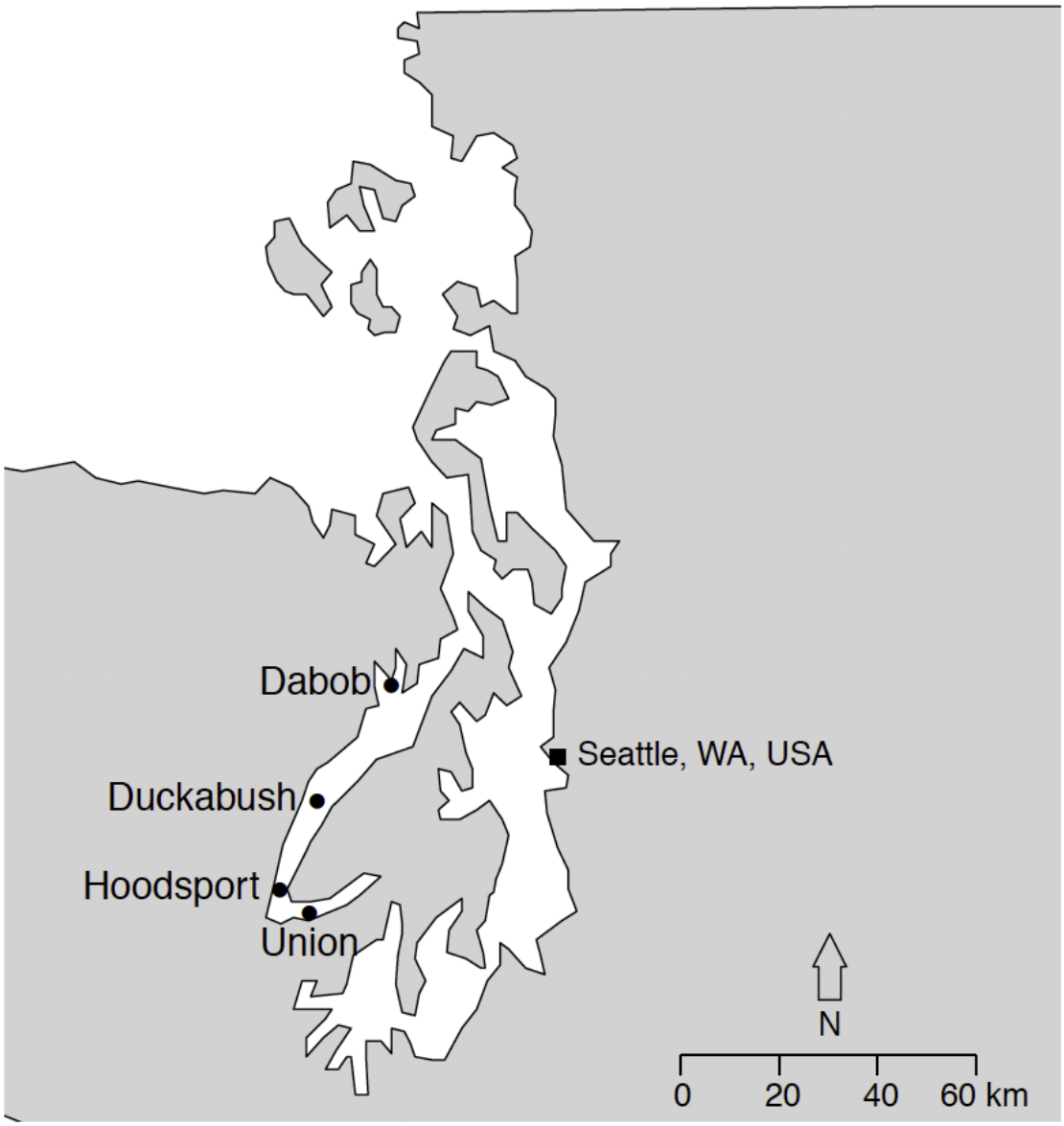

Figure 4.1 Map of the study area, Hood Canal, in Washington, USA. Black circles indicate the sampling sites.

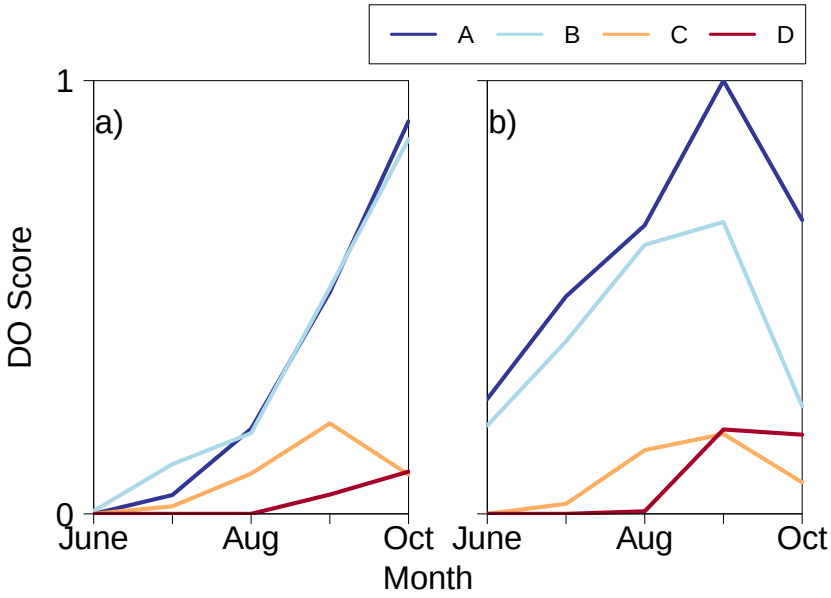

Figure 4.2 Dissolved oxygen levels at each sampling site over the season in both a) 2012 and b) 2013 (red). A dissolved oxygen score of 1 indicates the entire water column had DO < 4mg l^{-1}, while a score of 0 indicates none of the water column had DO < 4 mg l^{-1}.

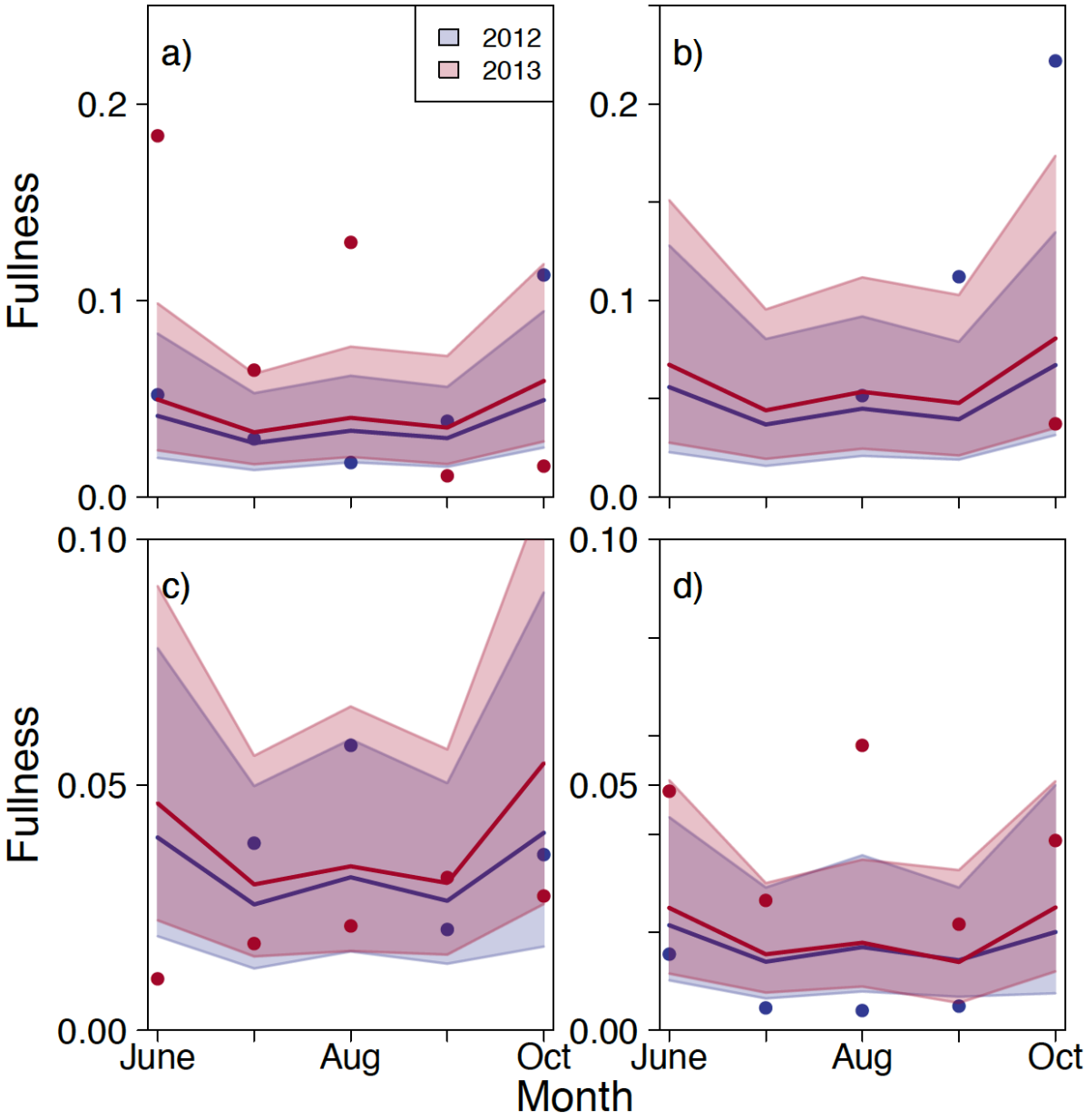

Figure 4.3 Stomach fullness for Pacific herring at sites a) Dabob, b) Duckabush, c) Hoodsport and d) Union (note that the y axes differ between plots). Stomach fullness is a function of mass of stomach contents and the length of the individual fish. Points are mean stomach fullness for Pacific herring caught at that site, month, and year. Lines are the mean model prediction and shaded areas represent the 95% prediction intervals.

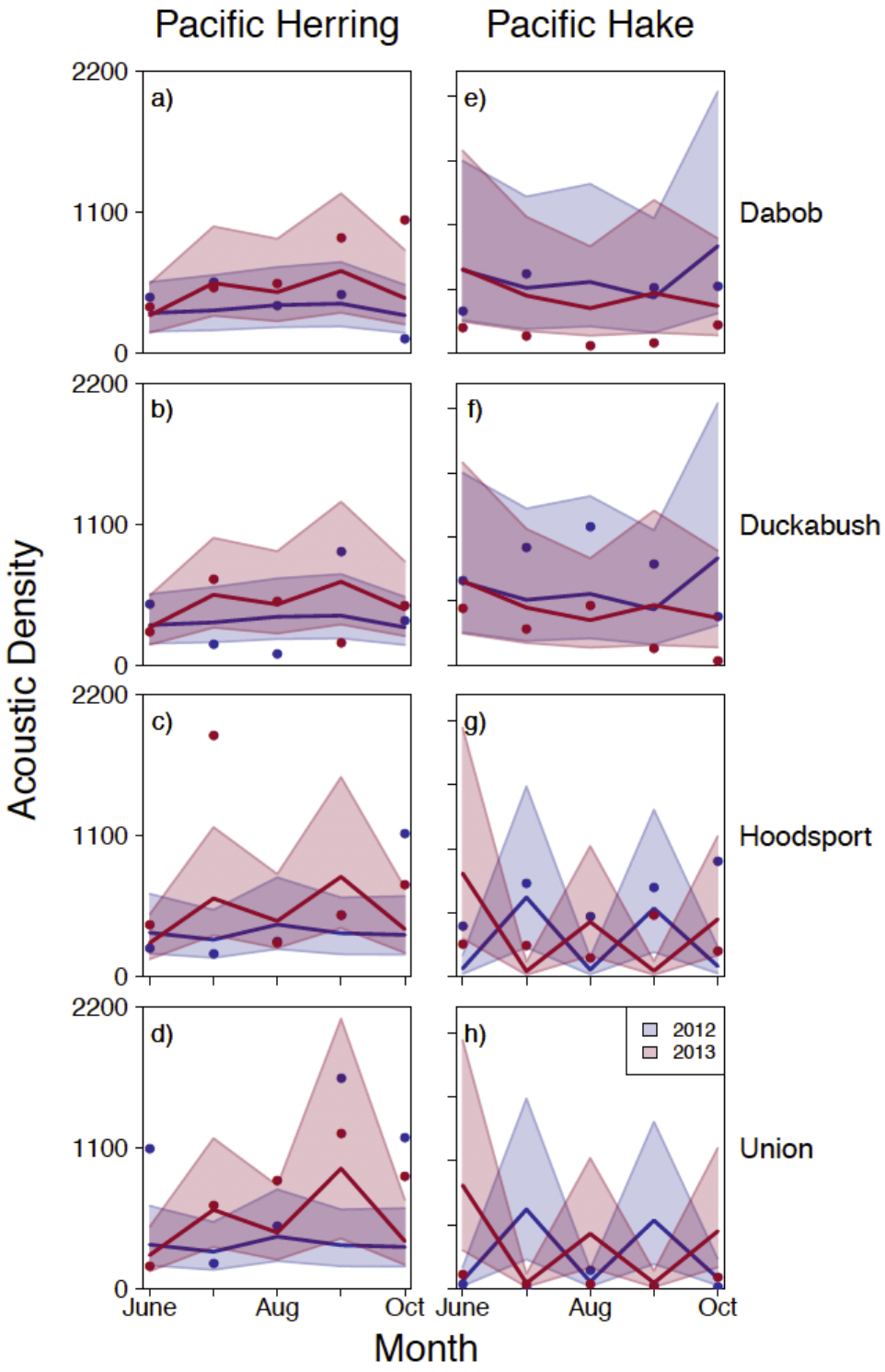

Figure 4.4 Acoustic densities for Pacific herring (a-d) and Pacific hake (e-h) at Union (a,e), Hoodsport (b, f), Duckabush (c, f), and Dabob (d, h) (units = m^2 nmi^{-2}). Points are mean acoustic densities for each species at that site, month, and year. Acoustic densities were averaged over the water column along each transect and then across transects. Lines are the mean model prediction and shaded areas represent the 95% prediction intervals.

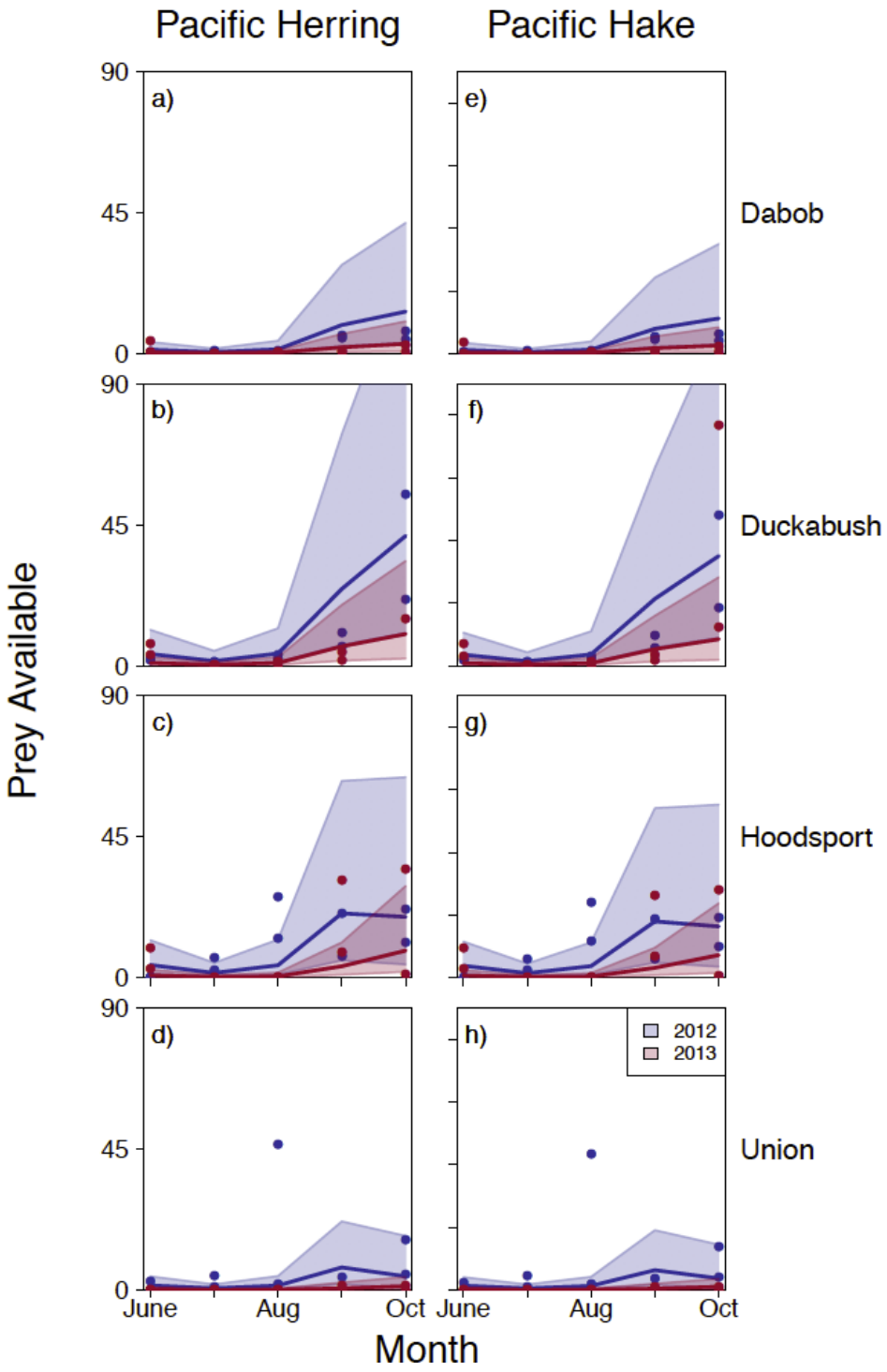

Figure 4.5. Euphausiids available for consumption by Pacific herring (a-d) and Pacific hake (e-h) at Union (a,e), Hoodsport (b,f), Duckabush (c,g), and Dabob (d,h) (units = m^2 nmi^{-2}). Prey availability is a function of zooplankton community composition, size selectivity by the predator in that month, and zooplankton acoustic densities. Points are mean prey availability for that species at that site, month, and year. Lines are the mean model prediction and shaded areas represent the 95% prediction intervals.

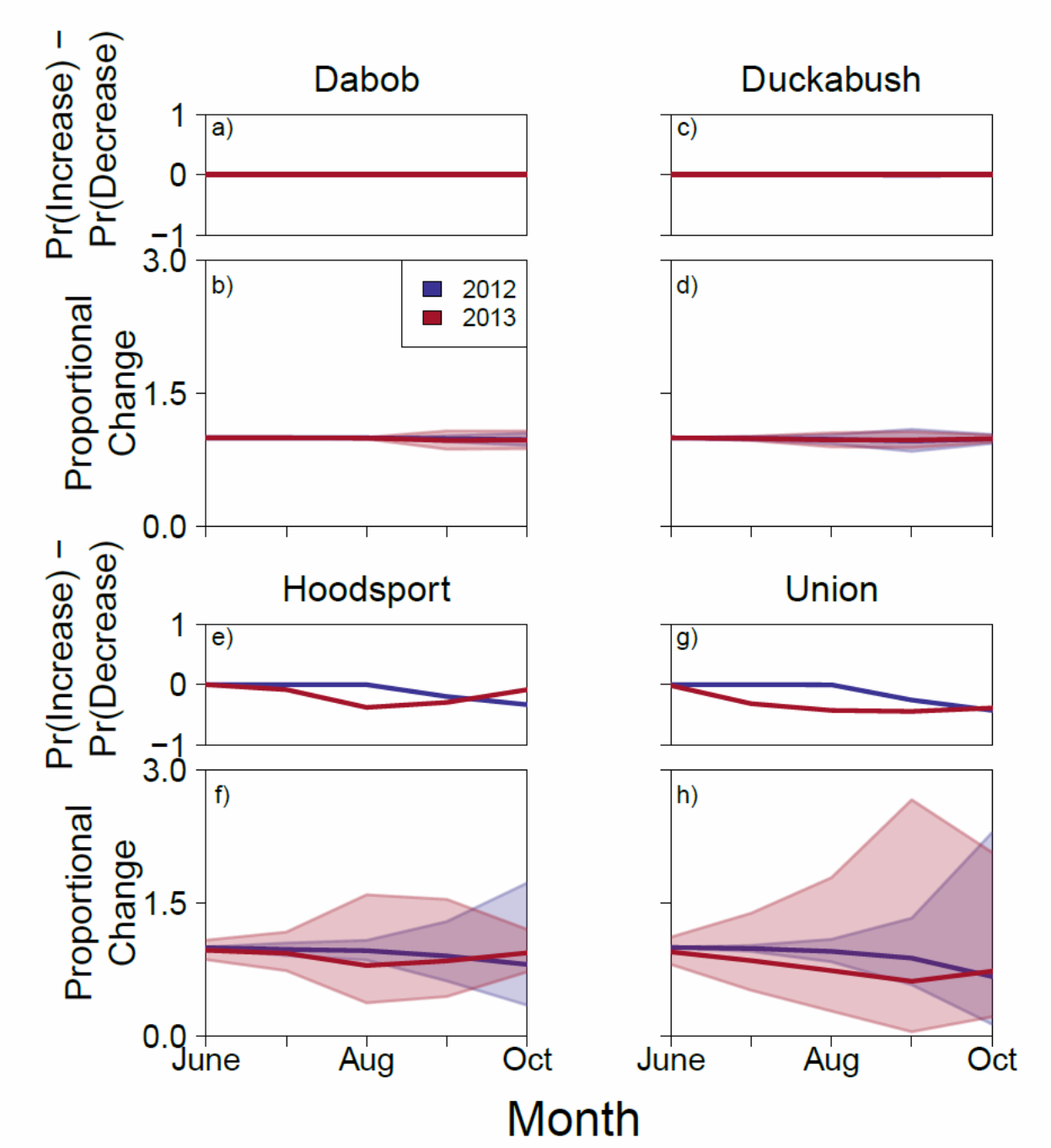

Figure 4.6 The difference in predicted mean per-capita consumption under actual hypoxic conditions and no hypoxia by Pacific herring over the season at Union (a, b), Hoodsport (c, d), Duckabush (e, f), Dabob (g, h). Per-capita consumption depends on stomach fullness and diet composition of the predator. Top panel in each panel pair depicts the difference in the probabilities of at least a 20% increase in per-capita consumption and a 20% decrease in per-capita consumption. The lower panel in each panel pair depicts the proportional change of per-capita consumption. The line is the mean predicted proportional change and the shaded area shows the 95% prediction intervals.

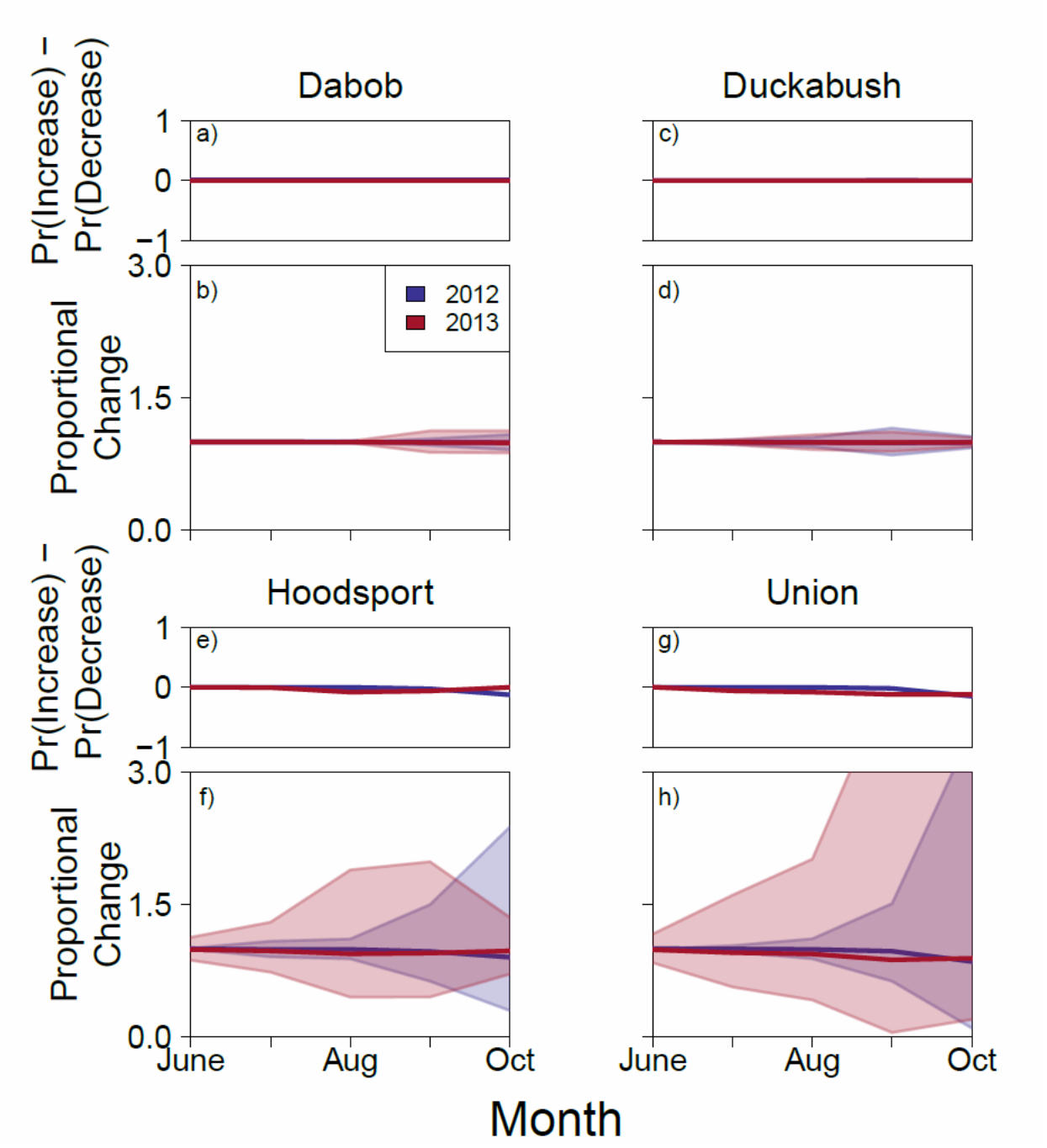

Figure 4.7 The difference in predicted mean per-capita consumption under actual hypoxic conditions and no hypoxia by Pacific hake over the season at Union (a, b), Hoodsport (c, d), Duckabush (e, f), Dabob (g, h). Per-capita consumption depends on stomach fullness and diet composition of the predator. Top panel in each panel pair depicts the difference in the probabilities of at least a 20% increase in per-capita consumption and a 20% decrease in per-capita consumption. The lower panel in each panel pair depicts the proportional change of per-capita consumption. The line is the mean predicted proportional change and the shaded area shows the 95% prediction intervals.

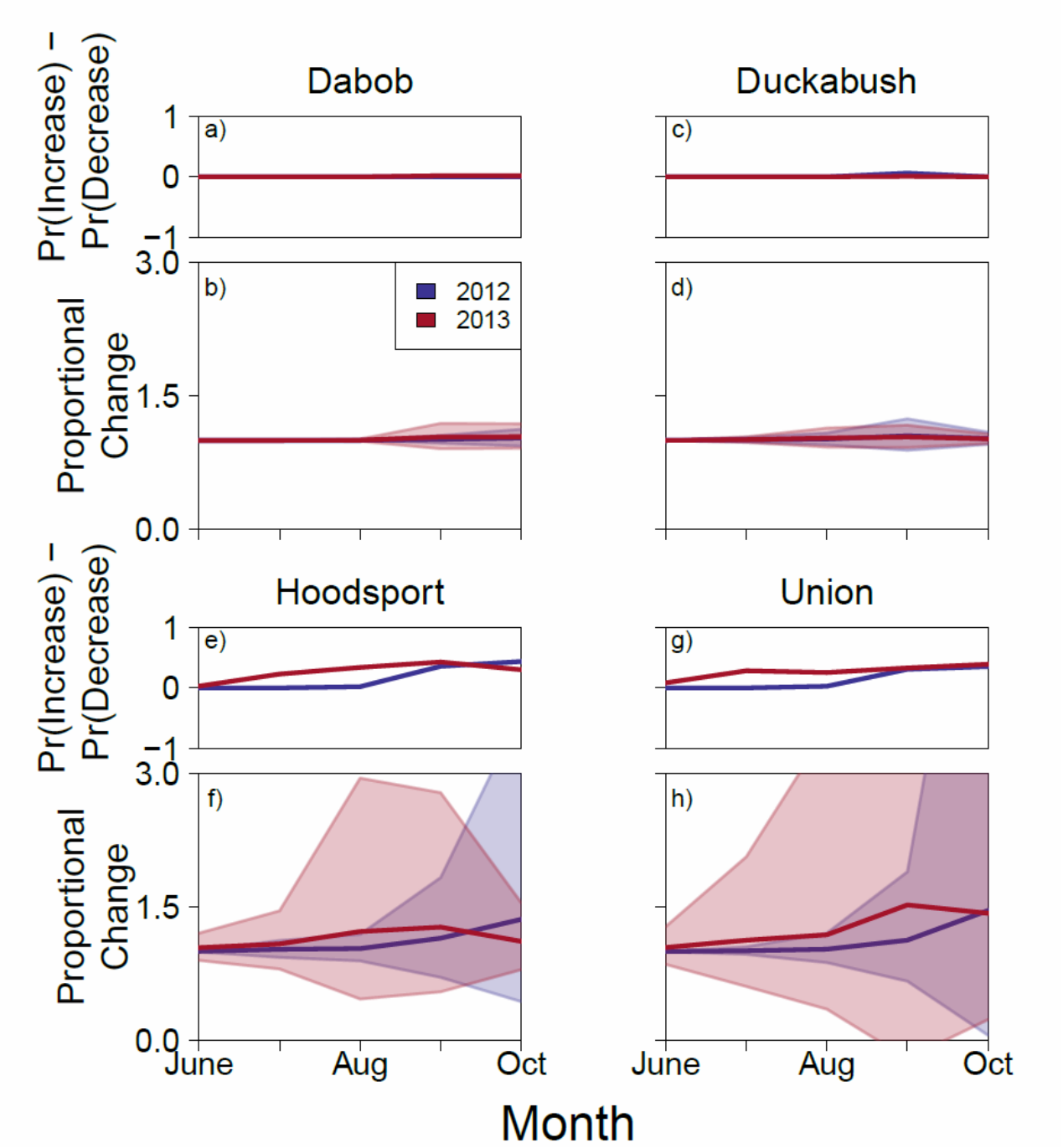

Figure 4.8 The difference in predicted mean population consumption under actual hypoxic conditions and no hypoxia of euphausiids by Pacific herring over the season at sites Union (a, b), Hoodsport (c, d), Duckabush (e, f), Dabob (g, h). Population-level consumption depends on per-capita consumption and acoustic density of the predator. Top panel in each panel pair depicts the difference in the probabilities of at least a 20% increase in per-capita consumption and a 20% decrease in per-capita consumption. The lower panel in each panel pair depicts the proportional change of per-capita consumption. The line is the mean predicted proportional change and the shaded area shows the 95% prediction intervals.

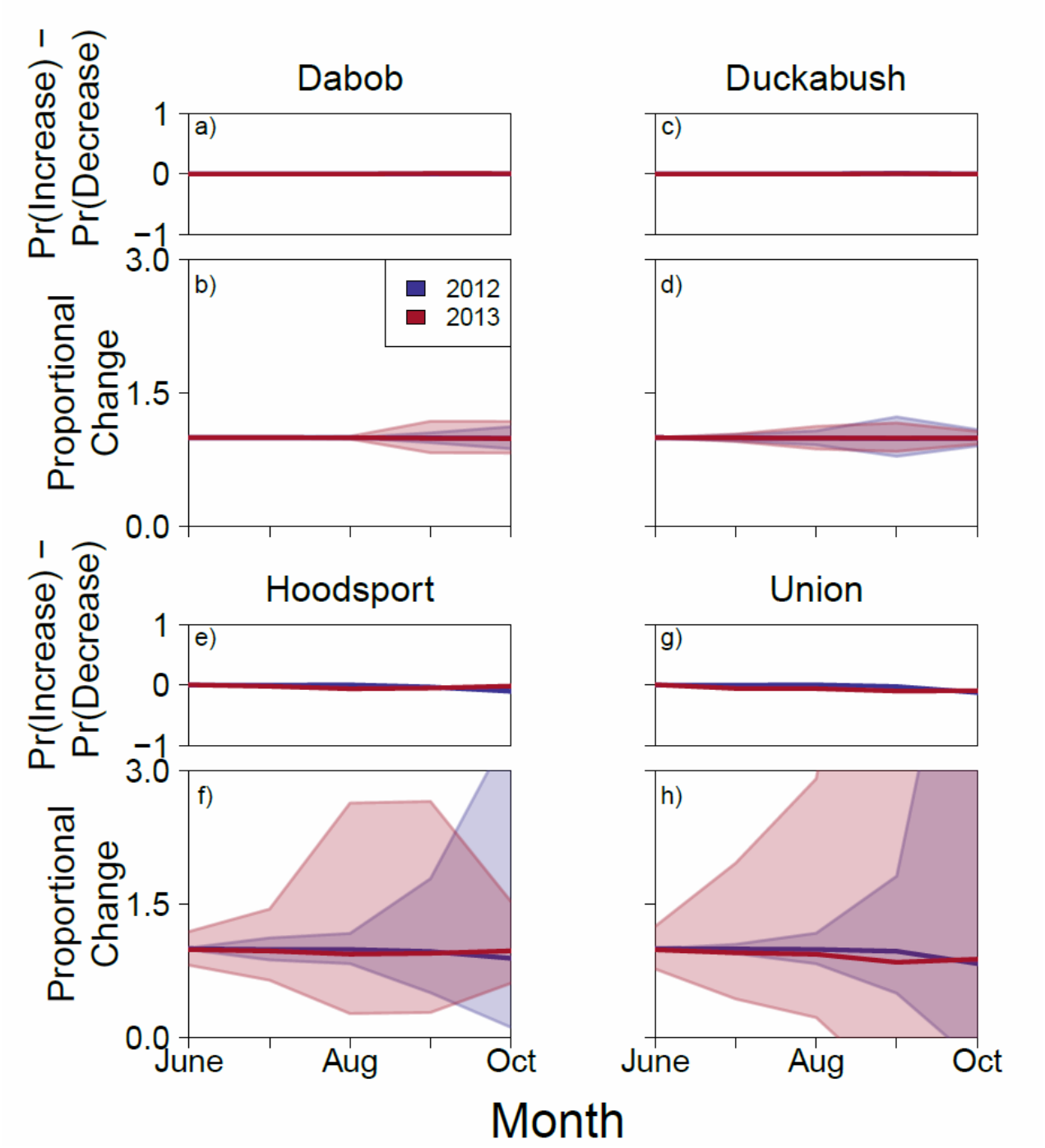

Figure 4.9 The difference in predicted mean population consumption under actual hypoxic conditions and no hypoxia of euphausiids by Pacific hake over the season at sites Union (a, b), Hoodsport (c, d), Duckabush (e, f), Dabob (g, h). Population-level consumption depends on per-capita consumption and acoustic density of the predator. Top panel in each panel pair depicts the difference in the probabilities of at least a 20% increase in per-capita consumption and a 20% decrease in per-capita consumption. The lower panel in each panel pair depicts the proportional change of per-capita consumption. The line is the mean predicted proportional change and the shaded area shows the 95% prediction intervals.

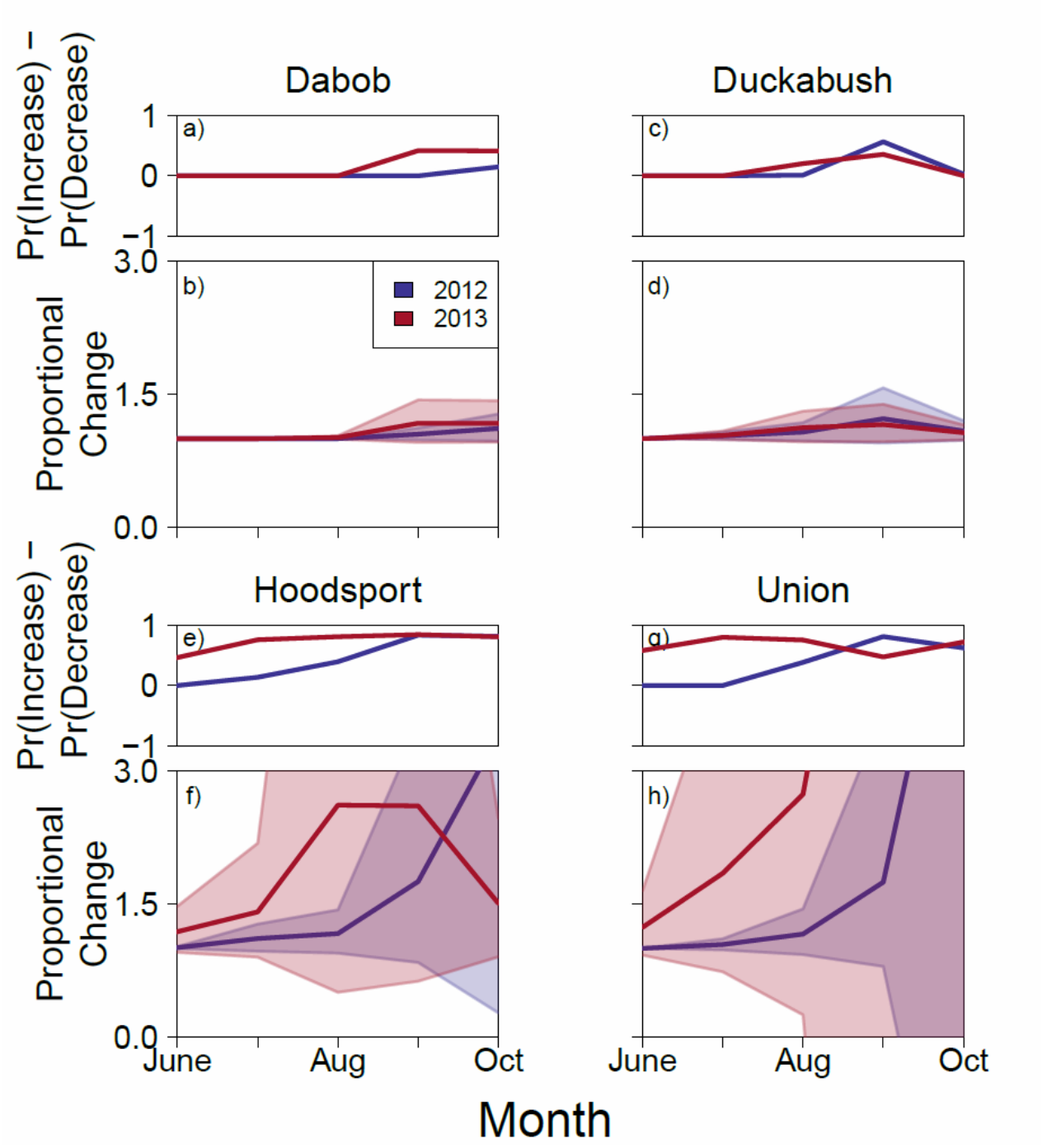

Figure 4.10 The difference in predicted mean relative consumption under actual hypoxic conditions and no hypoxia of euphausiids by Pacific herring over the season at sites A (a, b), site B (c, d), site C (e, f), site D (g, h). Relative consumption depends on euphausiid availability and the total consumption by the herring population. Top panel in each panel pair depicts the difference in the probabilities of at least a 20% increase in relative predation and a 20% decrease in relative predation. The lower panel in each panel pair depicts the proportional change of relative predation. The line is the mean predicted proportional change and the shaded area shows the 95% prediction intervals.

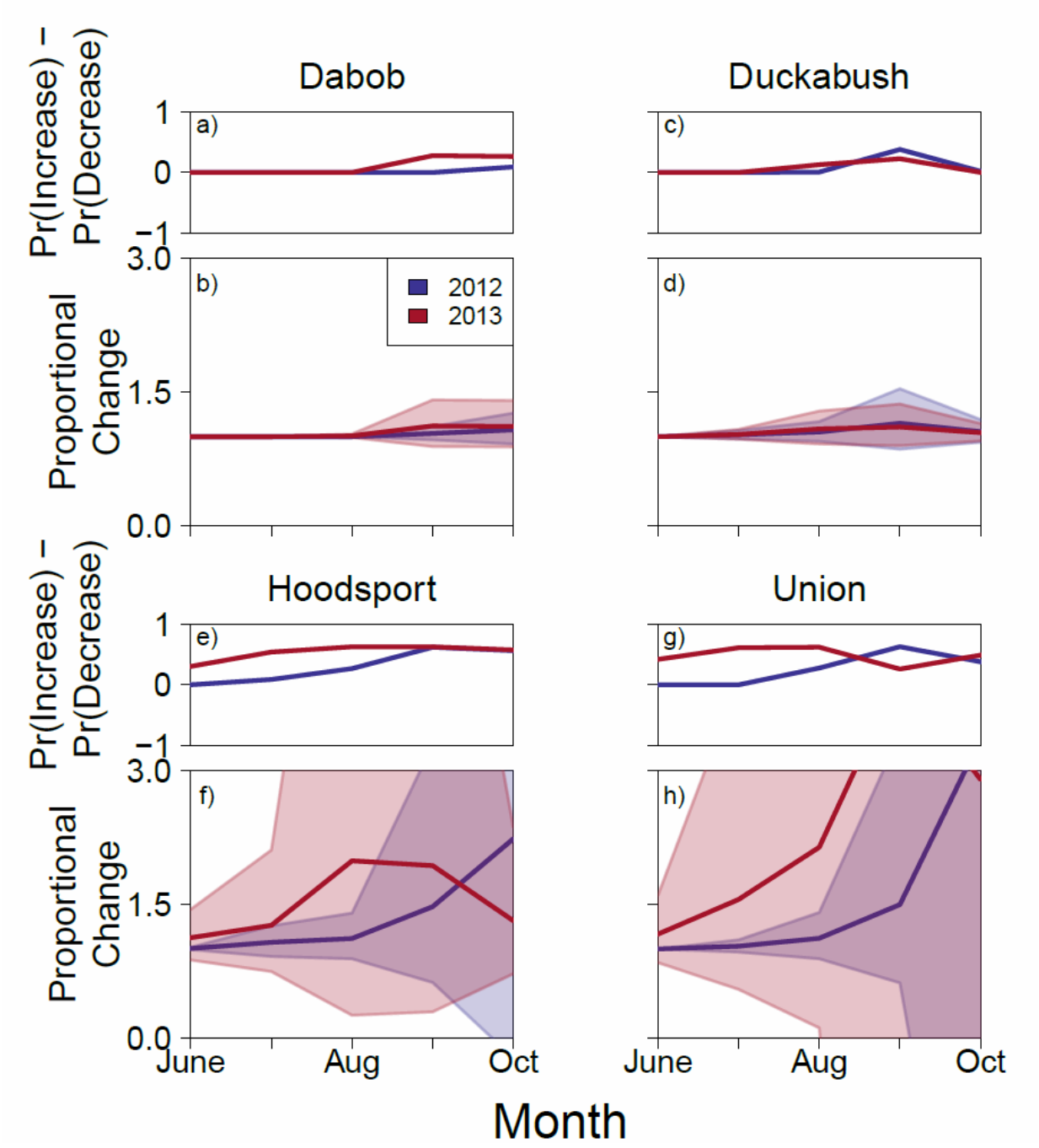

Figure 4.11 The difference in predicted mean relative consumption under actual hypoxic conditions and no hypoxia of euphausiids by Pacific hake Union (a, b), Hoodsport (c, d), Duckabush (e, f), Dabob (g, h). Relative consumption depends on euphausiid availability and the total consumption by the hake population. Top panel in each panel pair depicts the difference in the probabilities of at least a 20% increase in relative predation and a 20% decrease in relative predation. The lower panel in each panel pair depicts the proportional change of relative predation. The line is the mean predicted proportional change and the shaded area shows the 95% prediction intervals.

APPENDIX A4.

Table A4.1. Priors for diet model used in Stan. Any parameters not specified here used default priors derived by Stan (Stan Development Team 2017).

Parameter	**Prior**
μ_{mult}	Normal(0, 1)
σ_{mult}	Normal(0, 1)
r_{Φ}	Beta(1, 1)
$r_{\Phi_{p1}}$	Beta(1, 1)

APPENDIX B4.

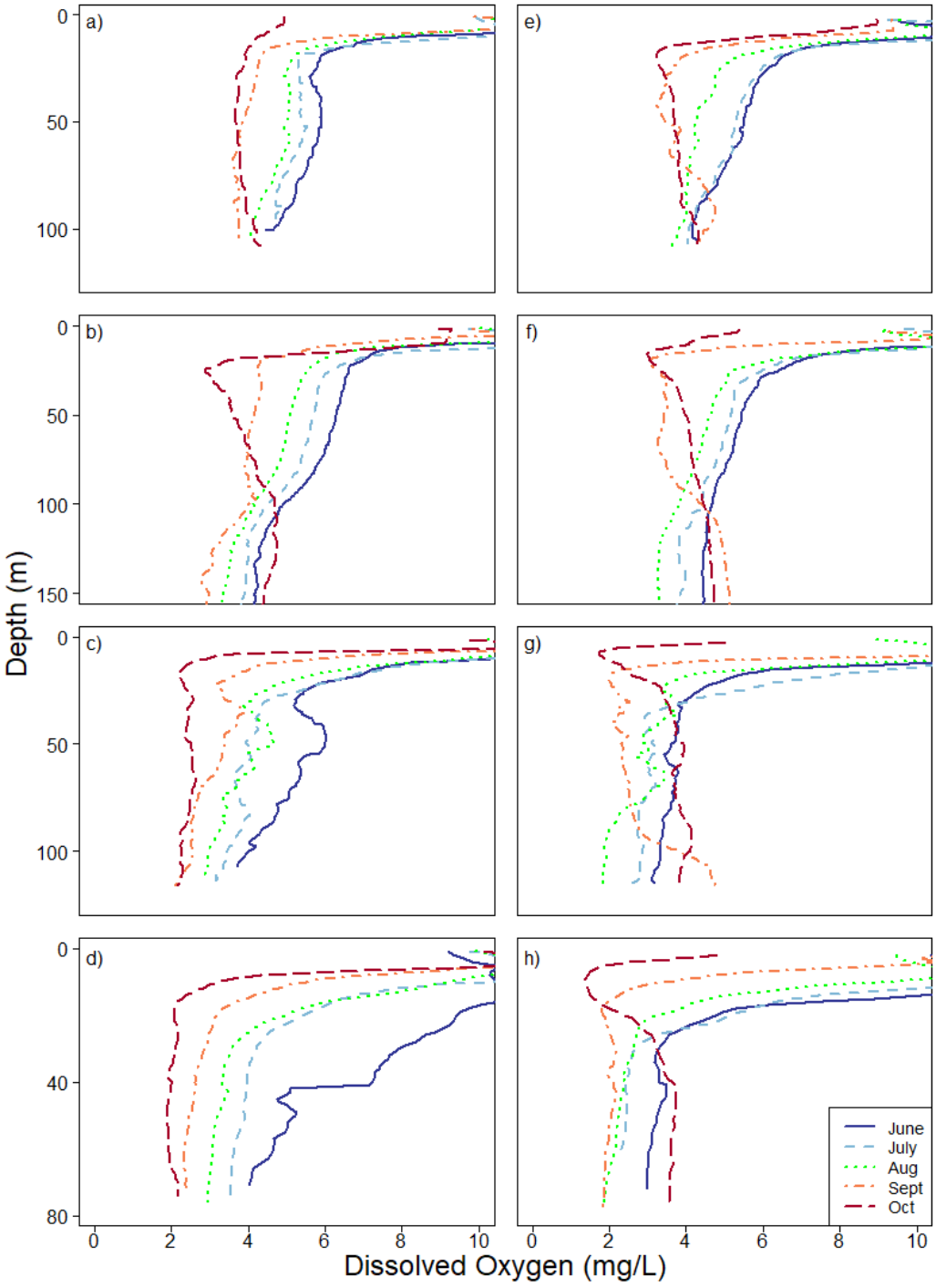

Figure B4.1.
Dissolved oxygen profiles at all sites in each month. Each line is the average of 2-4 separate CTD casts. Year 2012 (a-d) and 2013 (e-h) are plotted at sites Dabob (a, e), Duckabush (b, f), Hoodsport (c, g), and Union (d, h).

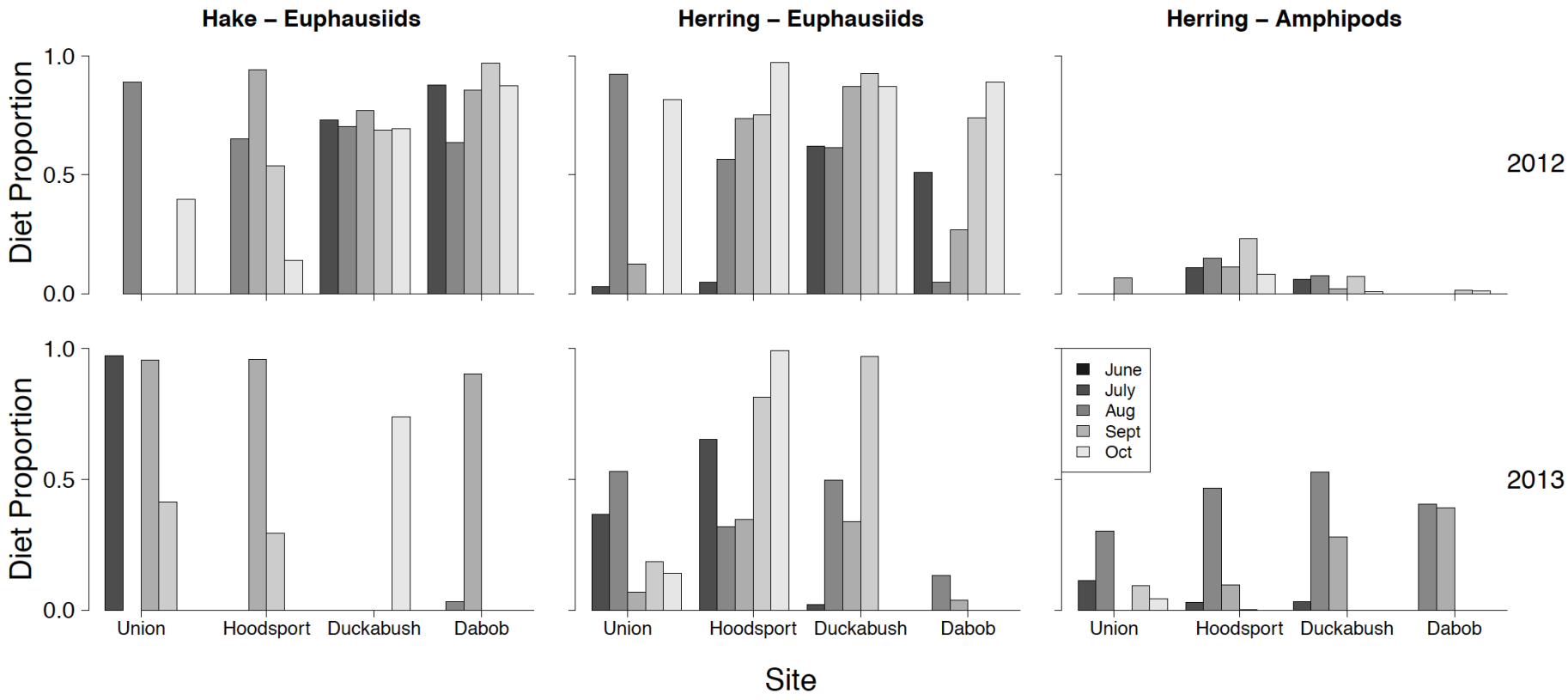

Figure B4.2. The diet contribution of euphausiids and amphipods to Pacific herring, and the contribution of euphausiids to Pacific hake. Diet contributions are shown for each site in each month.

APPENDIX C4.

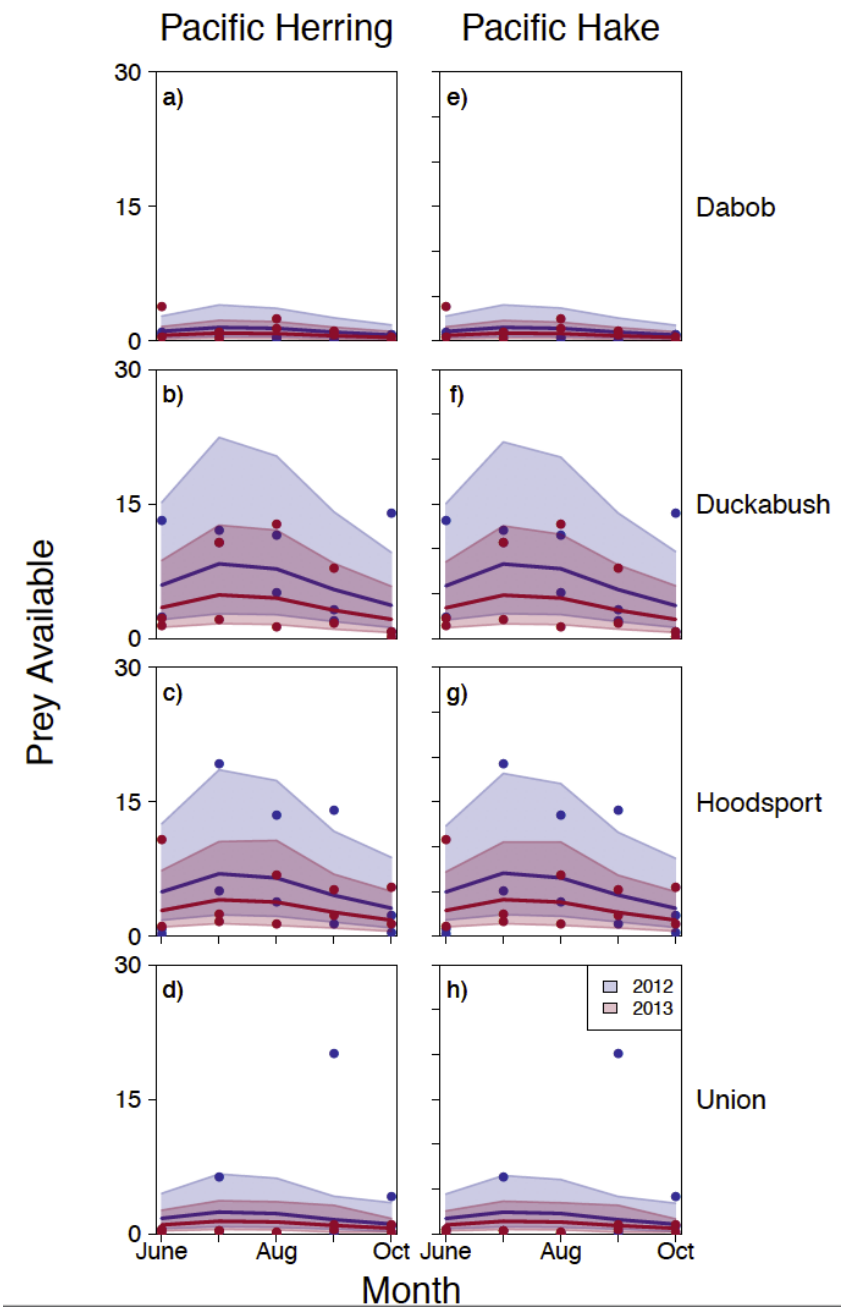

Figure B4.3. Amphipods available for consumption by Pacific herring (a-d) and Pacific hake (e-h) at Union (a,e), Hoodsport (b,f), Duckabush (c,g), and Dabob (d,h) (units = m^2 nmi^{-2}). Prey availability is a function of zooplankton community composition, size selectivity by the predator in that month, and zooplankton acoustic densities. Points are mean prey availability for that species at that site, month, and year. Lines are the mean model prediction and shaded areas represent the 95% prediction intervals.

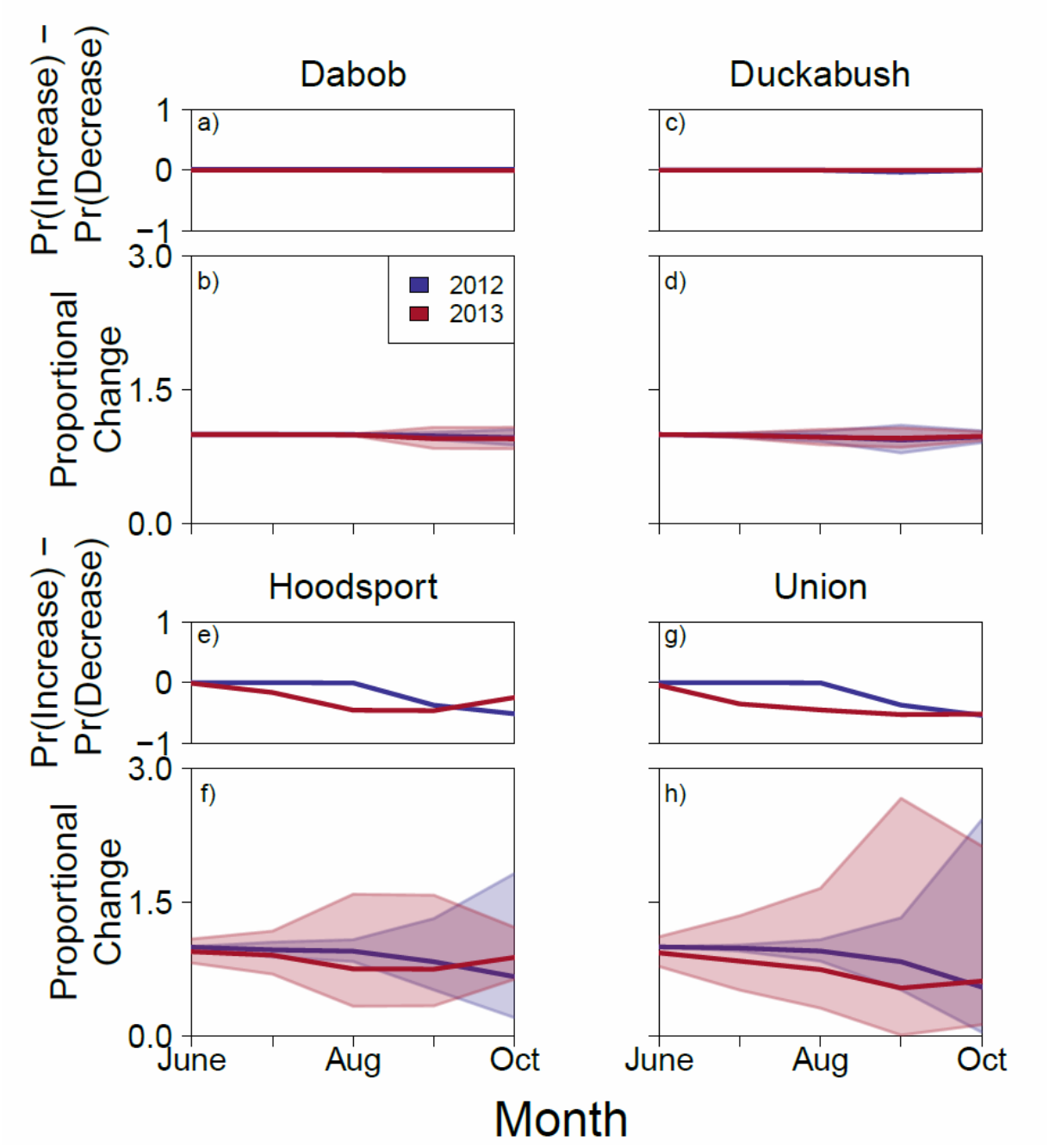

Figure B4.4. The difference in predicted mean per-capita consumption by Pacific herring of amphipods over the season at Union (a, b), Hoodsport (c, d), Duckabush (e, f), Dabob (g, h). Per-capita consumption depends on stomach fullness and diet composition of the predator. Top panel in each panel pair depicts the difference in the probabilities of at least a 20% increase in per-capita consumption and a 20% decrease in per-capita consumption. The lower panel in each panel pair depicts the proportional change of per-capita consumption. The line is the mean predicted proportional change and the shaded area shows the 95% prediction intervals.

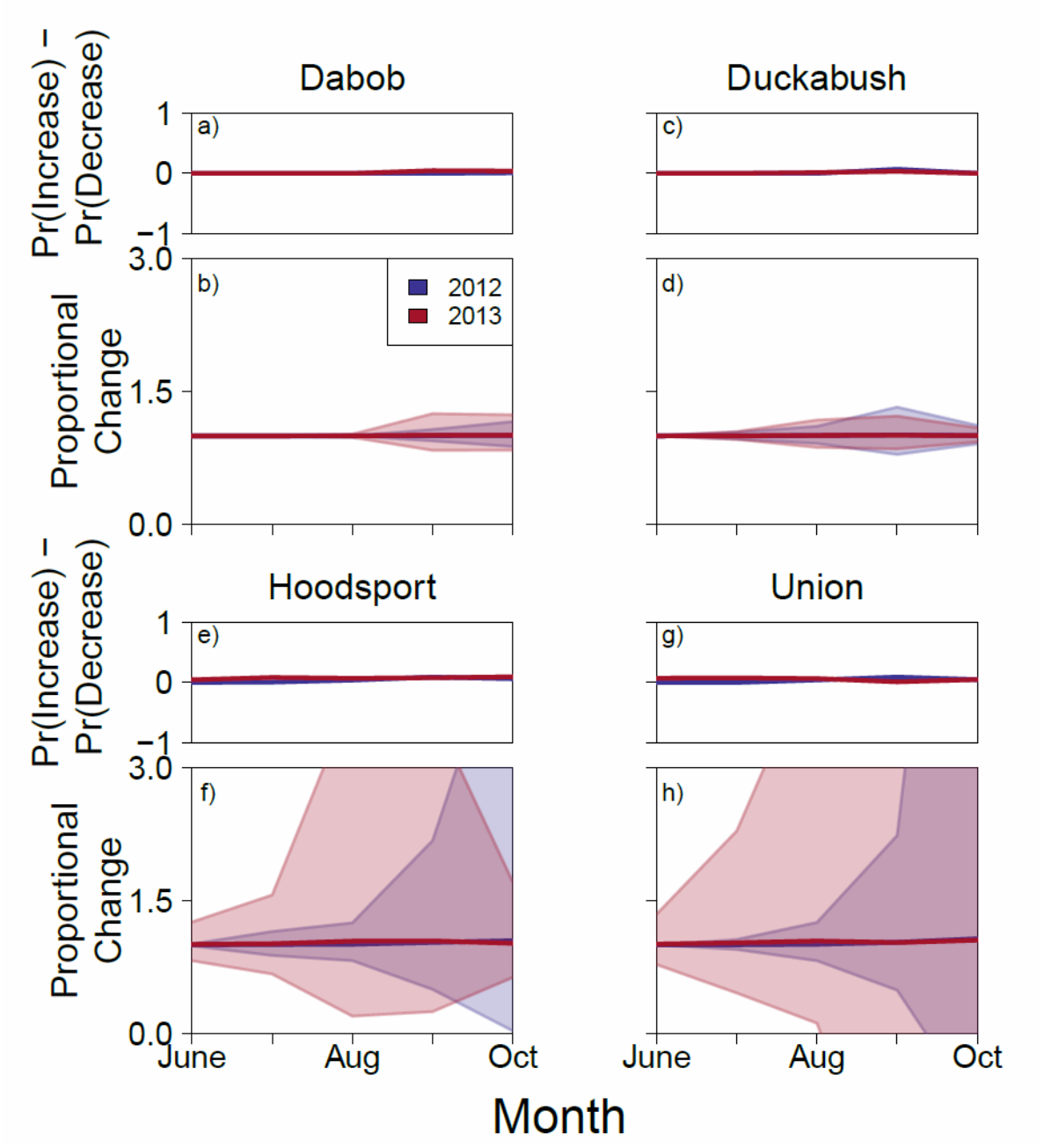

Figure B4.5. The difference in predicted mean per-capita consumption of amphipods by Pacific hake over the season at Union (a, b), Hoodsport (c, d), Duckabush (e, f), Dabob (g, h). Per-capita consumption depends on stomach fullness and diet composition of the predator. Top panel in each panel pair depicts the difference in the probabilities of at least a 20% increase in per-capita consumption and a 20% decrease in per-capita consumption. The lower panel in each panel pair depicts the proportional change of per-capita consumption. The line is the mean predicted proportional change and the shaded area shows the 95% prediction intervals.

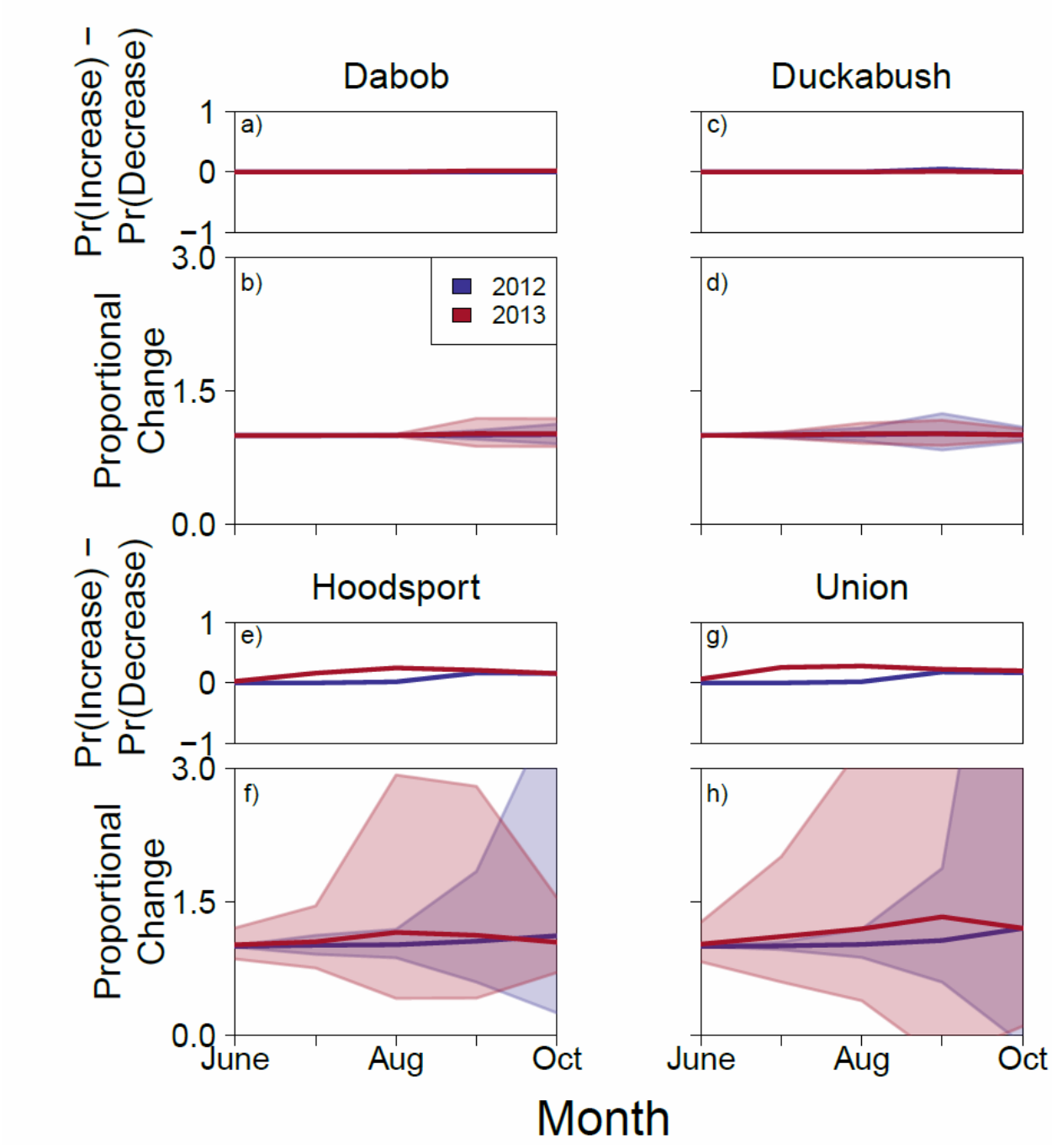

Figure B4.6. The difference in predicted mean population consumption of amphipods by Pacific herring over the season at sites Union (a, b), Hoodsport (c, d), Duckabush (e, f), Dabob (g, h). Population-level consumption depends on per-capita consumption and acoustic density of the predator. Top panel in each panel pair depicts the difference in the probabilities of at least a 20% increase in per-capita consumption and a 20% decrease in per-capita consumption. The lower panel in each panel pair depicts the proportional change of per-capita consumption. The line is the mean predicted proportional change and the shaded area shows the 95% prediction intervals.

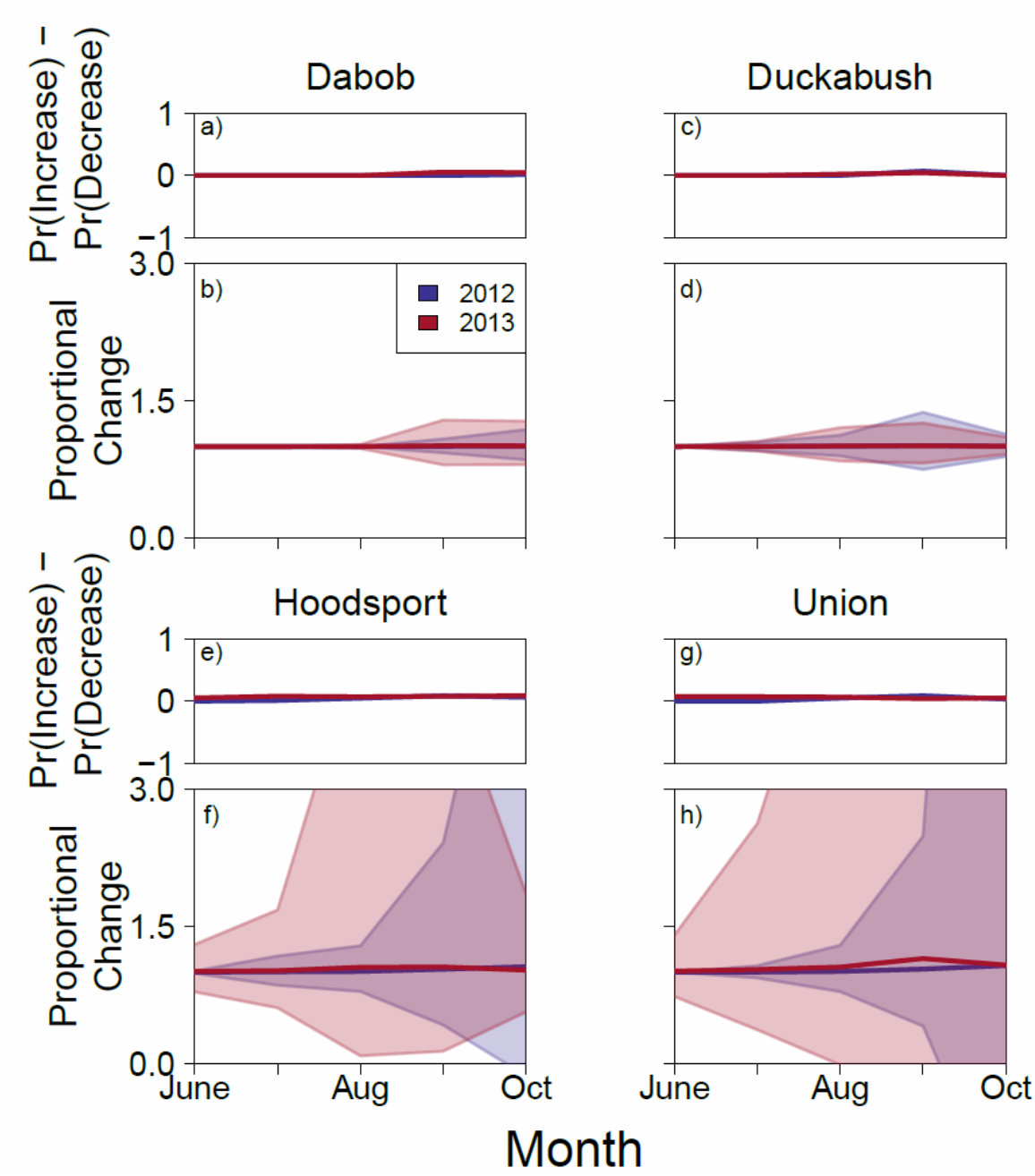

Figure B4.7. The difference in predicted mean population consumption of amphipods by Pacific hake over the season at sites Union (a, b), Hoodsport (c, d), Duckabush (e, f), Dabob (g, h). Population-level consumption depends on per-capita consumption and acoustic density of the predator. Top panel in each panel pair depicts the difference in the probabilities of at least a 20% increase in per-capita consumption and a 20% decrease in per-capita consumption. The lower panel in each panel pair depicts the proportional change of per-capita consumption. The line is the mean predicted proportional change and the shaded area shows the 95% prediction intervals.

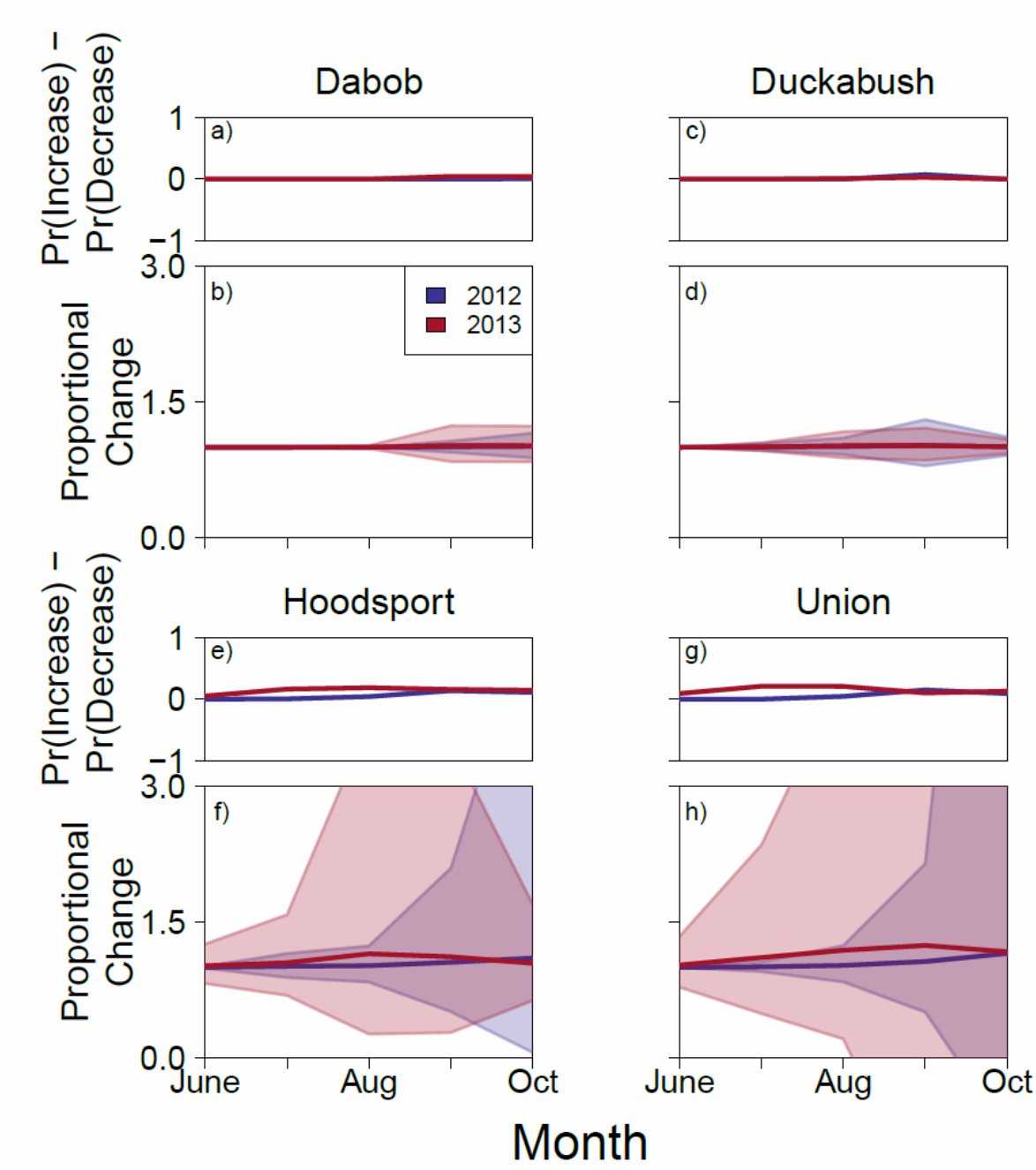

Figure B4.8. The difference in predicted mean relative consumption of amphipods by Pacific herring over the season at sites A (a, b), site B (c, d), site C (e, f), site D (g, h). Relative consumption depends on amphipod availability and the total consumption by the herring population. Top panel in each panel pair depicts the difference in the probabilities of at least a 20% increase in relative predation and a 20% decrease in relative predation. The lower panel in each panel pair depicts the proportional change of relative predation. The line is the mean predicted proportional change and the shaded area shows the 95% prediction intervals.

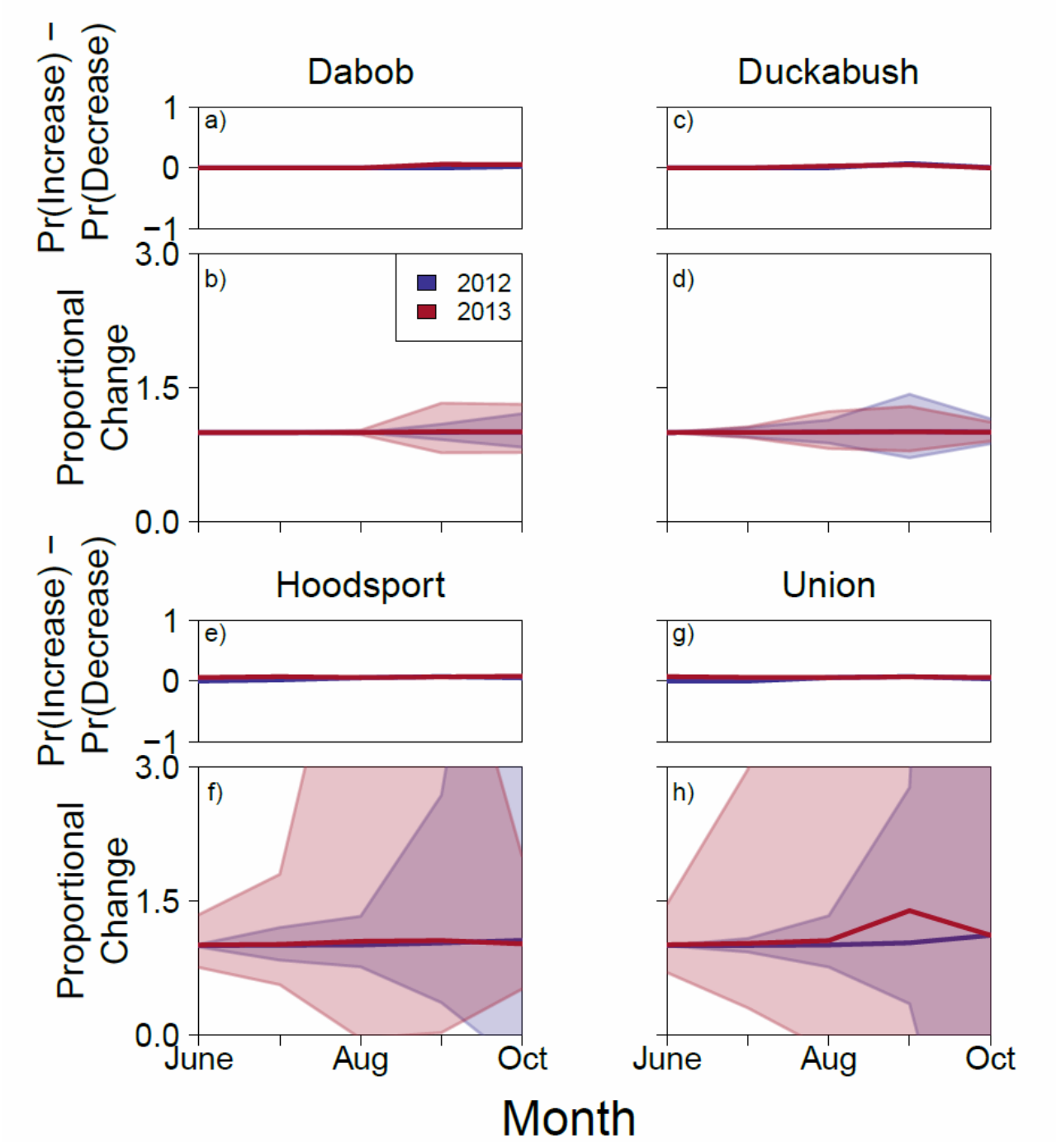

Figure B4.9. The difference in predicted mean relative consumption of amphipods by Pacific hake Union (a, b), Hoodsport (c, d), Duckabush (e, f), Dabob (g, h). Relative consumption depends on amphipod availability and the total consumption by the hake population. Top panel in each panel pair depicts the difference in the probabilities of at least a 20% increase in relative predation and a 20% decrease in relative predation. The lower panel in each panel pair depicts the proportional change of relative predation. The line is the mean predicted proportional change and the shaded area shows the 95% prediction intervals.

SYNTHESIS

Individual predator-prey interactions cannot always be considered in isolation, but are influenced by biotic and abiotic processes, each of which has direct and indirect effects. Every interaction ("link") between a particular predator and a particular prey type occurs within a larger food web that is affected by abiotic factors. Other linkages may influence the predator-prey link of interest directly, such as through competition for prey from another predator (e.g. Purcell and Sturdevant 2001, Schnedler-Meyer et al. 2016). It may also indirectly affect the predator-prey interaction, such as through a trophic cascade (Casini et al. 2008, Heath et al. 2014). The abiotic environment also directly and indirectly affects predator-prey interactions by altering the surrounding food web, such as a change in oxygen level directly changing predator or prey abundance, which then causes predator abundance to further change as well (e.g. Baird et al. 2004, Guinotte and Fabry 2008). Finally, these biotic and abiotic effects interact, expanding the complexity of possible effects of the food web on a specific predator-prey interaction (Conley et al. 2009, Clark et al. 2013).

The complexity of predator-prey interactions makes quantifying these interactions challenging. For instance, considering indirect and direct effects of a single abiotic process, hypoxia, required sampling multiple ecosystem components to obtain a variety of data sources, choosing appropriate methods to analyze each, and creating an analysis framework that could combine multiple data sources, while incorporating the error corresponding to each data source. Merging all the necessary components of information to fully understand the effect of just one abiotic process on a single predator-prey linkage was challenging, but provides valuable information from an ecosystem perspective. Moving forward, this form of analysis is likely to be

progressively important as attempts to predict the effects of environmental stressors become increasingly common.

Perhaps as a result of this complexity, there is a wide variety of methods for characterizing predator-prey interactions and each data source presents unique challenges. In aquatic sciences, these are predominantly stomach content data and stable isotope data (Boecklen et al. 2011, Baker et al. 2014). However, other potential data sources include fecal matter (Trites and Joy 2005) and cameras (e.g. Weckel et al. 2006, Yasuhiko et al. 2013). Each data source has its benefits and drawbacks. For example, stomach content data is well-known to bias diet estimates towards harder organisms over soft-bodied organisms, only provides a snapshot in time of an individual's consumption, and until recently lacked strong analytical methods (Rindorf and Lewy 2004, Deroba 2018). However, it is straightforward to collect and inexpensive to process. Stable isotope data provides a longer time scale of diet information (Fry 2006, Boecklen et al. 2011) and the low costs permits widespread use. Yet, stable isotope interpretation depends on an organism's specific physiology, requiring more mechanistic understanding before it can be applied to new taxa and sometimes, new contexts.

Together, the research presented here provides several improvements in being able to quantify predator-prey linkages, while also elucidating improvements still needed. Perhaps foremost, the consequences of seemingly benign assumptions need to be considered carefully. Choosing methods while being mindful of their limitations and how they can actually be interpreted is a vital step towards developing an accurate understanding of trophic interactions. The applications of stable isotopes to jellyfish is one example of this, though is not unique. For instance, indices are commonly applied across ecology and natural resource management, but again, are frequently not developed in clearly interpretable ways, despite being applied in this

manner (Moriarty et al. 2018). As data sources and data analysis methods are developed and/or their applications are expanded beyond what they were originally developed for, it is vital that we understand how to interpret the results. Doing so will aid in developing a more thorough understanding of ecological processes and therefore improve our ability to predict the effects of environmental stressors.

Improved statistical methods for diet data, particularly stomach contents data, will provide more accurate and precise information about trophic linkages (Chapters 1-2). In other cases, novel ways to combine multiple data sources can help elucidate patterns not otherwise apparent (Chapter 4). However, it is important to recognize that while improved statistical methodology can help counteract some of the biases of data sources, flaws cannot be erased. No matter how excellent our statistical methods become, data sources will always have inherent biases. Keeping these biases in mind when choosing methods for an ecological question and interpreting the results will always be an essential step, so that apparently straightforward assumptions are not changing our conclusions.

The work presented here emphasizes the complexity of approaches to studying food webs, which are an important aspect of many subfields of ecology. Ultimately, fully understanding predator-prey interactions requires a multifaceted approach. Yet, the best methods and interpretation of results are highly dependent on the ecological question and context.

REFERENCES

Adams, T. S., and R. W. Sterner. 2000. The effect of dietary nitrogen content on trophic level N-15 enrichment. Limnology and Oceanography **45**:601-607.

Ahlbeck, I., S. Hansson, and O. Hjerne. 2012. Evaluating fish diet analysis methods by individual-based modelling. Canadian Journal of Fisheries and Aquatic Sciences **69**:1184-1201.

Ainsworth, C. H., I. C. Kaplan, P. S. Levin, and M. Mangel. 2010. A statistical approach for estimating fish diet compositions from multiple data sources: Gulf of California case study. Ecological Applications **20**:2188-2202.

Arai, M. N. 1997. A functional biology of Scyphozoa. 1st edition. Chapman & Hall, London ; New York.

Arni, M., P. A. E, and H. Ray. 2013. Measuring uncertainty in fisheries stock assessment: the delta method, bootstrap, and MCMC. Fish and Fisheries **14**:325-342.

Ashworth, E. C., M. Depczynski, T. H. Holmes, and S. K. Wilson. 2014. Quantitative diet analysis of four mesopredators from a coral reef. Journal of Fish Biology:n/a-n/a.

Babson, A. L., M. Kawase, and P. MacCready. 2006. Seasonal and Interannual Variability in the Circulation of Puget Sound, Washington: A Box Model Study. Atmosphere-Ocean **44**:29-45.

Baeta, A., L. R. Vieira, A. V. Lírio, C. Canhoto, J. C. Marques, and L. Guilhermino. 2017. Use of stable isotope ratios of fish larvae as indicators to assess diets and patterns of anthropogenic nitrogen pollution in estuarine ecosystems. Ecological Indicators **83**:112-121.

Baird, D., R. R. Christian, C. H. Peterson, and G. A. Johnson. 2004. Consequences of hypoxia on estuarine ecosystem function: Energy diversion from consumers to microbes. Ecological Applications **14**:805-822.

Baker, R., A. Buckland, and M. Sheaves. 2014. Fish gut content analysis: robust measures of diet composition. Fish and Fisheries **15**:170-177.

Barz, K., and H. J. Hirche. 2007. Abundance, distribution and prey composition of scyphomedusae in the southern North Sea. Marine Biology **151**:1021-1033.

Beaudreau, A. H., and T. E. Essington. 2009. Development of a new field-based approach for estimating consumption rates of fishes and comparison with a bioenergetics model for lingcod (Ophiodon elongatus). Canadian Journal of Fisheries and Aquatic Sciences **66**:565-578.

Boecklen, W. J., C. T. Yarnes, B. A. Cook, and A. C. James. 2011. On the Use of Stable Isotopes in Trophic Ecology. Annual Review of Ecology, Evolution, and Systematics, Vol 42 **42**:411-440.

Bosley, K. L., and S. C. Wainright. 1999. Effects of preservatives and acidification on the stable isotope ratios (15N:14N, 13C:12C) of two species of marine animals. Canadian Journal of Fisheries and Aquatic Sciences **56**:2181-2185.

Brandenberger, J. M., P. Louchouarn, and E. A. Crecelius. 2011. Natural and Post-Urbanization Signatures of Hypoxia in Two Basins of Puget Sound: Historical Reconstruction of Redox Sensitive Metals and Organic Matter Inputs. Aquatic Geochemistry **17**:645-670.

Breitburg, D., L. A. Levin, A. Oschlies, M. Grégoire, F. P. Chavez, D. J. Conley, V. Garçon, D. Gilbert, D. Gutiérrez, K. Isensee, G. S. Jacinto, K. E. Limburg, I. Montes, S. W. A. Naqvi, G. C. Pitcher, N. N. Rabalais, M. R. Roman, K. A. Rose, B. A. Seibel, M. Telszewski, M. Yasuhara, and J. Zhang. 2018. Declining oxygen in the global ocean and coastal waters. Science **359**.

Brodeur, R. D., H. Sugisaki, and G. L. Hunt. 2002. Increases in jellyfish biomass in the Bering Sea: implications for the ecosystem. Marine Ecology-Progress Series **233**:89-103.

Burnham, K. P., and D. R. Anderson. 1998. Model selection and inference : a practical information-theoretic approach. Springer, New York.

Candy, S. G. 2008. Estimation of effective sample size for catch-at-age and catch-at-length data using simulated data from the dirichlet-multinomial distribution. Ccamlr Science **15**:115-138.

Carpenter, B., A. Gelman, M. D. Hoffman, D. Lee, B. Goodrich, M. Betancourt, M. Brubaker, J. Guo, P. Li, and A. Riddell. 2017. Stan: A Probabilistic Programming Language. 2017 **76**:32.

Carpenter, J. H. 1965. The accuracy of the Winkler method for dissolved oxygen analysis. Limnology and Oceanography **10**:135-140.

Casini, M., J. Lovgren, J. Hjelm, M. Cardinale, J. C. Molinero, and G. Kornilovs. 2008. Multi-level trophic cascades in a heavily exploited open marine ecosystem. Proceedings of the Royal Society B-Biological Sciences **275**:1793-1801.

Catano, L. B., A. A. Shantz, and D. E. Burkepile. 2014. Predation risk, competition, and territorial damselfishes as drivers of herbivore foraging on Caribbean coral reefs. Marine Ecology Progress Series **511**:193-207.

Caut, S., E. Angulo, and F. Courchamp. 2008. Discrimination factors (Δ15N and Δ13C) in an omnivorous consumer: effect of diet isotopic ratio. Functional Ecology **22**:255-263.

Caut, S., E. Angulo, and F. Courchamp. 2009. Variation in discrimination factors (Δ15N and Δ13C): the effect of diet isotopic values and applications for diet reconstruction. Journal of Applied Ecology **46**:443-453.

Charnov, E. L. 1976. Optimal Foraging: attack strategy of a mantid. American Naturalist **110**:141-151.

Chave, J. 2013. The problem of pattern and scale in ecology: what have we learned in 20 years? Ecology Letters **16**:4-16.

Chikaraishi, Y., N. O. Ogawa, Y. Kashiyama, Y. Takano, H. Suga, A. Tomitani, H. Miyashita, H. Kitazato, and N. Ohkouchi. 2009. Determination of aquatic food-web structure based on compound-specific nitrogen isotopic composition of amino acids. Limnology And Oceanography-methods **7**:740-750.

Chikaraishi, Y., S. A. Steffan, N. O. Ogawa, N. F. Ishikawa, Y. Sasaki, M. Tsuchiya, and N. Ohkouchi. 2014. High-resolution food webs based on nitrogen isotopic composition of amino acids. Ecology and Evolution:n/a-n/a.

Christensen, V., and C. J. Walters. 2004. Ecopath with Ecosim: methods, capabilities and limitations. Ecological Modelling **172**:109-139.

Clark, M. S., G. Husmann, M. A. S. Thorne, G. Burns, M. Truebano, L. S. Peck, D. Abele, and E. E. R. Philipp. 2013. Hypoxia impacts large adults first: consequences in a warming world. Global Change Biology **19**:2251-2263.

Coblentz, K. E., A. E. Rosenblatt, and M. Novak. 2017. The application of Bayesian hierarchical models to quantify individual diet specialization. Ecology **98**:1535-1547.

Colman, L. P., C. L. S. Sampaio, M. I. Weber, and J. C. de Castilhos. 2014. Diet of Olive Ridley Sea Turtles, Lepidochelys olivacea, in the Waters of Sergipe, Brazil. Chelonian Conservation and Biology **13**:266-U178.

Condon, R. H., D. K. Steinberg, P. A. del Giorgio, T. C. Bouvier, D. A. Bronk, W. M. Graham, and H. W. Ducklow. 2011. Jellyfish blooms result in a major microbial respiratory sink of carbon in marine systems. Proceedings of the National Academy of Sciences of the United States of America **108**:10225-10230.

Conley, D. J., J. Carstensen, R. Vaquer-Sunyer, and C. M. Duarte. 2009. Ecosystem thresholds with hypoxia. Hydrobiologia **629**:21-29.

Cornelissen, I. J. M., J. Vijverberg, A. M. van den Beld, N. R. Helmsing, J. A. J. Verreth, and L. A. J. Nagelkerke. 2018. Heterogeneity in food-web interactions of fish in the Mwanza Gulf, Lake Victoria: a quantitative stable isotope study. Hydrobiologia **805**:113-130.

Cortes, E. 1997. A critical review of methods of studying fish feeding based on analysis of stomach contents: Application to elasmobranch fishes. Canadian Journal of Fisheries and Aquatic Sciences **54**:726-738.

D'Ambra, I., R. H. Carmichael, and W. M. Graham. 2014. Determination of delta C-13 and delta N-15 and trophic fractionation in jellyfish: implications for food web ecology. Marine Biology **161**:473-480.

D'Ambra, I., W. M. Graham, R. H. Carmichael, A. Malej, and V. Onofri. 2013. Predation patterns and prey quality of medusae in a semi-enclosed marine lake: implications for food web energy transfer in coastal marine ecosystems. Journal of Plankton Research **35**:1305-1312.

Dalsgaard, J., M. St John, G. Kattner, D. Muller-Navarra, and W. Hagen. 2003. Fatty acid trophic markers in the pelagic marine environment. Advances in Marine Biology, Vol 46 **46**:225-340.

Dannheim, J., U. Struck, and T. Brey. 2007. Does sample bulk freezing affect stable isotope ratios of infaunal macrozoobenthos? Journal of Experimental Marine Biology and Ecology **351**:37-41.

Davis, C. S., and P. H. Wiebe. 1985. Macrozooplankton biomass in a warm-core Gulf Stream ring: Time series changes in size structure, taxonomic composition, and vertical distribution. Journal of Geophysical Research: Oceans **90**:8871-8884.

de Valpine, P., and A. N. Harmon-Threatt. 2013. General models for resource use or other compositional count data using the Dirichlet-multinomial distribution. Ecology **94**:2678-2687.

Demer, D. A., and R. P. Hewitt. 1995. Bias in acoustic biomass estimates of Euphausia superba due to diel vertical migration. Deep Sea Research Part I: Oceanographic Research Papers **42**:455-475.

DeNiro, M., and S. Epstein. 1977. Mechanism of carbon isotope fractionation associated with lipid synthesis. Science **197**:261-263.

Deniro, M. J., and S. Epstein. 1978. Influence of Diet on Distribution of Carbon Isotopes in Animals. Geochimica Et Cosmochimica Acta **42**:495-506.

Dennis, C. A., M. A. MacNeil, J. Y. Rosati, T. E. Pitcher, and A. T. Fisk. 2010. Diet discrimination factors are inversely related to δ15N and δ13C values of food for fish under controlled conditions. Rapid Communications in Mass Spectrometry **24**:3515-3520.

Deroba, J. J. 2018. Sources of variation in stomach contents of predators of Atlantic herring in the Northwest Atlantic during 1973–2014. Ices Journal of Marine Science:fsy013-fsy013.
Doak, D. F., J. A. Estes, B. S. Halpern, U. Jacob, D. R. Lindberg, J. Lovvorn, D. H. Monson, M. T. Tinker, T. M. Williams, J. T. Wootton, I. Carroll, M. Emmerson, F. Micheli, and M. Novak. 2008. Understanding and predicting ecological dynamics: are major surprises inevitable. Ecology **89**:952-961.
Doyle, T. K., J. D. R. Houghton, R. McDevitt, J. Davenport, and G. C. Hays. 2007. The energy density of jellyfish: Estimates from bomb-calorimetry and proximate-composition. Journal of Experimental Marine Biology and Ecology **343**:239-252.
Dunne, J. P., A. H. Devol, and S. Emerson. 2002. The Oceanic Remote Chemical/Optical Analyzer (ORCA)—An Autonomous Moored Profiler. Journal of Atmospheric and Oceanic Technology **19**:1709-1721.
Ekau, W., H. Auel, H. O. Portner, and D. Gilbert. 2010. Impacts of hypoxia on the structure and processes in pelagic communities (zooplankton, macro-invertebrates and fish). Biogeosciences **7**:1669-1699.
Elliot, J. M., and L. Persson. 1978. Estimation of daily rates of food consumption for fish. Journal of Animal Ecology **47**:977-991.
Essington, T. E., and C. E. Paulsen. 2010. Quantifying Hypoxia Impacts on an Estuarine Demersal Community Using a Hierarchical Ensemble Approach. Ecosystems **13**:1035-1048.
Fernandez, R., G. J. Pierce, C. D. Macleod, A. Brownlow, R. J. Reid, E. Rogan, M. Addink, R. Deaville, P. D. Jepson, and M. B. Santos. 2014. Strandings of northern bottlenose whales, Hyperoodon ampullatus, in the north-east Atlantic: seasonality and diet. Journal of the Marine Biological Association of the United Kingdom **94**:1109-1116.
Feuchtmayr, H., and J. Grey. 2003. Effect of preparation and preservation procedures on carbon and nitrogen stable isotope determinations from zooplankton. Rapid Communications in Mass Spectrometry **17**:2605-2610.
Fleming, N. E. C., C. Harrod, J. Newton, and J. D. R. Houghton. 2015. Not all jellyfish are equal: isotopic evidence for inter- and intraspecific variation in jellyfish trophic ecology. Peerj **3**:21.
Fleming, N. E. C., J. D. R. Houghton, C. L. Magill, and C. Harrod. 2011. Preservation methods alter stable isotope values in gelatinous zooplankton: implications for interpreting trophic ecology. Marine Biology **158**:2141-2146.
Fletcher, D., D. MacKenzie, and E. Villouta. 2005. Modelling skewed data with many zeros: A simple approach combining ordinary and logistic regression. Environmental and Ecological Statistics **12**:45-54.
Foote, K. G. 1983. Linearity of fisheries acoustics, with addition theorems. The Journal of the Acoustical Society of America **73**:1932-1940.
Frost, J. R., A. Denda, C. J. Fox, C. A. Jacoby, R. Koppelmann, M. H. Nielsen, and M. J. Youngbluth. 2012. Distribution and trophic links of gelatinous zooplankton on Dogger Bank, North Sea. Marine Biology **159**:239-253.
Fry, B. 2006. Stable isotope ecology. Springer, New York, NY.
Fulton, E. A., J. S. Link, I. C. Kaplan, M. Savina-Rolland, P. Johnson, C. Ainsworth, P. Horne, R. Gorton, R. J. Gamble, A. D. M. Smith, and D. C. Smith. 2011. Lessons in modelling and management of marine ecosystems: the Atlantis experience. Fish and Fisheries **12**:171-188.

Fulton, E. A., A. D. M. Smith, and C. R. Johnson. 2004. Biogeochemical marine ecosystem models I: IGBEM - a model of marine bay ecosystems. Ecological Modelling **174**:267-307.

Gannes, L. Z., C. M. n. del Rio, and P. Koch. 1998. Natural Abundance Variations in Stable Isotopes and their Potential Uses in Animal Physiological Ecology. Comparative Biochemistry and Physiology Part A: Molecular & Integrative Physiology **119**:725-737.

Gannes, L. Z., D. M. O'Brien, and C. M. del Rio. 1997. Stable isotopes in animal ecology: assumptions, caveats, and a call for more laboratory experiments. Ecology **78**:1271-1276.

Gelman, A. 2006. Prior distributions for variance parameters in hierarchical models (comment on article by Browne and Draper). Bayesian Anal. **1**:515-534.

Gelman, A. 2014. Bayesian data analysis. Third edition. edition. CRC Press, Boca Raton.

Gelman, A., and J. Hill. 2007. Data analysis using regression and multilevel/hierarchical models. Cambridge University Press, Cambridge ; New York.

Gelman, A., and D. B. Rubin. 1992. Inference from Iterative Simulation Using Multiple Sequences. Statist. Sci. **7**:457-472.

Germain, L. R., P. L. Koch, J. Harvey, and M. D. McCarthy. 2013. Nitrogen isotope fractionation in amino acids from harbor seals: implications for compound-specific trophic position calculations. Marine Ecology Progress Series **482**:265-+.

Guinotte, J. M., and V. J. Fabry. 2008. Ocean acidification and its potential effects on marine ecosystems. Year in Ecology and Conservation Biology 2008 **1134**:320-342.

Gurney, W. S. C., and R. M. Nisbet. 1998. Ecological dynamics. Oxford University Press, New York.

Hare, E. P., M. L. Fogel, T. W. Stafford, A. D. Mitchell, and T. C. Hoering. 1991. The isotopic composition of carbon and nitrogen in individual amino acids isolated from modern and fossil proteins. Journal of Archaeological Science **18**:277-292.

Heaslip, S. G., S. J. Iverson, W. D. Bowen, and M. C. James. 2012. Jellyfish Support High Energy Intake of Leatherback Sea Turtles (Dermochelys coriacea): Video Evidence from Animal-Borne Cameras. Plos One **7**:7.

Heath, M. R., D. C. Speirs, and J. H. Steele. 2014. Understanding patterns and processes in models of trophic cascades. Ecology Letters **17**:101-114.

Heffernan, J. B., P. A. Soranno, M. J. Angilletta, L. B. Buckley, D. S. Gruner, T. H. Keitt, J. R. Kellner, J. S. Kominoski, A. V. Rocha, J. Xiao, T. K. Harms, S. J. Goring, L. E. Koenig, W. H. McDowell, H. Powell, A. D. Richardson, C. A. Stow, R. Vargas, and K. C. Weathers. 2014. Macrosystems ecology: understanding ecological patterns and processes at continental scales. Frontiers in Ecology and the Environment **12**:5-14.

Heithaus, M. R., A. Frid, A. J. Wirsing, and B. Worm. 2008. Predicting ecological consequences of marine top predator declines. Trends in Ecology & Evolution **23**:202-210.

Higham, T. E., W. J. Stewart, and P. C. Wainwright. 2015. Turbulence, Temperature, and Turbidity: The Ecomechanics of Predator-Prey Interactions in Fishes. Integrative and Comparative Biology **55**:6-20.

Hilborn, R., and M. Mangel. 1997. The ecological detective : confronting models with data. Princeton University Press, Princeton, NJ.

Hobson, K. A., and A. L. Bond. 2012. Extending an indicator: year-round information on seabird trophic ecology from multiple-tissue stable-isotope analyses. Marine Ecology Progress Series **461**:233-243.

Holyoak, M., M. A. Leibold, R. D. Holt, and Ecological Society of America. Meeting. 2005. Metacommunities : spatial dynamics and ecological communities. University of Chicago Press, Chicago.
Homan, M. D., and A. Gelman. 2014. The No-U-Turn Sampler: adaptively setting path lengths in Hamiltonian Monte Carlo. J. Mach. Learn. Res. **15**:1593-1623.
Hooten, M. B., and N. T. Hobbs. 2014. A Guide to Bayesian Model Selection for Ecologists. Ecological Monographs.
Hopkins, J. B., and J. M. Ferguson. 2012. Estimating the Diets of Animals Using Stable Isotopes and a Comprehensive Bayesian Mixing Model. Plos One **7**.
Hrycik, A. R., L. Z. Almeida, and T. O. Hook. 2017. Sub-lethal effects on fish provide insight into a biologically-relevant threshold of hypoxia. Oikos **126**:307-317.
Hussey, N. E., M. A. MacNeil, B. C. McMeans, J. A. Olin, S. F. J. Dudley, G. Cliff, S. P. Wintner, S. T. Fennessy, and A. T. Fisk. 2014. Rescaling the trophic structure of marine food webs. Ecology Letters **17**:239-250.
Huxel, G. R., and K. McCann. 1998. Food web stability: the influence of trophic flows across habitats. American Naturalist **152**:460-469.
Hyslop, E. J. 1980. Stomach contents analysis - a review of methods and their application. Journal of Fish Biology **17**:411-429.
Iglesias, C., M. Meerhoff, L. S. Johansson, I. González-Bergonzoni, N. Mazzeo, J. P. Pacheco, F. T.-d. Mello, G. Goyenola, T. L. Lauridsen, M. Søndergaard, T. A. Davidson, and E. Jeppesen. 2017. Stable isotope analysis confirms substantial differences between subtropical and temperate shallow lake food webs. Hydrobiologia **784**:111-123.
Ingram, B. A., K. A. Pitt, and P. Barnes. 2016. Stable isotopes reveal a potential kleptoparasitic relationship between an ophiuroid (Ophiocnemis marmorata) and the semaeostome jellyfish, Aurelia aurita. Journal of Plankton Research.
Iverson, S. J. 2009. Tracing Aquatic Food Webs Using Fatty Acids: From Qualitative Indicators to Quantitative Determination. Springer, 233 Spring Street, New York, Ny 10013, United States.
Iverson, S. J., C. Field, W. Don Bowen, and W. Blanchard. 2004. Quantitative fatty acid signature analysis: a new method of estimating predator diets. Ecological Monographs **74**:211-235.
Jaspers, C., J. L. Acuña, and R. D. Brodeur. 2015. Interactions of gelatinous zooplankton within marine food webs. Journal of Plankton Research **37**:985-988.
Kaehler, S., and E. A. Pakhomov. 2001. Effects of storage and preservation on the d13C and d15N signatures of selected marine organisms. Marine Ecology Progress Series **219**:299-304.
Kellnreitner, F., M. Pockberger, R. Asmus, and H. Asmus. 2013. Feeding interactions between the introduced ctenophore Mnemiopsis leidyi and juvenile herring Clupea harengus in the Wadden Sea. Biological Invasions **15**:871-884.
Kim, S. L., and P. L. Koch. 2012. Methods to collect, preserve, and prepare elasmobranch tissues for stable isotope analysis. Environmental Biology of Fishes **95**:53-63.
Kogovsek, T., T. T, K. K, and M. A. 2014. Jellyfish biochemical composition: importance of standardised sample processing. Marine Ecology Progress Series **510**:275-288.
Lavaniegos, B. E., and M. D. Ohman. 2007. Coherence of long-term variations of zooplankton in two sectors of the California Current System. Progress in Oceanography **75**:42-69.

Legendre, L., and R. B. Rivkin. 2008. Planktonic food webs: microbial hub approach. Marine Ecology Progress Series **365**:289-309.
Liao, H. S., C. L. Pierce, and J. G. Larscheid. 2001. Empirical assessment of indices of prey importance in the diets of predacious fish. Transactions of the American Fisheries Society **130**:583-591.
Link, J. S., and F. P. Almeida. 2000. An Overview and History of the Food Web Dynamics Program of the Northeast Fisheries Science Center, Woods Hole, Massachusetts. U.S. Department of Commerce.
Little, W. S., and N. J. Copley. 2003. WHOI silhouette digitizer version 1.0 User's guide. Woods Hole Oceanographic Institute Technical Report **5**:1-63.
Locke, S. A., G. Bulté, M. R. Forbes, and D. J. Marcogliese. 2012. Estimating diet in individual pumpkinseed sunfish Lepomis gibbosus using stomach contents, stable isotopes and parasites. Journal of Fish Biology.
Logan, J. M., T. D. Jardine, T. J. Miller, S. E. Bunn, R. A. Cunjak, and M. E. Lutcavage. 2008. Lipid corrections in carbon and nitrogen stable isotope analyses: comparison of chemical extraction and modelling methods. Journal of Animal Ecology **77**:838-846.
Ludsin, S. A., X. S. Zhang, S. B. Brandt, M. R. Roman, W. C. Boicourt, D. M. Mason, and M. Costantini. 2009. Hypoxia-avoidance by planktivorous fish in Chesapeake Bay: Implications for food web interactions and fish recruitment. Journal of Experimental Marine Biology and Ecology **381**:S121-S131.
Lynch, H. J., J. T. Thorson, and A. O. Shelton. 2014. Dealing with under- and over-dispersed count data in life history, spatial, and community ecology. Ecology **95**:3173-3180.
MacKenzie, K. M., C. N. Trueman, C. H. Lucas, and J. Bortoluzzi. 2017. The preparation of jellyfish for stable isotope analysis. Marine Biology **164**:219.
Maclennan, D. N., P. G. Fernandes, and J. Dalen. 2002. A consistent approach to definitions and symbols in fisheries acoustics. Ices Journal of Marine Science **59**:365-369.
Malej, A., J. Faganeli, and J. Pezdic. 1993. Stable-Isotope and Biochemical Fractionation in the Marine Pelagic Food-Chain - the Jellyfish Pelagia-Noctiluca and Net Zooplankton. Marine Biology **116**:565-570.
Mandic, M., A. E. Todgham, and J. G. Richards. 2009. Mechanisms and evolution of hypoxia tolerance in fish. Proceedings of the Royal Society B: Biological Sciences **276**:735-744.
Marshall, K. N. 2007. Integrating energetics and interaction strengths in natural ecosystems. MSc Thesis. University of Washington, Seattle,WA.
Matley, J. K., A. T. Fisk, and T. A. Dick. 2015. Foraging ecology of ringed seals (*Pusa hispida*), beluga whales (*Delphinapterus leucas*) and narwhals (*Monodon monoceros*) in the Canadian High Arctic determined by stomach content and stable isotope analysis. Polar Research **34**:11.
Mauchline, J. 1980. Measurement of body length of *Euphausia superba* Dana. BIOMASS Handbook No. 4, SCAR/SCOR/IABO/ACMRR:4-9.
McAllister, M. K., and J. N. Ianelli. 1997. Bayesian stock assessment using catch-age data and the sampling - importance resampling algorithm. Canadian Journal of Fisheries and Aquatic Sciences **54**:284-300.
McCann, K., A. Hastings, and G. R. Huxel. 1998. Weak trophic interactions and the balance of nature. Nature **395**:794-798.

McClellan, C. M., J. Braun-McNeill, L. Avens, B. P. Wallace, and A. J. Read. 2010. Stable isotopes confirm a foraging dichotomy in juvenile loggerhead sea turtles. Journal of Experimental Marine Biology and Ecology **387**:44-51.

McMahon, K. W., and M. D. McCarthy. 2016. Embracing variability in amino acid δ15N fractionation: mechanisms, implications, and applications for trophic ecology. Ecosphere **7**:e01511.

Melzner, F., J. Thomsen, W. Koeve, A. Oschlies, M. A. Gutowska, H. W. Bange, H. P. Hansen, and A. Körtzinger. 2013. Future ocean acidification will be amplified by hypoxia in coastal habitats. Marine Biology **160**:1875-1888.

Michener, R. H., and K. Lajtha. 2007. Stable isotopes in ecology and environmental science. 2nd edition. Blackwell Pub., Malden, MA.

Minagawa, M., and E. Wada. 1984. STEPWISE ENRICHMENT OF N-15 ALONG FOOD-CHAINS - FURTHER EVIDENCE AND THE RELATION BETWEEN DELTA-N-15 AND ANIMAL AGE. Geochimica Et Cosmochimica Acta **48**:1135-1140.

Mohan, J. A., S. D. Smith, T. L. Connelly, E. T. Attwood, J. W. McClelland, S. Z. Herzka, and B. D. Walther. 2016. Tissue-specific isotope turnover and discrimination factors are affected by diet quality and lipid content in an omnivorous consumer. Journal of Experimental Marine Biology and Ecology **479**:35-45.

Molina-Ramírez, A., C. Cáceres, S. Romero-Romero, J. Bueno, J. I. González-Gordillo, X. Irigoien, J. Sostres, A. Bode, C. Mompeán, M. Fernández Puelles, F. Echevarria, C. M. Duarte, and J. L. Acuña. 2015. Functional differences in the allometry of the water, carbon and nitrogen content of gelatinous organisms. Journal of Plankton Research.

Montalti, D., and N. Ruben Coria. 1993. The use of the stomach-flushing technique to obtain stomach contents samples of Antarctic seabirds. Rivista Italiana di Ornitologia **63**:69-73.

Moore, J. C., and P. C. De Ruiter. 2012. Energetic food webs : an analysis of real and model ecosystems. 1st edition. Oxford University Press, Oxford.

Moriarty, P. E., T. E. Essington, and E. J. Ward. 2017. A novel method to estimate prey contributions to predator diets. Canadian Journal of Fisheries and Aquatic Sciences **74**:168-177.

Moriarty, P. E., E. E. Hodgson, H. E. Froehlich, S. M. Hennessey, K. N. Marshall, K. L. Oken, M. C. Siple, S. Ko, L. E. Koehn, B. D. Pierce, and C. C. Stawitz. 2018. The need for validation of ecological indices. Ecological Indicators **84**:546-552.

Nagata, R. M., M. Z. Moreira, C. R. Pimentel, and A. C. Morandini. 2015a. Food web characterization based on delta N-15 and delta C-13 reveals isotopic niche partitioning between fish and jellyfish in a relatively pristine ecosystem. Marine Ecology Progress Series **519**:13-27.

Nagata, R. M., M. Z. Moreira, C. R. Pimentel, and A. C. Morandini. 2015b. Food web characterization based on Î´15N and Î´13C reveals isotopic niche partitioning between fish and jellyfish in a relatively pristine ecosystem. Marine Ecology Progress Series **519**:13-27.

Naman, S. M., C. M. Greene, C. A. Rice, J. Chamberlin, L. Conway-Cranos, J. R. Cordell, J. E. Hall, and L. D. Rhodes. 2016. Stable isotope-based trophic structure of pelagic fish and jellyfish across natural and anthropogenic landscape gradients in a fjord estuary. Ecology and Evolution **6**:8159-8173.

Navia, A. F., P. A. Mejia-Falla, and A. Giraldo. 2007. Feeding ecology of elasmobranch fishes in coastal waters of the Colombian Eastern Tropical Pacific. BMC Ecology **7**:8.

Newsome, S. D., M. T. Clementz, and P. L. Koch. 2010. Using stable isotope biogeochemistry to study marine mammal ecology. Marine Mammal Science **26**:509-572.
Newton, J., C. Bassin, D. A., M. Kawase, W. Ruef, M. Warner, D. Hannafious, and R. Rose. 2007. Hypoxia in Hood Canal: an overview of status and contributing factors.*in* Georgia Basic Puget Sound Research Conference.
Nielsen, L. A., D. L. Johnson, and American Fisheries Society. 1983. Fisheries techniques. American Fisheries Society, Bethesda, Md.
Ott, M. W. 2005. The accuracy of acoustic vertical velocity measurements: instrument biases and the effect of Zooplankton migration. Continental Shelf Research **25**:243-257.
Paine, R. T. 1980. Food Webs - Linkage, Interaction Strength and Community Infrastructure - the 3rd Tansley Lecture. Journal of Animal Ecology **49**:667-685.
Parker-Stetter, S. L., and J. K. Horne. 2009. Nekton distribution and midwater hypoxia: A seasonal, diel prey refuge? Estuarine, Coastal and Shelf Science **81**:13-18.
Pearson, S. F., D. J. Levey, C. H. Greenberg, and C. Martínez del Rio. 2003. Effects of elemental composition on the incorporation of dietary nitrogen and carbon isotopic signatures in an omnivorous songbird. Oecologia **135**:516-523.
Peterson, B. J. 1999. Stable isotopes as tracers of organic matter input and transfer in benthic food webs: A review. Acta Oecologica-International Journal of Ecology **20**:479-487.
Peterson, B. J., and B. Fry. 1987. Stable Isotopes in Ecosystem Studies. Annual Review of Ecology and Systematics **18**:293-320.
Phillips, D. L., S. D. Newsome, and J. W. Gregg. 2005. Combining sources in stable isotope mixing models: alternative methods. Oecologia **144**:520-527.
Pierson, J. J., M. R. Roman, D. G. Kimmel, W. C. Boicourt, and X. S. Zhang. 2009. Quantifying changes in the vertical distribution of mesozooplankton in response to hypoxic bottom waters. Journal of Experimental Marine Biology and Ecology **381**:S74-S79.
Pitt, K. A., R. M. Connolly, and T. Meziane. 2009a. Stable isotope and fatty acid tracers in energy and nutrient studies of jellyfish: a review. Hydrobiologia **616**:119-132.
Pitt, K. A., C. M. Duarte, C. H. Lucas, K. R. Sutherland, R. H. Condon, H. Mianzan, J. E. Purcell, K. L. Robinson, and S.-I. Uye. 2013. Jellyfish Body Plans Provide Allometric Advantages beyond Low Carbon Content. Plos One **8**:e72683.
Pitt, K. A., D. T. Welsh, and R. H. Condon. 2009b. Influence of jellyfish blooms on carbon, nitrogen and phosphorus cycling and plankton production. Hydrobiologia **616**:133-149.
Plagányi, É. E., A. E. Punt, R. Hillary, E. B. Morello, O. Thébaud, T. Hutton, R. D. Pillans, J. T. Thorson, E. A. Fulton, A. D. M. Smith, F. Smith, P. Bayliss, M. Haywood, V. Lyne, and P. C. Rothlisberg. 2014. Multispecies fisheries management and conservation: tactical applications using models of intermediate complexity. Fish and Fisheries **15**:1-22.
Polis, G. A., and S. D. Hurd. 1996. Linking marine and terrestrial food webs: allochthonous input from the ocean supports high secondary productivity on small islands and coastal land communities. The American Naturalist **147**:396-423.
Pollock, M. S., L. M. J. Clarke, and M. G. Dube. 2007. The effects of hypoxia on fishes: from ecological relevance to physiological effects. Environmental Reviews **15**:1-14.
Ponsard, S., and P. Averbuch. 1999. Should growing and adult animals fed on the same diet show different δ15N values? Rapid Communications in Mass Spectrometry **13**:1305-1310.
Pörtner, H. O., and R. Knust. 2007. Climate Change Affects Marine Fishes Through the Oxygen Limitation of Thermal Tolerance. Science **315**:95-97.

Pörtner, H. O., M. Langenbuch, and B. Michaelidis. 2005. Synergistic effects of temperature extremes, hypoxia, and increases in CO2 on marine animals: From Earth history to global change. Journal of Geophysical Research: Oceans **110**:n/a-n/a.
Post, D. M. 2002. Using stable isotopes to estimate trophic position: models, methods, and assumptions. Ecology **83**:703-718.
Post, D. M., C. A. Layman, D. A. Arrington, G. Takimoto, J. Quattrochi, and C. G. Montana. 2007. Getting to the fat of the matter: models, methods and assumptions for dealing with lipids in stable isotope analyses. Oecologia **152**:179-189.
Pothoven, S. A., H. A. Vanderploeg, T. O. Hook, and S. A. Ludsin. 2012. Hypoxia modifies planktivore-zooplankton interactions in Lake Erie. Canadian Journal of Fisheries and Aquatic Sciences **69**:2018-2028.
Prugh, L. R. 2005. Coyote prey selection and community stability during a decline in food supply. Oecologia **110**:253-264.
Purcell, J. E., and M. V. Sturdevant. 2001. Prey selection and dietary overlap among zooplanktivorous jellyfish and juvenile fishes in Prince William Sound, Alaska. Marine Ecology Progress Series **210**:67-83.
R Core Team. 2017. R: A language and environment for statistical computing.
Rahel, F. J., and J. W. Nutzman. 1994. Foraging in a Lethal Environment - Fish Predation in Hypoxic Waters of a Stratified Lake. Ecology **75**:1246-1253.
Randall, P. J., and A. A. Myers. 2001. Effects of resource matrix, gut region analysed and sample size on diet statistics in co-existing species of flatfish. Journal of the Marine Biological Association of the United Kingdom **81**:1041-1048.
Rastetter, E. B., J. D. Aber, D. P. C. Peters, D. S. Ojima, and I. C. Burke. 2003. Using Mechanistic Models to Scale Ecological Processes across Space and Time. Bioscience **53**:68-76.
Reum, J. C. P., and T. E. Essington. 2008. Seasonal variation in guild structure of the Puget Sound demersal fish community. Estuaries and Coasts **31**:790-801.
Richardson, A. J., A. Bakun, G. C. Hays, and M. J. Gibbons. 2009. The jellyfish joyride: causes, consequences and management responses to a more gelatinous future. Trends in Ecology & Evolution **24**:312-322.
Rindorf, A., and P. Lewy. 2004. Bias in estimating food consumption of fish by stomach-content analysis. Canadian Journal of Fisheries and Aquatic Sciences **61**:2487-2498.
Robbins, C. T., L. A. Felicetti, and S. T. Florin. 2010. The impact of protein quality on stable nitrogen isotope ratio discrimination and assimilated diet estimation. Oecologia **162**:571-579.
Robbins, C. T., L. A. Felicetti, and M. Sponheimer. 2005. The effect of dietary protein quality on nitrogen isotope discrimination in mammals and birds. Oecologia **144**:534-540.
Roberts, J. J., P. A. Grecay, S. A. Ludsin, S. A. Pothoven, H. A. Vanderploeg, and T. O. HÖÖK. 2012. Evidence of hypoxic foraging forays by yellow perch (Perca flavescens) and potential consequences for prey consumption. Freshwater Biology **57**:922-937.
Roman, M. R., A. L. Gauzens, W. K. Rhinehart, and J. R. White. 1993. Effects of Low-Oxygen Waters on Chesapeake Bay Zooplankton. Limnology and Oceanography **38**:1603-1614.
Roman, M. R., J. J. Pierson, D. G. Kimmel, W. C. Boicourt, and X. Zhang. 2012. Impacts of Hypoxia on Zooplankton Spatial Distributions in the Northern Gulf of Mexico. Estuaries and Coasts **35**:1261-1269.

Rose, K., B. Megrey, D. Hay, F. Werner, and J. Schweigert. 2008. Climate regime effects on Pacific herring growth using coupled nutrient-phytoplankton-zooplankton and bioenergetics models. Transactions of the American Fisheries Society **137**:278-297.
Rose, K. A. 2000. Why are quantitative relationships between environmental quality and fish populations so elusive? Ecological Applications **10**:367-385.
Ruzicka, J. J., E. A. Daly, and R. D. Brodeur. 2016. Evidence that summer jellyfish blooms impact Pacific Northwest salmon production. Ecosphere **7**:22.
Samhouri, J. F., P. S. Levin, and C. J. Harvey. 2009. Quantitative Evaluation of Marine Ecosystem Indicator Performance Using Food Web Models. Ecosystems **12**:1283-1298.
Sandberg, E. 1997. Benthic predator-prey relationships and abiotic stress. The effects of physical disturbance and oxygen deficiency. Acta Academiae Aboensis Ser B Mathematica et Physica **56**:1-42.
Sato, M., J. K. Horne, S. L. Parker-Stetter, T. E. Essington, J. E. Keister, P. E. Moriarty, L. Li, and J. Newton. 2016. Impacts of moderate hypoxia on fish and zooplankton prey distributions in a coastal fjord. Marine Ecology Progress Series **560**:57-72.
Sato, M., J. K. Horne, S. L. Parker-Stetter, and J. E. Keister. 2015. Acoustic classification of coexisting taxa in a coastal ecosystem. Fisheries Research **172**:130-136.
Schnedler-Meyer, N. A., P. Mariani, and T. Kiorboe. 2016. The global susceptibility of coastal forage fish to competition by large jellyfish. Proceedings of the Royal Society B-Biological Sciences **283**:8.
Semmens, B. X., E. J. Ward, J. W. Moore, and C. T. Darimont. 2009. Quantifying Inter- and Intra-Population Niche Variability Using Hierarchical Bayesian Stable Isotope Mixing Models. Plos One **4**.
Sentis, A., J.-L. Hemptinne, and J. Brodeur. 2014. Towards a mechanistic understanding of temperature and enrichment effects on species interaction strength, omnivory and food-web structure. Ecology Letters **17**:785-793.
Sick, H., N. Roos, E. Saggau, K. Haas, V. Meyn, B. Walch, and N. Trugo. 1997. Amino acid utilization and isotope discrimination of amino nitrogen in nitrogen metabolism of rat liver in vivo. Zeitschrift Fur Ernahrungswissenschaft **36**:340-346.
Skikne, S. A., R. E. Sherlock, and B. H. Robison. 2009. Uptake of dissolved organic matter by ephyrae of two species of scyphomedusae. Journal of Plankton Research **31**:1563-1570.
Sokolova, I. M. 2013. Energy-Limited Tolerance to Stress as a Conceptual Framework to Integrate the Effects of Multiple Stressors. Integrative and Comparative Biology **53**:597-608.
Sondre, A., and M. Pennington. 2003. On estimating the age composition of the commercial catch of Northeast Arctic cod from a sample of clusters. Ices Journal of Marine Science **60**:297-303.
Sosik, E. A., and C. A. Simenstad. 2013. Isotopic evidence and consequences of the role of microbes in macroalgae detritus-based food webs. Marine Ecology Progress Series **494**:107-119.
Stan Development Team. 2017a. RStan: the R interface to Stan. R package version 2.16.2.
Stan Development Team. 2017b. Stan Modeling Language Users Guide and Reference Manual, Version 2.17.0.
Stewart, D. J., J. F. Kitchell, and L. B. Crowder. 1981. Forage Fishes and Their Salmonid Predators in Lake-Michigan. Transactions of the American Fisheries Society **110**:751-763.

Stewart, I. J., and O. S. Hamel. 2014. Bootstrapping of sample sizes for length- or age-composition data used in stock assessments. Canadian Journal of Fisheries and Aquatic Sciences **71**:581-588.

Stillman, R. A., S. F. Railsback, J. Giske, U. Berger, and V. Grimm. 2015. Making Predictions in a Changing World: The Benefits of Individual-Based Ecology. Bioscience **65**:140-150.

Sutherland, D. A., P. MacCready, N. S. Banas, and L. F. Smedstad. 2011. A Model Study of the Salish Sea Estuarine Circulation. Journal of Physical Oceanography **41**:1125-1143.

Sweeting, C. J., J. T. Barry, N. V. C. Polunin, and S. Jennings. 2007. Effects of body size and environment on diet-tissue δ13C fractionation in fishes. Journal of Experimental Marine Biology and Ecology **352**:165-176.

Syvaranta, J., C. Harrod, L. Kubicek, V. Cappanera, and J. D. R. Houghton. 2012. Stable isotopes challenge the perception of ocean sunfish Mola mola as obligate jellyfish predators. Journal of Fish Biology **80**:225-231.

Thiebot, J.-B., J. P. Y. Arnould, A. Gómez-Laich, K. Ito, A. Kato, T. Mattern, H. Mitamura, T. Noda, T. Poupart, F. Quintana, T. Raclot, Y. Ropert-Coudert, J. E. Sala, P. J. Seddon, G. J. Sutton, K. Yoda, and A. Takahashi. Jellyfish and other gelata as food for four penguin species – insights from predator-borne videos. Frontiers in Ecology and the Environment:n/a-n/a.

Thomas, P., M. S. Rahman, M. E. Picha, and W. Tan. 2015. Impaired gamete production and viability in Atlantic croaker collected throughout the 20,000km2 hypoxic region in the northern Gulf of Mexico. Marine Pollution Bulletin **101**:182-192.

Thurber, A. R. 2014. Diet-dependent incorporation of biomarkers: implications for food-web studies using stable isotope and fatty acid analyses with special application to chemosynthetic environments. Marine Ecology:n/a-n/a.

Tirasin, E. M., and T. Jorgensen. 1999. An evaluation of the precision of diet description. Marine Ecology Progress Series **182**:243-252.

Trites, A. W., and R. Joy. 2005. Dietary analysis from fecal samples: how many scats are enough? Journal of Mammalogy **86**:704-712.

Turk, V., D. Lucic, V. Flander-Putrle, and A. Malej. 2008. Feeding of Aurelia sp (Scyphozoa) and links to the microbial food web. Marine Ecology-an Evolutionary Perspective **29**:495-505.

Tylianakis, J. M., R. K. Didham, J. Bascompte, and D. A. Wardle. 2008. Global change and species interactions in terrestrial ecosystems. Ecology Letters **11**:1351-1363.

Uye, S. 1994. Replacement of Large Copepods by Small Ones with Eutrophication of Embayments - Cause and Consequence. Hydrobiologia **293**:513-519.

Val, A. L., Silva, M.N.P., amp, and V. M. F. Almeida-Val. 1998. Hypoxia adaptation in fish of the Amazon: a never-ending task. African Zoology **33**:107-114.

van der Bank, M. G., A. C. Utne-Palm, K. Pittman, A. K. Sweetman, N. B. Richoux, V. Bruchert, and M. J. Gibbons. 2011. Dietary success of a 'new' key fish in an overfished ecosystem: evidence from fatty acid and stable isotope signatures. Marine Ecology-Progress Series **428**:219-233.

Vander Zanden, M. J., M. K. Clayton, E. K. Moody, C. T. Solomon, and B. C. Weidel. 2015. Stable Isotope Turnover and Half-Life in Animal Tissues: A Literature Synthesis. Plos One **10**:e0116182.

Vanderklift, M. A., and S. Ponsard. 2003. Sources of variation in consumer-diet delta(15)N enrichment: a meta-analysis. Oecologia **136**:169-182.

Vanderploeg, H. A., S. A. Ludsin, S. A. Ruberg, T. O. Hook, S. A. Pothoven, S. B. Brandt, G. A. Lang, J. R. Liebig, and J. F. Cavaletto. 2009. Hypoxia affects spatial distributions and overlap of pelagic fish, zooplankton, and phytoplankton in Lake Erie. Journal of Experimental Marine Biology and Ecology **381**:S92-S107.

Vansteenbrugge, L., K. Hostens, B. Vanhove, A. De Backer, L. De Clippele, and M. De Troch. 2016. Trophic ecology of Mnemiopsis leidyi in the southern North Sea: a biomarker approach. Marine Biology **163**:17.

Vaquer-Sunyer, R., and C. M. Duarte. 2008. Thresholds of hypoxia for marine biodiversity. Proceedings of the National Academy of Sciences of the United States of America **105**:15452-15457.

Vaquer-Sunyer, R., and C. M. Duarte. 2011. Temperature effects on oxygen thresholds for hypoxia in marine benthic organisms. Global Change Biology **17**:1788-1797.

Ward, E. J., B. X. Semmens, D. L. Phillips, J. W. Moore, and N. Bouwes. 2011. A quantitative approach to combine sources in stable isotope mixing models. Ecosphere **2**:art19.

Watanabe, S., M. Kodama, J. G. Sumbing, and M. J. H. Lebata-Ramos. 2013. Diet-tissue Stable Isotopic Fractionation of Tropical Sea Cucumber, Holothuria scabra. Jarq-Japan Agricultural Research Quarterly **47**:127-134.

Webber, M. K., and J. C. Roff. 1995. Annual biomass and production of the oceanic copepod community off Discovery Bay, Jamaica. Marine Biology **123**:481-495.

Weckel, M., W. Giuliano, and S. Silver. 2006. Jaguar (Panthera onca) feeding ecology: distribution of predator and prey through time and space. Journal of Zoology **270**:25-30.

Wernberg, T., D. A. Smale, F. Tuya, M. S. Thomsen, T. J. Langlois, T. de Bettignies, S. Bennett, and C. S. Rousseaux. 2013. An extreme climatic event alters marine ecosystem structure in a global biodiversity hotspot. Nature Climate Change **3**:78-82.

Wiebe, P. H., G. L. Lawson, A. C. Lavery, N. J. Copley, E. Horgan, and A. Bradley. 2013. Improved agreement of net and acoustical methods for surveying euphausiids by mitigating avoidance using a net-based LED strobe light system. ICES Journal of Marine Science: Journal du Conseil.

Williams, N. C., K. A. Bjorndal, M. M. Lamont, and R. R. Carthy. 2014. Winter Diets of Immature Green Turtles (Chelonia mydas) on a Northern Feeding Ground: Integrating Stomach Contents and Stable Isotope Analyses. Estuaries and Coasts **37**:986-994.

Williams, R., and D. Robins. 1979. Calorific, ash, carbon and nitrogen content in relation to length and dry weight of Parathemisto gaudichaudi (Amphipoda: Hyperiidea) in the North East Atlantic Ocean. Marine Biology **52**:247-252.

Yasuhiko, N., C. D. P., A. Taiki, R. P. W., F. Melinda, and T. Akinori. 2013. Unravelling the mysteries of a mesopelagic diet: a large apex predator specializes on small prey. Functional Ecology **27**:710-717.

Zhang, H. Y., S. A. Ludsin, D. M. Mason, A. T. Adamack, S. B. Brandt, X. S. Zhang, D. G. Kimmel, M. R. Roman, and W. C. Boicourt. 2009. Hypoxia-driven changes in the behavior and spatial distribution of pelagic fish and mesozooplankton in the northern Gulf of Mexico. Journal of Experimental Marine Biology and Ecology **381**:S80-S91.